

Functional Architecture of Molecular Complexes involved in DNA double-strand break Repair

Functionele architectuur van moleculaire complexen
betrokken bij DNA dubbelstrengsbreuk herstel

Proefschrift

ter verkrijging van de graad van doctor
aan de Erasmus Universiteit Rotterdam
op gezag van de Rector Magnificus Prof.dr. S.W.J. Lamberts
en volgens besluit van het College voor Promoties.

De openbare verdediging zal plaatsvinden op
woensdag 29 juni 2005 om 11.45 uur

door

Dejan Ristić

geboren te Sremska Mitrovica (Joegoslavië)

Promotiecommissie

Promotoren: Prof.dr. R. Kanaar
Prof.dr. J.H.J. Hoeijmakers

Overige leden: Prof.dr. P. Verrijzer
Prof.dr. P. van der Vliet
Dr. N. Galjart

Copromotor: Dr. C. Wyman

Cover design: Dejan Ristić

Printed by: Optima Grafische Communicatie, Rotterdam
ISBN

© Dejan Ristić, 2005

No part of this book may be reproduced, stored in a retrieval system or transmitted in any form or by any means without permission of the author. The copyright of the publications remains with the publishers.

The work presented in this thesis have been performed at the Department of Cell Biology and Genetics at the Erasmus Medical Center in Rotterdam.
The research have been supported by the Nederland Organisatie voor Wetenschappelijk Onderzoek (NWO)

Mami i tati

Vesni i Milošu

Contents

Chapter 1	
Introduction	7
I Microscopy in Life Sciences	9
II Structure-Function relations of the DNA repair machines	11
III Scanning force microscopy analysis of the mechanism of homologous recombination	12
IV Scope of the thesis	16
Chapter 2	
The molecular machines of DNA repair: scanning force microscopy analysis of their architecture	19
Chapter 3	
Homologous recombination-mediated double-strand break repair	31
Chapter 4	
Rad52 and Ku bind to different DNA structures produced early in double-strand break repair	41
Chapter 5	
The architecture of the human Rad54–DNA complex provides evidence for protein translocation along DNA	53
Chapter 6	
ATP hydrolysis affects stability of hRad51 nucleoprotein filaments	63
Summary	89
Samenvatting	90
List of publications	91
Curriculum vitae	92
Acknowledgments	93

Chapter 1

Introduction



I Microscopy in Life Sciences

We see interesting things around us and wonder what they are and how they work. Science founded upon direct observation of the world tries to explain its nature. Our efforts to understand the natural world are often dependent on technology. Available technology also limits things that can be observed and, to some extent, determines how we describe nature. Thus, technological advances often provide more than incremental improvements in our ability to describe and understand the natural world. As stated by the philosopher of science Freeman Dyson "The effect of concept-driven revolution is to explain old things in new ways. The effect of tool-driven revolution is to discover new things that have to be explained."(Dyson, 1997).

In the beginning, our interest in the natural world was manifested through direct observation by our eyes. Resolution of our eyes limited us to observe only objects the size of fine human hair or bigger. Technological progress brought us tools to expand this resolution range. Tools, like telescopes in astronomy and microscopes in life sciences, "opened our eyes" for macro and micro cosmos. Only after the invention of the optical microscope by Anton van Leeuwenhoek in the 17th century did scientists become aware of a "new world": bacteria, yeast, microscopic nematodes etc., collectively known as microbes or "micron scale beings". Using the optical microscope, Robert Hooke was the first to describe and coin the phrase "cell" which revolutionized biology and medicine. After two centuries of research, which was based, to a large extent on optical microscopy, the idea that all living things are composed of cells was formulated as the "cell theory". Optical microscopy continues to be an indispensable tool for understanding many biological processes. The realization that cells are made of subcellular organelles and, at another level, of a collection of biomolecules, brought the attention of scientist from the cellular to the molecular level.

Subcellular and molecular components could be resolved by the electron microscope, developed in 1931 by Max Knott and Ernst Ruska. The electron microscope uses a beam of high-energy electrons instead of visible light to illuminate a sample. Electrons are scattered due to the interactions with the sample, and that scattering is detected and transformed into an image. In electron microscopy direct observation of an object was replaced by indirect visualization. Resolution of both the electron microscope and the optical microscope is limited, due to diffraction, to approximately half the wavelength of radiation used for illumination of the sample (Abbe, 1873). High-energy electrons, used in electron microscopy, have an effective wavelength of less than 1 nm, while the wavelength of visible light ranges from 400-700 nm. However, because of the difficulties in correction of the aberrations of electron lenses, problems of sample preparation, contrast and radiation damage, resolution in electron microscopy is limited to about 2 nm for purified biomolecules and to 3-8 nm for cells and organelles (McIntosh et al., 2005). This is still about 100 fold better than the resolution of the optical microscope. Thanks to its nanometer resolution, electron microscopy has been extensively used for imaging of subcellular components including biomolecules. However, electron microscopy has some limitations and difficulties. Since samples are exposed to very high vacuum in the electron microscope there is no possibility of viewing biological material in the living, wet state. Furthermore, contrast in electron microscopy depends on the atomic

number of the atoms in the sample: the higher atomic number, the more electrons are scattered and the greater the contrast. Biomolecules, composed mainly of carbon, oxygen, nitrogen and hydrogen are almost completely transparent in electron microscopy. Hence, to obtain contrast biological samples are usually stained with heavy metal compounds. Thus effective contrast depends on differential labeling of cell components with heavy atoms. In addition, complex sample preparation often requires chemical fixation of biomolecules which can influence structure. Also, due to the high radiation sensitivity of biological material, the electron dose has to be limited which compromises image quality. Passing through the entire thickness of the sample, electrons interact both with a surface and the internal structures. Therefore, objects with different internal structures can be distinguished. However, electrons create two-dimensional projections against the viewscreen and relations in the third dimension between structures are lost. In order to obtain three-dimensional information from electron microscope images mathematical processing and image reconstruction are required. These aspects place some limits on the use of electron microscopy in analyzing biomolecules and molecular processes, particularly dynamic molecular processes.

Although not developed with the life sciences in mind, the scanning force microscope (also called atomic force microscope) has overcome some of the limitations of optical and electron microscopy. The scanning force microscope was introduced in 1986 by Gerd Binnig and his colleagues Christoph Gerber and Calvin Quate (Binnig et al., 1986). The scanning force microscope, like all other scanning probe microscopes, produces an interaction map of the surface of a sample. In scanning force microscopy a small probe tip, mounted on a flexible cantilever, is scanned by a piezoelectric scanner over a sample. The attractive or repulsive forces between the tip and sample will cause height deflection of the cantilever, which can be measured and recorded. The height is recorded at a series of points, as the probe moves over the surface, in order to build up topographic information on the sample. Hence, visualization of the sample with the scanning force microscope is, like with the electron microscope, indirect. Resolution of the scanning force microscope is not limited by any kind of wavelength but rather depends mostly on the relative size of the tip and the sample. Absolute resolution depends on the sensitivity with which the piezo position can be moved and can be 0.1 nm or less. However, due to tip convolution and the elasticity of biomolecules, a working resolution of around 1 nm in the z dimension and 1-10 nm in the X-Y plane is typical for biomolecules (Santos et al., 2004). This resolution range of the scanning force microscope is similar to resolution of the electron microscope for biological samples. However, due to some important advantages, scanning force microscopy can provide more information than electron microscopy even though spatial resolution is not greater. Compared with electron microscopy, preparation of samples for scanning force microscopy is simply easier and does not require treatment with external contrast agents, which may introduce artefacts and affect the structure of the sample. In addition, scanning force microscopy provide a three-dimensional profile of biomolecules at nanometer resolution directly, in contrast to optical and electron microscopy, where three-dimensional relations have to be reconstructed from two-dimensional images. Biological material can be investigated in an unlabeled and unfixed state without damage for a long time (hours or even days). One unique feature of the scanning force microscope is its ability to

conduct high resolution imaging in an aqueous solution including a wide range of biologically relevant buffers (Bustamante et al., 1997). Because of these features, the scanning force microscope was quickly recognized and accepted as unique tool in biology for single molecule studies as well as visualization of dynamic interactions of biomolecules in their native state.

The direct observation approach to studying biological objects provides a wealth of information about multiple aspects of complex structures simultaneously. This makes visualization methods important complementary or, sometimes, alternative tools to the classical biochemical approach. Direct imaging of complex arrangements of biomolecules such as proteins and DNA is applicable in many processes, including DNA repair which is the focus of this thesis.

II Structure-Function relations of the DNA repair machines

Genetic and biochemical studies have identified gene products required for different aspects of DNA metabolism, including the network of DNA repair pathways. DNA repair is required in all living organisms for proper genome duplication and gene expression. Also, it plays a crucial role in preventing mutagenesis and genomic instability, which can lead to carcinogenesis, ageing or cell death (Hoeijmakers, 2001). Despite the different DNA lesions that must be repaired and the variety of mechanisms used to repair them, DNA repair pathways are conceptually similar in many aspects. Recognition of DNA damage is the first step followed by coordinated assembly of many proteins in molecular machines where repair reactions take place. Like other machines, these nanomachines of DNA repair require a very precise arrangement of their parts in order to function properly. One way to study how these nanomachines work is to describe their structure and correlate structural features with functional activities. Assembly of these protein machines and their three dimensional arrangements can be studied by direct observation with the scanning force microscope. The protein complexes are, for this purpose, reconstituted *in vitro* using purified components. Although powerful, this approach is based entirely on the currently identified list of proteins involved in a process, which might not be complete. However, a major advantage of *in vitro* experiments is the use of defined components, purified proteins and specific DNA substrates, which allows their detailed description. Specific mechanistic models derived from such *in vitro* analyses of molecular structures can then be tested for relevance in the context of intact, living cell.

Multimeric protein complexes are not static structures, their conformation and protein contents changes as repair processes progress. To understand the mechanism of action of the molecular machines of DNA repair, a description of these conformational dynamics is also required. Although, scanning force microscopy could be used to visualize dynamic DNA repair process, there are some limitations. In order to visualize molecules in scanning force microscopy they have to be immobilized on a surface. However, molecules have to be free from the surface to enable their dynamic interactions and to prevent steric hindrance by the surface, that might affect molecular interactions. Thus the immobilization of molecules on the surface has to be carefully controlled to enable both imaging and molecular interactions. Another limitation of applying scanning force microscopy to study dynamic reactions is its time resolution.

The frame rate of the scanning force microscope is typically about 1 image/minute. The kinetics of biological processes are in the order of seconds and milliseconds. Thus the scanning force microscope is still too slow for real time imaging of many biologically relevant reactions. However, it is not always necessary to observe dynamics directly in order to understand how a process works. Because *in vitro* reactions of DNA repair processes are not synchronous, at any given time, many different steps in a dynamic process of structural changes are present simultaneously. Scanning force microscopy, like other single molecules techniques, provide information about all complexes in a mixture, revealing multiple alternative conformations of protein complexes and their frequency. Analysis of conformational changes observed from static scanning force microscopy images can provide insight into pathway dynamics.

III Scanning force microscopy analysis of the mechanism of homologous recombination

Homologous recombination is a highly conserved biochemical process required for accurate repair of DNA double strand breaks (Wyman et al., 2004), for proper DNA replication (Cox et al. 2000) and for generating genetic diversity in meiosis (Paques et al., 1999).

Homologous recombination, the exchange of DNA sequence between homologous DNA molecules, is a complex process that requires the synchronized action of many proteins. Based on the state of the DNA partners, homologous recombination can be divided into three mechanistically distinct steps: 1. pre-synapsis (unjoined DNA partners), including DNA end processing and formation of active nucleoprotein filaments on the 3' single stranded overhangs, (Fig. 1A-B) 2. synapsis (joined DNA partners), including homology search and joint molecule formation, where the invading single-stranded DNA pairs with its homologous partner in template double-stranded DNA (Fig. 1C) 3. post-synapsis (processing of joined DNA to separate DNA products), including extension of the joint molecule and resolution of the recombined DNA molecules (Fig 1D-E)(For more details on the mechanism of homologous recombination see chapter 3).

Understanding homologous recombination will require a description of the structural features, as well as the dynamic rearrangements, of the recombination machinery involving DNA and the required proteins. Scanning force microscopy, being able to provide three-dimensional profiles of biomolecules at nanometer resolution, as well as information about transitional steps of dynamic processes, is a valuable tool for investigating the dynamic interactions of biomolecules involved in homologous recombination (For more details about recent applications of scanning force microscopy to the study of homologous recombination and the other DNA repair mechanisms see chapter 2).

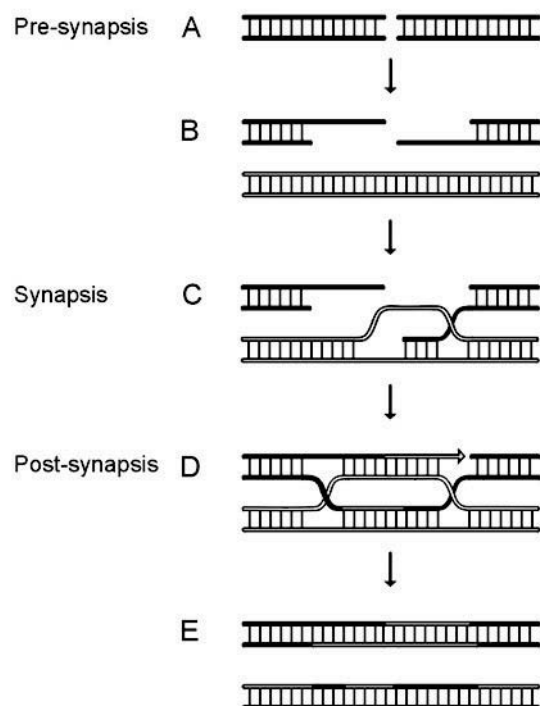


Figure 1. Schematic representation of the arrangement of DNA strands in homologous recombination. (A-B) Pre-synapsis. Upon the formation of double-stranded DNA break, the ends of the break are processed to result in 3' overhangs. (C) Synapsis. The processed broken DNA forms a joint molecule with the homologous template DNA. (D-E) Post-synapsis. DNA synthesis extends the joint molecule and the product DNA molecules are separated.

The mechanistic aspects of homologous recombination that can uniquely be described by scanning force microscopy are presented here. Extensive genetic and biochemical studies have identified the Rad52 group of proteins, including Rad51, Rad52 and Rad54, as the main players in the pre-synapsis and synapsis stages of homologous recombination (Symington, 2002). Rad51 catalyses the crucial steps of homologous recombination, homology search and joint molecule formation. The catalytic core of the process is Rad51 in a complex with single-stranded DNA in a form of a nucleoprotein filament. Rad52 and Rad54 are referred to as recombinant mediators that stimulate joint molecule formation (Wyman et al., 2004; Sung et al., 2003). The following is a brief summary of the relevant biochemical activities of Rad52 and Rad54. Rad52 interacts with Rad51 and ssDNA binding protein RPA (Sugiyama et al., 2002; Sung, 1997; Song et al., 2000; McIlwraith et al., 2000; New et al., 1998). The high affinity of Rad52 for ssDNA and its ability to recognize RPA-bound ssDNA are properties that allow Rad52 to overcome the inhibitory effect of RPA on loading of Rad51 on ssDNA (Krejci et al., 2002). In addition, Rad52 presumably plays a role in the stabilization of Rad51 filaments. Rad54 can interact with Rad51 and stimulates DNA strand exchange promoted by Rad51 (Jiang et al., 1996; Clever et al., 1997;

Golub et al., 1997; Petukhova et al., 1998; Mazin et al., 2000; Solinger et al., 2001). Rad54 has ATPase activity that is dsDNA-dependent (Swagemakers et al., 1998; Petukhova et al., 1998). Rad54 uses the energy of ATP hydrolysis to translocate along DNA, which can generate topological changes in the DNA. Topological stress may result in a local melting of target DNA, which would promote joint molecule formation. Removing histones and other bound proteins from the target DNA by Rad54 action may be another (or additional) way to stimulate homologous recombination.

Based on the accumulated data, molecular mechanisms for the coordinated action of these proteins in homologous recombination have been proposed (see chapter 3). To test these proposed models of homologous recombination, direct visualization can be employed to describe the structure of the predicted recombination intermediates. Direct imaging of *in vitro* reconstituted recombination intermediates with increasing complexity, such as complexes of DNA plus Rad51, DNA plus Rad51/Rad52, DNA plus Rad51/Rad54, DNA plus Rad51/Rad52/Rad54, can be used to investigate how the individual recombination protein activities are synchronized. The multiple features, such as relative position of recombination proteins and distortion of their DNA substrates, stoichiometric ratio of molecules, oligomeric status of proteins, revealed by direct observation have important mechanistic implications. Examples of applying direct imaging to further our understanding of the mechanism of homologous recombination are briefly described below.

Initially, Rad51 filaments were analyzed in a context of different DNA substrates and reaction conditions that influence *in vitro* recombination. Rad51 is widely assumed to function as a highly regular helical structure bound to DNA in a nucleoprotein filament. This structure is more conserved among all of the identified recombinases than their amino acid sequences. Understanding the mechanisms of action of Rad51 will require a description of the conformational dynamics of nucleoprotein filaments. The structural variations observed among filaments formed in different conditions but also along segments of the same filaments suggest that filaments are rather dynamic and not static regular structures (Yu et al., 2001; Conway et al., 2004). Binding of nucleotide cofactor by Rad51 has a major effect on the assembly and the structure of the filament and ATP hydrolysis by Rad51 is the source of the conformational dynamic of the filament. The nucleoprotein filament is an example of a complex structure that can be coherently analyzed by direct observation. The dynamics of filament assembly and disassembly as well as conformational dynamics of already formed filaments due to ATP binding and hydrolysis can be followed with scanning force microscopy. The visualization of recombination intermediates trapped by using ATPase defective mutants of Rad51 and/or non- or slowly-hydrolysable analogs of ATP can reveal the role of ATP hydrolysis at different steps of homologous recombination.

Although it has been proposed that Rad52 is involved in filament assembly and/or stabilization, the exact mechanism through which Rad52 performs its tasks is not understood. Determining the architectural arrangements of Rad52 in a complex with specific DNA substrates or Rad51 filaments will provide information to discriminate between alternative mechanisms of Rad52 action. Scanning force microscopy analysis can directly determine if Rad52 preferentially interacts with specific DNA structures, such as DNA ends, ssDNA, ds/ssDNA junctions, gaps etc., which has important functional implications. In addition, protein-induced changes in DNA, such as DNA bending and/or wrapping, stretching or condensation, can be quantitatively

described. Furthermore, association of distant DNA sites or different DNA molecules mediated by the protein can be directly described. Next, protein changes upon interaction with DNA, such as protein multimerisation, can be quantitatively described. Furthermore, the effect of Rad52 on the assembly, structure and stability of Rad51 filaments can be investigated by visualizing Rad52-Rad51 complexes in different steps of filament assembly and disassembly.

Rad54 interacts with Rad51 *in vivo* upon induction of DNA damage. Since Rad54 stabilizes the Rad51-ssDNA interaction *in vitro*, it is possible that Rad54 interacts with Rad51 that is in nucleoprotein filaments. Based on biochemical data, there are several models for the interaction of Rad54 with Rad51 filaments. One idea is that Rad54 in a monomeric form interacts with Rad51 all along the filament. This type of association would require stoichiometric amounts of Rad54 relative to Rad51. An alternative possibility is that Rad54 in the form of an oligomer interacts with Rad51 only at specific parts of filaments, for instance filament ends, ds/ssDNA junction etc. Direct observation of Rad54 interaction with Rad51 filaments should easily distinguish between these two possibilities. The combination of biochemical techniques to reconstruct functional recombination intermediates *in vitro* and scanning force microscopy imaging to determine the position and amount of Rad54 in complexes will provide direct evidence in support of the one of proposed models or possibly reveal other arrangements.

It has been shown that *in vitro* Rad54 stimulates Rad51 mediated joint molecule formation. In return, the interaction of Rad54 with the Rad51 nucleoprotein filament stimulates the ATPase activity of Rad54 and its ability to induce topological stress into DNA. The coordination of Rad54 activity on the target dsDNA with activity of Rad51-ssDNA complex can be addressed by scanning force microscopy. The visual analysis of individual complexes will reveal aspects of the relative arrangement of these two proteins and their DNA substrates. These features would either be lost in averaging of bulk analysis, or would require interpretation of indirect biochemical assays. Direct visualization will also be advantageous for the analysis of potentially irregular reaction intermediates such as joint molecule, with respect to features like the arrangements of DNA strands and relative position of individual proteins. Scanning force microscopy analysis of complexes in different steps of joint molecule formation will help us understand the mechanisms of the crucial but still mysterious processes of homology search, homology recognition and strand invasion.

The analysis of homologous recombination, described in this thesis, shows the advantages of direct observation for analysis of complex processes that involve multiple DNA-protein and protein-protein interactions. Direct observation by scanning force microscopy describes multiple features of complex structures. These features are characterized simultaneously, which allows their direct correlation. Scanning force microscopy, as a single molecule technique, can extract coherent structural information from asynchronous reactions. The description of all intermediate states of a multistep process can be used to build up a dynamic picture. Homologous recombination is a multistep pathway that involves complex assemblies with multiple important features. These aspects of homologous recombination make this pathway a suitable candidate for scanning force microscopy analysis and also make scanning force microscopy a tool that can produce unique information on this complex molecular process. Scanning force microscopy, expanding resolution from our eyes to

the nano world, will enable us to see homologous recombination. Direct observation of the nanomachines of homologous recombination at work and correlation of this information with biochemical data will explain the mechanism of this complex pathway in new ways.

IV Scope of the thesis

The application of scanning force microscopy to study the architecture of protein complexes involved in DNA repair processes is presented in chapter 2. High resolution imaging in buffer, three dimensional information on molecular structure at nanometer resolution and correlation of complex structural features by single complex visualisation are features of scanning force microscopy explored in this chapter to reveal information on the assembly, architecture and mechanisms of action of the molecular machines of DNA repair.

The role of homologous recombination, the exchange of strands between homologous DNA molecules, in DNA double-stranded break repair is described in chapter 3. The basic steps of homologous recombination as well as the protein machinery responsible for accomplishing these steps are first described for *E.coli*. Subsequently, eukaryotic proteins involved in homologous recombination and their roles are presented. Finally, recent cell biological approaches, used to reveal information on homologous recombination *in vivo*, are described.

A competition for binding to DNA ends by Ku70/80 and Rad52 has been proposed to direct DNA double-stranded break repair to either non-homologous end-joining or homologous recombination. In chapter 4 this idea was tested by comparing the binding of the human Ku70/80 and Rad52 proteins to different DNA substrates. Scanning force microscopy analysis showed that while Ku was preferentially bound to DNA with free ends, Rad52 did not have such a preference. Rad52 was preferentially bound to single-stranded DNA, independent of the presence of DNA ends. Based on these findings it is unlikely that competition between Ku and Rad52 for DNA end binding determine the choice of repair pathway.

Interactions of the human Rad54 protein with double-stranded DNA are described in chapter 5 in order to understand how Rad54 assist homologous DNA pairing by Rad51. Scanning force microscopy analysis of the architecture of Rad54-DNA complexes suggests that the protein translocates along DNA. We discuss how this Rad54 activity may stimulate homologous recombination.

Rad51, like other recombinases, forms distinct nucleoprotein filaments, which represent the "core" structure of homologous recombination. In chapter 6 we report on the effects of reaction conditions, which influence homologous recombination in biochemical assays, on the structure of human Rad51 nucleoprotein filaments by scanning force microscopy. Stable and regular filaments with elongated DNA were visualized under conditions which stimulated homologous recombination in biochemical assays. Conditions which allowed formation of an ADP bound Rad51 conformation resulted in irregular and unstable filaments. Furthermore, we showed that disassembly of filaments, that were followed either in solution or immobilized on mica was, unlike RecA, not a cooperative process but occurred from multiple places along the filament.

References

1. Abbe, E., *Beiträge zur Theorie des Mikroskops und der mikroskopischen Wahrnehmung*. Arch Mikroskop Anat, 1873. **9**: p. 413-420.
2. Binnig, G., C.F. Quate, and C. Gerber, *Atomic force microscope*. Physical Review Letters, 1986. **56**(9): p. 930-933.
3. Jiang, H., et al., *Direct association between the yeast Rad51 and Rad54 recombination proteins*. J Biol Chem, 1996. **271**(52): p. 33181-33186.
4. Bustamante, C., C. Rivetti, and D.J. Keller, *Scanning force microscopy under aqueous solutions*. Curr Opin Struct Biol, 1997. **7**(5): p. 709-716.
5. Clever, B., et al., *Recombinational repair in yeast: functional interactions between Rad51 and Rad54 proteins*. Embo J, 1997. **16**(9): p. 2535-2544.
6. Dyson, F., *Imagined Worlds*. Harvard University Press, 1997.
7. Golub, E.I., et al., *Interaction of human recombination proteins Rad51 and Rad54*. Nucleic Acids Res, 1997. **25**(20): p. 4106-4110.
8. Sung, P., *Function of yeast Rad52 protein as a mediator between replication protein A and the Rad51 recombinase*. J Biol Chem, 1997. **272**(45): p. 28194-28197.
9. New, J.H., et al., *Rad52 protein stimulates DNA strand exchange by Rad51 and replication protein A*. Nature, 1998. **391**(6665): p. 407-410.
10. Petukhova, G., S. Stratton, and P. Sung, *Catalysis of homologous DNA pairing by yeast Rad51 and Rad54 proteins*. Nature, 1998. **393**(6680): p. 91-94.
11. Swagemakers, S.M., et al., *The human RAD54 recombinational DNA repair protein is a double-stranded DNA-dependent ATPase*. J Biol Chem, 1998. **273**(43): p. 28292-28297.
12. Paques, F. and J.E. Haber, *Multiple pathways of recombination induced by double-strand breaks in Saccharomyces cerevisiae*. Microbiol Mol Biol Rev, 1999. **63**(2): p. 349-404.
13. Cox, M.M., et al., *The importance of repairing stalled replication forks*. Nature, 2000. **404**(6773): p. 37-41.
14. Mazin, A.V., et al., *Rad54 protein is targeted to pairing loci by the Rad51 nucleoprotein filament*. Mol Cell, 2000. **6**(3): p. 583-592.
15. McIlwraith, M.J., et al., *Reconstitution of the strand invasion step of double-strand break repair using human Rad51 Rad52 and RPA proteins*. J Mol Biol, 2000. **304**(2): p. 151-164.
16. Song, B. and P. Sung, *Functional interactions among yeast Rad51 recombinase, Rad52 mediator, and replication protein A in DNA strand exchange*. J Biol Chem, 2000. **275**(21): p. 15895-15904.
17. Hoeijmakers, J.H., *Genome maintenance mechanisms for preventing cancer*. Nature, 2001. **411**(6835): p. 366-374.
18. Ristic, D., et al., *The architecture of the human Rad54-DNA complex provides evidence for protein translocation along DNA*. Proc Natl Acad Sci U S A, 2001. **98**(15): p. 8454-8460.
19. Solinger, J.A., et al., *Rad54 protein stimulates heteroduplex DNA formation in the synaptic phase of DNA strand exchange via specific interactions with the presynaptic Rad51 nucleoprotein filament*. J Mol Biol, 2001. **307**(5): p. 1207-1221.
20. Yu, X., et al., *Domain structure and dynamics in the helical filaments formed by RecA and Rad51 on DNA*. Proc Natl Acad Sci U S A, 2001. **98**(15): p. 8419-8424.
21. Krejci, L., et al., *Interaction with Rad51 is indispensable for recombination mediator function of Rad52*. J Biol Chem, 2002. **277**(42): p. 40132-40141.

22. Sugiyama, T. and S.C. Kowalczykowski, *Rad52 protein associates with replication protein A (RPA)-single-stranded DNA to accelerate Rad51-mediated displacement of RPA and presynaptic complex formation*. J Biol Chem, 2002. **277**(35): p. 31663-31672.
23. Symington, L.S., *Role of RAD52 epistasis group genes in homologous recombination and double-strand break repair*. Microbiol Mol Biol Rev, 2002. **66**(4): p. 630-670, table of contents.
24. Sung, P., et al., *Rad51 recombinase and recombination mediators*. J Biol Chem, 2003. **278**(44): p. 42729-42732.
25. Conway, A.B., et al., *Crystal structure of a Rad51 filament*. Nat Struct Mol Biol, 2004. **11**(8): p. 791-796.
26. Santos, N.C. and M.A. Castanho, *An overview of the biophysical applications of atomic force microscopy*. Biophys Chem, 2004. **107**(2): p. 133-149.
27. Wyman, C., D. Ristic, and R. Kanaar, *Homologous recombination-mediated double-strand break repair*. DNA Repair (Amst), 2004. **3**(8-9): p. 827-833.
28. McIntosh, R., D. Nicastro, and D. Mastronarde, *New views of cells in 3D: an introduction to electron tomography*. Trends Cell Biol, 2005. **15**(1): p. 43-51.

Chapter 2

**The molecular machines of DNA repair: scanning force
microscopy analysis of their architecture**



The molecular machines of DNA repair: scanning force microscopy analysis of their architecture

A. JANIĆIJEVIĆ^{1*}, D. RISTIĆ^{1*} & C. WYMAN^{*†}

^{*}Department of Cell Biology and Genetics, Erasmus MC and [†]Radiation Oncology, Erasmus MC-Daniel, PO Box 1738, 3000 DR Rotterdam, The Netherlands

Key words. Atomic force microscopy, DNA repair, DNA–protein complexes, scanning force microscopy.

Summary

The application of scanning force microscope (SFM, also called atomic force microscope or AFM) imaging to study the architecture of proteins and their functional assemblies on DNA has provided new and exciting information on the mechanism of vital cellular processes. Rapid progress in molecular biology has resulted in the identification and isolation of proteins and protein complexes that function in specific DNA transactions. These proteins and protein complexes can now be analysed at the single molecule level, whereby the functional assemblies are often described as nanomachines. Understanding how they work requires understanding their structure and functional arrangement in three dimensions. The SFM is uniquely suited to provide three-dimensional structural information on biomolecules at nanometre resolution. In this review we focus on recent applications of SFM to reveal detailed information on the architecture and mechanism of action of protein machinery involved in safeguarding genome stability through DNA repair processes.

Introduction

The limits of our understanding of biological processes are determined by the technology available to study and define them. Recent advances in microscopy techniques have provided new tools that expand these limits. This review will consider advances in understanding molecular mechanisms of complex genome transactions, specifically repair of DNA damage, that have been made possible by the application of scanning force microscope (SFM also called atomic force

microscope or AFM) imaging to determine molecular architecture. SFM provides three-dimensional (3-D) information on molecular structure at nanometre resolution without the need for external contrast agents. Molecules and complexes are individually analysed providing information on the variety of arrangements possible and their frequency in a mixture. Importantly, this type of single molecule structural analysis allows coherent description of features that would otherwise be lost in the averaging of bulk analysis. In addition, direct observation allows correlation of multiple structural features of individual molecular complexes.

The study of cellular processes has reached the level at which we can identify and isolate the required molecular components for functional analysis. There is intense effort along these lines to understand vital processes such as maintenance of genomic information. One aspect of genome maintenance is the repair of DNA damage that otherwise would result in disruption of cellular function, cell death or mutations. DNA repair pathways are generally classified by the type of damage they correct. The DNA repair pathways that will be considered here are the repair of structural damage, specifically double-strand breaks (DSBs), the removal of chemically modified bases by nucleotide excision repair (NER) and the correction of replication mistakes by mismatch repair (MMR). These various pathways differ widely in required components and mechanism. However, a common salient feature of these pathways is their requirement for the co-ordinated action of several proteins with specific DNA lesions in the genome in order to ensure accurate and efficient repair.

It is at the level of determining the arrangement and functional rearrangement of components that SFM has contributed to our understanding of the mechanisms of several DNA repair pathways. The unique contributions of SFM imaging to understanding mechanisms of DNA transactions can be divided into three categories. First, the size of individual molecules can be accurately determined from SFM images.

Correspondence to: Claire Wyman. Tel.: +31 10 4088337; fax: +31 10 4089468; e-mail: c.wyman@erasmusmc.nl

[†]These authors contributed equally to this work.

Second, protein-induced changes in DNA can be quantitatively described at the single molecule level. Third, through direct observation complex structures such as protein-mediated interaction of multiple and/or distant DNA sites resulting in DNA looping, condensation or supercoiling can be described. This review will present examples of the application of these three features of SFM imaging that have provided novel insight into DNA repair processes.

Protein structure, size and association constant

SFM produces topographic images of molecules from which it is possible to relate their measured volume to molecular weight (Henderson *et al.*, 1996; Wyman *et al.*, 1997; Ratcliff & Erie, 2001). Information on molecular weight can describe the multimer state of a protein or the composition of a complex. There are several techniques to determine the multimeric state of proteins that all have limitations in practical application, certainty of result or relevance to *in vivo* function. SFM imaging can overcome some of these limitations and also provide new possibilities for determining protein–protein interactions and multimer state where other methods have failed. A practical advantage of SFM imaging is that it does not require large amounts of concentrated material. In addition, deposition of material for analysis is rapid and often occurs with molecules in functional conditions, thus more accurately reflecting relevant associations. A convenient method to determine molecular weight from SFM images has recently been developed and demonstrated to be quite robust (Ratcliff & Erie, 2001). Although absolute dimensions of biomolecules are distorted in SFM images as a result of tip convolution (Bustamante *et al.*, 1993), it was shown that there is a linear relationship between SFM measured volume and molecular weight for proteins in the range of 41–670 kDa. This method was then applied to determine the proportion of dimers and monomers of the UvrD protein. Thus these experiments were connected to DNA repair only peripherally as UvrD is a helicase required for nucleotide excision repair in *E. coli*. However, UvrD was used here in a proof of principle experiment to show that the association constant determined from the distribution of dimers and monomers from SFM volume measurements was similar to that determined previously by biochemical methods.

SFM imaging was used to provide new information on the multimer state of another DNA repair-related helicase, the human Werner syndrome protein (hWRN) (Xue *et al.*, 2002). This protein is mutated in an autosomal recessive disease with phenotypic consequences consistent with DNA repair defects (Hickson, 2003), although the exact role of the protein and the pathway it takes part in are not yet known. Volume measurements indicate that the exonuclease domain of hWRN studied exists in trimer–hexamer equilibrium. When bound to PCNA, a trimeric DNA replication processivity factor also involved in DNA repair, hWRN was in a hexameric form. In addition, volume measurements indicated that hWRN formed

hexamers when bound to DNA. These results indicate that the active form of hWRN is a hexamer, a unique insight into the functional forms of hWRN protein. This set of experiments also provided an example of the value of SFM imaging in revealing the unexpected. Images of hWRN bound to some DNA substrates revealed unexpectedly short DNA fragments, suggesting a previously undescribed endonuclease activity that was then tested and confirmed. Further SFM analysis will surely play an important part in describing the role of hWRN in DNA repair.

In addition to the rather general description of molecular weight, SFM images reveal important details of protein structure. The size and shape of some proteins and protein complexes are very amenable to SFM structural analysis. One such complex that is important in DSB repair is the human Rad50–Mre11 complex (Rad50/Mre11). Rad50/Mre11 is a required component of DSB repair and has been implicated to participate in two mechanistically distinct repair pathways, homologous recombination and non-homologous end joining. In addition, it has important functions in diverse aspects of genome metabolism that share an involvement of DNA ends (de Jager & Kanaar, 2002). SFM imaging of human Rad50/Mre11 provided new insight into its structure, indicated an architecture different from what had been accepted and suggested new mechanistic functions.

The amino acid sequence of Rad50 places it in the SMC family of proteins. These proteins all have a very interesting predicted structure with a bipartite ATPase domain, half of which is at the C-terminus and half of which is at the N-terminus, separated by a region of 600–900 amino acids that is predicted to form a coiled-coil structure (Strunnikov & Jessberger, 1999). Based on electron microscope images of a few bacterial SMC examples it was proposed that this class of protein formed complete ATPases by dimerizing into antiparallel intermolecular coiled-coils with a globular ATPase at each end (Melby *et al.*, 1998). SFM images of the human homologue of Rad50, which exists in complex with another protein Mre11, were inconsistent with this arrangement (de Jager *et al.*, 2001). They revealed a central globular domain from which two long thin structures protruded (Fig. 1A). The length and width of the long thin structures were consistent with a coiled-coil half the length of the predicted intermolecular structure. This suggested that the antiparallel coiled-coils were intramolecular with a functional ATPase at one end. Other data had shown that the Rad50/Mre11 complex consisted of two Rad50 molecules and two Mre11 molecules, associated via Mre11 dimerization and Mre11 interacting with Rad50 near the globular ATPase (Hopfner *et al.*, 2001). Taken together with the SFM images, these data lead to the model of Rad50/Mre11 architecture shown in Fig. 1. Subsequently, detailed structural data on the central portion of the Rad50 coiled-coil as well as other SMC family members has confirmed that the intramolecular coiled-coil structure is general for proteins of this family (reviewed in Wyman & Kanaar, 2002).

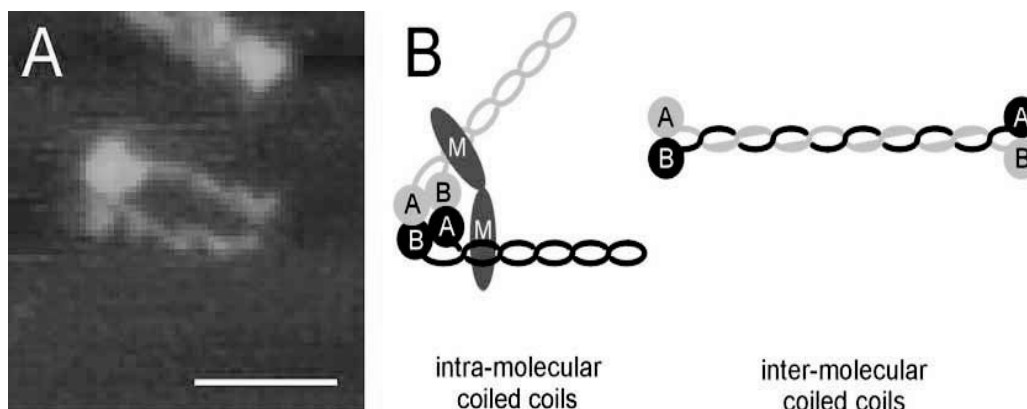


Fig. 1. The architecture of the human Rad50/Mre11 complex revealed by SFM imaging. (A) SFM image of a human Rad50/Mre11 complex. Scale bar = 50 nm. Height is represented by dark to light colours, 0–5 nm. (B) Cartoon diagram of the arrangement of Rad50 and Mre11 in the complex. A and B represent halves of the ATPase domain of Rad50 that are located at the N- and C-terminus of the amino acid sequence. M represents Mre11. The human complex shown here is arranged as a heterotetramer of two Rad50s with intramolecular coiled-coils associated near their ATPase domains via an Mre11 dimer. For comparison, the previously accepted model for Rad50 dimerization via intermolecular coiled-coils is shown to the right. (Image courtesy of M. de Jager.)

SFM imaging, like other single molecule techniques, reveals a wealth of information about the variation and distribution of different structures in a mixture. This was especially interesting in the analysis of Rad50/Mre11 structure. The molecules deposited and imaged in air displayed a variety of conformations of the Rad50 coiled-coils (de Jager *et al.*, 2001). These could represent either a mixture of static forms or flexibility of individual molecules. The ability to image molecules in buffer was successfully exploited here to demonstrate that individual Rad50 coiled-coils were indeed flexible. Subsequent high-resolution imaging and quantification of the local flexibility along the Rad50 coiled-coils identified two regions of increased flexibility that correspond to interruptions in the predicted coiled-coil structure (van Noort *et al.*, 2003).

Protein–DNA complexes

SFM analysis of protein–DNA complexes involved in a variety of DNA repair pathways has helped to elucidate mechanistic details of these vital cellular reactions. In many cases detailed aspects of molecular structure can be quantitatively described from direct observation by SFM. The examples reviewed include: (1) data on the stoichiometry of DNA-bound proteins, (2) protein-induced changes in DNA structure and (3) complex arrangements of proteins on DNA such as oligomerization and simultaneous interaction of multiple sites on one DNA or multiple DNA molecules.

Photo-reactivation

The required first step in any DNA repair pathway is recognition of damage. The ability to image biomolecules in buffer by

SFM has been exploited to study dynamic protein–DNA interactions as a basis for understanding damage recognition. There are two general mechanisms that describe the interaction of proteins with specific DNA sites (Berg *et al.*, 1981). Facilitated 1-D diffusion involves non-specific binding of a protein to DNA followed by translocation of the protein along the DNA strand to find a specific site. The alternative is location of a specific site on DNA by 3-D diffusion of the protein from solution. A simple protein–DNA interaction was studied in SFM experiments in order to optimize imaging parameters and test SFM as a means of distinguishing these two mechanisms of protein location of a specific DNA site. The reaction studied involved bacterial photolyase, a monomeric 55-kDa protein that binds to UV-induced thymidine dimers and uses the energy of visible light to reverse the crosslink chemically (reviewed in Sancar, 1994). By optimizing imaging parameters and modifying the SFM set-up, dynamic interaction of photolyase with partially immobilized DNA could be visualized (van Noort *et al.*, 1998). The DNA in this study was undamaged so all interactions were non-specific. Photolyase association with DNA, disassociation from DNA and sliding over DNA were observed. The latter indicates that facilitated 1-D diffusion over DNA to locate damage is at least possible.

Protein–DNA interactions often result in distortion of DNA, which can have important implications for the mechanism of site recognition. SFM imaging has the advantage over most bulk biochemical methods in that protein-induced changes in DNA structure at non-specific sites can be measured and compared to the changes in DNA structure induced at specific binding sites (Erie *et al.*, 1994). For the case of photolyase this has provided some provocative results. It was determined that photolyase bound to damaged DNA induced a bend of 36°

whereas undamaged DNA was not bent by photolyase (van Noort *et al.*, 1999). The surprising finding of this study was that the distribution of bend angles for the specifically bound complexes was larger than that for both protein non-specifically bound and for free DNA. This indicates an increase in flexibility of DNA (Rivetti *et al.*, 1996) with photolyase bound to damaged sites. This puzzling result is, however, consistent with one model for photolyase action, which requires the damaged bases to be flipped out of the helix and could account for increased flexibility of the DNA. However, these imaging experiments were done with a DNA substrate randomly damaged by UV light, and the difference between specifically and non-specifically bound photolyase was based on statistical subtraction of characteristics of known non-specific complexes. Confirmation awaits analysis of photolyase bound to a known specific damaged site.

Nucleotide excision repair

The mechanism of DNA damage recognition is particularly intriguing in the NER pathway. NER is responsible for removing a wide variety of chemically distinct lesions from DNA that disrupt transcription and replication and that can lead to cell death or mutagenesis (Wood, 1999; Friedberg, 2003). This is a multistep pathway that is conserved from bacteria to humans. Mechanistically, NER can be divided into a series of steps that involve the assembly and modification of distinct protein complexes on DNA: (1) damage recognition, (2) damage demarcation and opening of the double-stranded DNA around the damage, (3) incision of one DNA strand on both sides of the damage and removal of the damaged oligonucleotide and (4) gap filling DNA synthesis and ligation to restore the correct DNA sequence. In bacteria, damage recognition is accomplished by a complex of the UvrA and UvrB proteins. Subsequently, UvrA is released, UvrC recognizes the UvrB bound to damaged DNA and incision on both sides of the damage occurs. SFM analysis of complexes formed by the Uvr proteins and DNA with a single damaged base at a defined site has provided new insight into the mechanism of bacterial NER. First it was demonstrated that in the damage recognition process DNA is wrapped around UvrB and that this wrapping is dependent on ATP binding by UvrB (Verhoeven *et al.*, 2001). DNA wrapping is obvious in SFM images by a decrease in DNA contour length measured through a bound protein complex. The amount of DNA wrapped was about 70 base pairs and the wrap was asymmetric with respect to the damage. This asymmetry is possibly important for determining the position of the incisions as they occur asymmetrically around the damage. DNA was also wrapped around UvrB when it was bound to undamaged DNA. This suggests that damage recognition depends in part on the fact that damaged DNA can more easily be distorted into a wrap and forms a more stable complex with UvrB (Verhoeven *et al.*, 2001).

It had long been accepted that the bacterial damage recognition complex consisted of two UvrA protomers and one UvrB

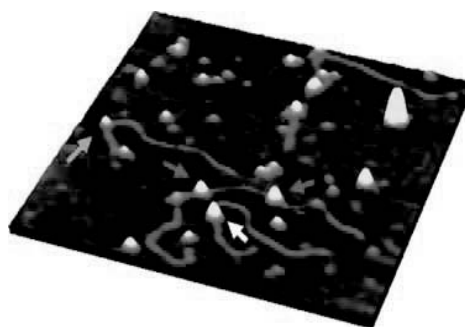


Fig. 2. SFM image reveals that UvrB bound to damaged DNA as a dimer. This image shows a combination of DNA protein complexes. The size standard, Ku70/80 (155 kDa), was bound to a 1500-bp DNA fragment. UvrB (76-kDa monomer) was bound to a 1020-bp DNA fragment with a single damaged base at one-third of its length from one end. In this experiment, ATP was washed out after UvrB binding, which releases the DNA wrap and results in two sizes of UvrB complexes bound to the damaged DNA. The larger UvrB complex, white arrow, is about the same size as Ku70/80, blue arrow. The smaller UvrB complex, green arrow, is half the size of Ku70/80. Thus, the larger UvrB complexes can only logically be UvrB dimers. The image is presented as if it were tilted to emphasize topography. Height is represented as colour from dark to light, 0–3 nm. (Image courtesy of E. Verhoeven and N. Goosen.)

protomer. Volume measurements from SFM images of DNA-bound UvrB complexes clearly indicated the presence of two UvrB protomers (Fig. 2). The damage recognition complex must logically consist of two UvrA protomers and two UvrB protomers, thus correcting a long-standing misconception in the literature (Verhoeven *et al.*, 2002). The size and DNA distortion, in this case a wrap, was simultaneously determined for the individual UvrB–DNA complexes. Using conditions in which both dimers and monomers of UvrB were bound to DNA it was shown that the same amount of DNA was wrapped in both cases. This indicated that DNA was wrapped around one UvrB monomer. Furthermore, after addition of UvrC it was shown that one UvrB monomer was released. From these data it was proposed that two UvrB monomers are needed in the pre-incision complex to detect damage in either DNA strand (Verhoeven *et al.*, 2002).

NER in mammalian systems follows the same basic steps as in bacteria, but more than 20 proteins are required (de Laat *et al.*, 1999). The damage recognition step of mammalian NER is also by extension more complex. Damage recognition in mammalian NER is believed to occur either via RNA polymerase stalled by a DNA lesion (de Laat *et al.*, 1999) or by initially binding the XPC-HR23B complex to damaged sites in non-transcribed regions of the genome (Sugasawa *et al.*, 1998; Volker *et al.*, 2001). As a start to understanding the architectural build up of a functional mammalian NER complex, changes in DNA structure induced by XPC-HR23B binding to damaged sites were investigated by SFM. It was shown that

unlike the bacterial UvrB damage recognition protein, XPC-HR23B did not wrap DNA upon binding or damage recognition. Instead, upon binding damaged DNA, XPC-HR23B induced a DNA bend of 39° and a slightly larger bend of 49° when bound to undamaged DNA (Janicijevic *et al.*, 2003). The significance of the difference in these bend angles is not yet certain as it was not statistically tested. It was proposed that the bend angle at the damaged site is an important structural feature required for subsequent build up of an active NER complex.

Mismatch repair

Another type of DNA damage is caused by replication errors resulting from the incorporation of mismatched bases as DNA is synthesized. In order to avoid introducing mutations, these mistakes are corrected in the MMR pathway. MMR of course involves recognition of mispaired bases, but correct repair critically depends on distinguishing the newly synthesized DNA strand from the parental DNA strand. After this distinction is made, the newly synthesized DNA including the incorrect base is removed and re-synthesized correctly from the parental template. In bacteria, the proteins required to accomplish MMR have been identified and their mechanistic roles in mismatch recognition, strand discrimination, error removal and re-synthesis have been defined. In eukaryotes, homologues of the bacterial MMR proteins have been identified. It is clear that the overall mechanism has been conserved; however, many more proteins are involved in eukaryotes and mechanistic roles have not yet been defined for all of them (reviewed in Kolodner & Marsischky, 1999; Hsieh, 2001). The availability of purified MMR proteins allows detailed dissection of their mechanistic functions. It has been determined that in eukaryotes the heterodimer complexes Msh2–Msh6 and Msh2–Msh3 are responsible for mismatch recognition (Kolodner & Marsischky, 1999; Hsieh, 2001). The role of additional eukaryotic MMR proteins is still being unravelled and SFM imaging has played an important role here.

After mismatch recognition, the steps of strand discrimination, error removal and re-synthesis have to occur in a co-ordinated fashion. SFM imaging has provided clues to the mechanistic role of the yeast Mlh1–Pms2 heterodimer, which acts downstream of mismatch recognition. Mlh1–Pms2 is known to interact with Msh2-containing complexes bound to mismatched bases, but models of MMR had not included Mlh1–Pms2 interactions with DNA. Biochemical and SFM imaging experiments did reveal high affinity and co-operative binding of yeast Mlh1–Pms2 to double-stranded DNA. Importantly, the SFM images showed long tracts of Mlh1–Pms2 bound to double-stranded DNA (Hall *et al.*, 2001; Drotschmann *et al.*, 2002). This sort of relatively non-specific DNA interaction is difficult to define by bulk biochemical assays but obvious by direct inspection of images. In addition, the SFM images showed that the long tracts of Mlh1–Pms2 often included the association of two separate regions of double-

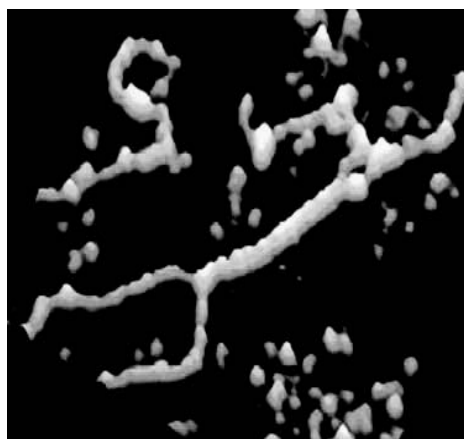


Fig. 3. The mismatch repair complex Mlh1–Pms2 binds cooperatively to DNA and can associate two regions of double-stranded DNA. An SFM image of the yeast Mlh1–Pms2 heterodimer bound to linear M13mp2 double-stranded DNA. Two double-stranded DNA molecules can be distinguished in the lower left corner and these are held together in a long tract of bound Mlh1–Pms2. The image is presented as a surface plot to emphasize topography. Height is represented by colour from dark to light, 0–3.5 nm. (Image courtesy of D. Erie and T. Kunkel.)

stranded DNA (Fig. 3). The association of two DNA strands could indicate that Mlh1–Pms2 has two DNA binding sites or that the arrangement in long tracts produces binding sites favouring association of multiple DNA strands. The mechanistic significance of this Mlh1–Pms2 cooperative binding to DNA and association of multiple DNA strands has not yet been defined, but it was suggested that this activity could facilitate strand discrimination by communication with the mismatch and other MMR factors (Hall *et al.*, 2001). These observations will surely spur new directions of investigation into the functional architecture of mammalian MMR complexes.

DSB repair

DNA DSBs, arising during genome duplication and from exogenous DNA damaging agents, are among the most toxic DNA lesions. Unrepaired DSBs can be lethal whereas misrepaired DSBs can cause chromosomal rearrangements, genome instability and eventually carcinogenesis. Eukaryotic cells primarily repair DSBs in one of two ways, homologous recombination and non-homologous end joining (reviewed in Kanaar *et al.*, 1998). Homologous recombination repairs DSBs accurately using the information from the undamaged sister chromatid or homologous chromosome. Non-homologous end joining rejoins ends directly in a manner that is more error-prone. Both pathways are complex processes, which involve the co-ordinated action of a large number of proteins. Homologous recombination requires proteins originally identified as the Rad52 epistasis

group of yeast and later found to be conserved in other species: Rad50, Rad51, Rad52, Rad54, Rad55, Rad57, Rad59, Mre11 and Xrs2 (Nbs1 in mammals) (Symington, 2002). The proteins specifically required for non-homologous end joining include Ku70/80, DNA-PK_{cs}, DNA ligase IV and XRCC4 (Critchlow & Jackson, 1998). In yeast, the Rad50/Mre11 complex is implicated in non-homologous end joining as well.

Repair of DSBs must begin by recognizing the ends and keeping them close for further processing. Several of the proteins in homologous recombination and non-homologous end joining are known to have important interactions with DNA ends. SFM imaging has helped to characterize and define these interactions as well as provide new ideas about the assembly of complexes that may be needed for DSB repair. One protein complex, the Rad50/Mre11 complex discussed above with respect to the architecture of the proteins, may be involved in both pathways. SFM images of human Rad50/Mre11 bound to DNA revealed structures that could account for a common role in these otherwise mechanistically distinct pathways (de Jager *et al.*, 2001). Rad50/Mre11 was seen to bind to DNA via its globular domain with the long coiled-coils protruding. Large oligomeric assemblies of many Rad50/Mre11 complexes were often observed on linear DNA but never on circular DNA. The large oligomeric DNA-bound Rad50/Mre11 complexes could tether different DNAs apparently via interaction of the protruding coiled-coil domains. It was suggested that this would provide a means of keeping broken DNA ends in close proximity to allow co-ordinated processing and eventual repair via either homologous recombination or non-homologous end joining. SFM images of yeast Rad50/Mre11/Xrs2 complex bound to DNA showed a different picture (Chen *et al.*, 2001). Here protein was observed bound to DNA ends or to internal positions believed to be junctions between short linear fragments. Large oligomers were not observed in this study although the short DNA substrate would have been almost completely obscured if oligomers were formed. In addition, the long coiled-coil structures of Rad50, apparently responsible for tethering DNA by the human protein, were not resolved in this study.

SFM imaging identified large DNA-bound oligomers of Rad50/Mre11 as the functional form in tethering DNA and presumably important for biological activity. The DNA-bound Rad50/Mre11 oligomers are difficult to characterize or quantify by bulk biochemical assays because of their irregular nature and large size. Therefore, SFM imaging was used to test the influence of ATP on formation of DNA-bound Rad50/Mre11 oligomers. Rad50 includes an ATPase activity but the effect of ATP on Rad50 function had not been defined. The formation of large oligomeric complexes was quantified on DNA substrates with different end structures in the presence of ATP or non-hydrolysable ATP analogues. In this way, it was shown that the preference of Rad50/Mre11 to form oligomers on DNA with different end structures was influenced by ATP binding (de Jager *et al.*, 2002). The mechanistic significance of

this ATP-induced change in end binding preference still needs to be defined. One possibility is that it influences the nuclease activity of the Mre11 subunit at different end structures, believed to be important for non-homologous end joining reactions (Hopfner *et al.*, 2001; de Jager *et al.*, 2002).

The other DSB repair proteins that interact with DNA ends, Ku70/80 and DNA-PK_{cs}, are involved exclusively in non-homologous end joining and not homologous recombination. Biochemical studies and electron microscopy visualization of DNA bound by Ku70/80 had shown many years ago that this protein needed an end to bind but did not remain at an end (de Vries *et al.*, 1989). This was confirmed by SFM and extended to analyse the interaction of DNA-bound Ku70/80 with DNA-PK_{cs}. An SFM study reported frequent end-joining events in the presence of Ku70/80 and DNA-PK_{cs}, 16–23% of protein-bound DNA, but the images presented were not very easy to interpret and non-specific aggregations may have occurred (Cary *et al.*, 1997). In another study, it was observed that DNA-PK_{cs} and Ku70/80 could bind separately to DNA, and once bound they could interact to form a complex at a DNA end (Yaneva *et al.*, 1997). This study took advantage of the quantitative 3-D information of SFM images to determine that the size and shape of the protein complex at DNA ends most likely represented DNA-PK_{cs} at the DNA end with an adjacent DNA-internal Ku70/80. In the images presented, DNA ends were joined inter- and intramolecularly in the presence of DNA-PK_{cs} with and without Ku70/80, but this was not quantified. Although not specifically analysed, joining of ends by Ku70/80 alone was not prominent here or in previous electron microscopy studies (de Vries *et al.*, 1989).

In mammals, the Ligase IV-XRCC4 complex is responsible for the final step in non-homologous end joining (Critchlow & Jackson, 1998). The interaction of the Ligase IV-XRCC4 complex with DNA ends with and without Ku70/80 or DNA-PK_{cs} has also been studied by a combination of biochemistry and SFM imaging (Chen *et al.*, 2000). SFM imaging revealed Ligase IV-XRCC4 bound to DNA ends and at the junction of two linear DNA fragments if their ends were complementary, a reassuring position for a ligase. Ligase IV-XRCC4 was also observed together with either Ku70/80 or DNA-PK_{cs} at DNA ends. However, the functional significance of these two interactions cannot be equivalent because biochemical experiments in the same study indicated that Ku70/80 inhibited ligation by Ligase IV-XRCC4 whereas DNA-PK_{cs} shifted the Ligase IV-XRCC4 ligation reaction to favour intermolecular products. The SFM analysis of DNA ends bound by increasingly complex assemblies of end-joining proteins will continue to be important for understanding the complete mechanism of this reaction.

Proteins working on DNA

Many of the DNA repair pathways include steps that require dynamic changes in DNA structure or large-scale rearrangement and movement of proteins on DNA. It is not always necessary

actually to observe movement of molecules to understand their dynamic interactions. Static SFM images can reveal complicated features of molecules as evidence of dynamic reactions that have occurred. A few examples have already been described. The association of distant DNA sites by both Rad50/Mre11 and Mlh1-Pms2 and association of DNA ends by DNA-PK_{cs} and Ku70/80 were obvious from inspection of SFM images (Yaneva *et al.*, 1997; de Jager *et al.*, 2001; Hall *et al.*, 2001). The dynamic process of DNA wrapping by the bacterial NER damage recognition complex involved ATP binding, and hydrolysis at specific steps was determined from the structures of static complexes formed in defined conditions and with informative mutant components (Verhoeven *et al.*, 2001, 2002).

The homologous recombination reaction that is responsible for accurate repair of DSBs also involves dramatic rearrangement of DNA molecules. The central step in homologous recombination is formation of a joint molecule between a broken DNA processed to a single-stranded end and a homologous sequence in the intact double-stranded template. Homologous recombination can be divided into a series of steps that probably occur in a co-ordinated fashion *in vivo*. In eukaryotic cells the broken DNA end is processed to expose a single-stranded region that is bound by Rad51 in a nucleoprotein filament. The structure of this nucleoprotein filament is much like its bacterial homologue, the RecA filament, for which there are some nice SFM images (Seitz *et al.*, 1998). The Rad51 single-stranded DNA filament then has to invade the double-stranded template and eventually basepair with its complementary strand in the template. This requires melting

of the template double-strand and possible removal of proteins bound to the template that would block the reaction. Rad54 is one of the accessory proteins in Rad51-mediated joint molecule formation that probably plays a role at these steps. Rad54 can interact with a Rad51 single-stranded DNA filament (Jiang *et al.*, 1996; Clever *et al.*, 1997; Golub *et al.*, 1997; Tan *et al.*, 1999) and has ATPase activity, which is stimulated by double-stranded DNA (Petukhova *et al.*, 1998; Swagemakers *et al.*, 1998). Rad54 can use the energy of ATP hydrolysis to change DNA topology (Tan *et al.*, 1999; Mazin *et al.*, 2000; Van Komen *et al.*, 2000). Introducing superhelical stress into the template double-strand would help in joint molecule formation by either favouring template melting, removal of proteins bound to the template or both (Petukhova *et al.*, 1999; Tan *et al.*, 1999; Mazin *et al.*, 2000; Petukhova *et al.*, 2000; Van Komen *et al.*, 2000; Ristic *et al.*, 2001).

SFM imaging helped to elucidate the mechanism by which Rad54 uses ATP hydrolysis to change DNA topology (Ristic *et al.*, 2001). Images of DNA-Rad54 complexes formed after incubation of human Rad54 (hRad54) with singly nicked circular DNA show small proteins, presumably hRad54 monomers, bound to DNA in the absence of ATP. Addition of ATP to the binding reaction resulted in formation of much larger complexes. However, there was no evidence for protein-constrained supercoils, such as DNA wrapped around protein or DNA stretched in a protein filament. The large hRad54 complexes were observed anchoring the junction between relaxed and plectonemically supercoiled domains of the plasmid (Fig. 4). The occurrence of these structures was demonstrated

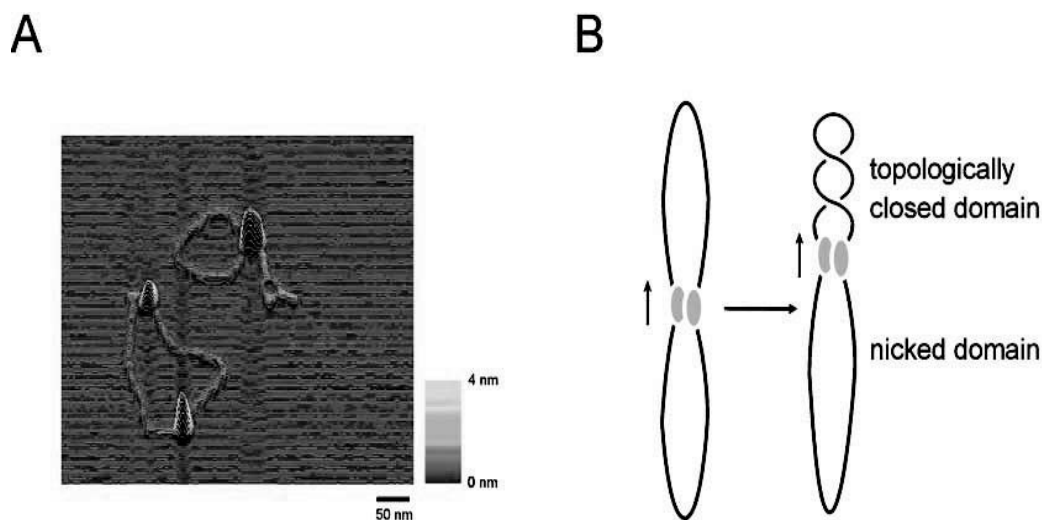


Fig. 4. The hRad54 protein anchoring a supercoiled domain in a singly nicked plasmid. (A) Human Rad54 was bound to a 2-kbp singly nicked plasmid in the presence of ATP before deposition for SFM imaging. The relaxed plasmid to the left has two hRad54 complexes bound. The plasmid to the right has a single large hRad54 complex bound at the junction between relaxed and supercoiled domains. (B) A diagram illustrating the association of two DNA-bound proteins (grey ovals). Movement of the associated proteins, indicated by the vertical arrow, along the DNA helix would create supercoils in plasmid domain without a nick.

to require ATP hydrolysis by hRad54. The creation of an hRad54 anchored supercoiled domain in these plasmids was interpreted to be the result of interaction between two DNA-bound hRad54 complexes and movement of one of them along DNA. Volume measurements of the presumably functional large hRad54 complexes bound to DNA in the presence of ATP indicate they are at least trimers and may be as large as hexamers.

Perspective

Here we have reviewed studies that applied SFM imaging of molecules and complexes in order to better understand the mechanism of DNA repair reactions. Most of these studies used the SFM as a straightforward imaging tool and were able to reveal structural information that would have been difficult to obtain by other methods. Similar information, in some cases, could have been obtained by electron microscopy. However, SFM has the advantage of requiring much simpler sample preparation and being accessible to many more investigators. These advantages and the wealth of interesting protein–DNA structures still to be analysed will ensure that SFM imaging continues to play a productive role in molecular biology.

There are also challenges to overcome in order to learn even more from direct imaging of biomolecules and their functional complexes. As the functional assemblies become more complex and include more components, it will be necessary to develop methods to identify specifically individual proteins within these assemblies. The work reviewed here was all done with purified components combined in defined conditions. There is always the possibility that important components have been omitted. In order to avoid this problem it will also be necessary to develop methods to isolate material from cells or complex mixtures with purity and abundance sufficient for SFM imaging. The combination of SFM imaging with single molecule manipulation techniques, such as magnetic or optical tweezers, will also open new doors for understanding dynamic details of DNA repair and other vital genome transactions.

Acknowledgements

We would like to thank Roland Kanaar for comments on the manuscript and Martijn de Jager for Fig. 1. We thank Dorothy Erie and Esther Verhoeven for providing the images used in the Figs 2 and 3, respectively. These authors were supported by grants from the Netherlands Organization for Scientific Research (NOW-CW and FOM-ALW).

References

Berg, O.G., Winter, R.B. & von Hippel, P.H. (1981) Diffusion-driven mechanisms of protein translocation on nucleic acids. 1. Models and theory. *Biochemistry*, **20**, 6929–6948.

Bustamante, C., Keller, D. & Yang, G. (1993) Scanning force microscopy of nucleic acids and nucleoprotein assemblies. *Curr. Opin. Struct. Biol.* **3**, 363–372.

Cary, R.B., Peterson, S.R., Wang, J., Bear, D.G., Bradbury, E.M. & Chen, D.J. (1997) DNA looping by Ku and the DNA-dependent protein kinase. *Proc. Natl Acad. Sci. USA*, **94**, 4267–4272.

Chen, L., Trujillo, K., Ramos, W., Sung, P. & Tomkinson, A.E. (2001) Promotion of Dnl4-catalyzed DNA end-joining by the Rad50/Mre11/Xrs2 and Hdf1/Hdf2 complexes. *Mol. Cell*, **8**, 1105–1115.

Chen, L., Trujillo, K., Sung, P. & Tomkinson, A.E. (2000) Interactions of the DNA ligase IV-XRCC4 complex with DNA ends and the DNA-dependent protein kinase. *J. Biol. Chem.* **275**, 26196–26205.

Clever, B., Interthal, H., Schmuckli-Maurer, J., King, J., Sigrist, M. & Heyer, W.D. (1997) Recombinational repair in yeast: functional interactions between Rad51 and Rad54 proteins. *EMBO J.* **16**, 2535–2544.

Critchlow, S.E. & Jackson, S.P. (1998) DNA end-joining: from yeast to man. *Trends Biochem. Sci.* **23**, 394–398.

Drotschmann, K., Hall, M.C., Shcherbakova, P.V., Wang, H., Erie, D.A., Brownell, F.R., Kool, E.T. & Kunkel, T.A. (2002) DNA binding properties of the yeast Msh2-Msh6 and Mlh1-Pms1 heterodimers. *Biol. Chem.* **383**, 969–975.

Erie, D.A., Yang, G., Schultz, H.C. & Bustamante, C. (1994) DNA bending by Cro protein in specific and nonspecific complexes: implications for protein site recognition and specificity. *Science*, **266**, 1562–1566.

Friedberg, E.C. (2003) DNA damage and repair. *Nature*, **421**, 436–440.

Golub, E.I., Kovalenko, O.V., Gupta, R.C., Ward, D.C. & Radding, C.M. (1997) Interaction of human recombination proteins Rad51 and Rad54. *Nucl Acids Res.* **25**, 4106–4110.

Hall, M.C., Wang, H., Erie, D.A. & Kunkel, T.A. (2001) High affinity cooperative DNA binding by the yeast Mlh1-Pms1 heterodimer. *J. Mol. Biol.* **312**, 637–647.

Henderson, R.M., Schneider, S., Li, Q., Hornby, D., White, S.J. & Oberleithner, H. (1996) Imaging ROMK1 inwardly rectifying ATP-sensitive K⁺ channel protein using atomic force microscopy. *Proc. Natl Acad. Sci. USA*, **93**, 8756–8760.

Hickson, I.D. (2003) RecQ helicases: caretakers of the genome. *Nat. Rev. Cancer*, **3**, 169–178.

Hopfner, K.P., Karcher, A., Craig, L., Woo, T.T., Carney, J.P. & Tainer, J.A. (2001) Structural biochemistry and interaction architecture of the DNA double-strand break repair Mre11 nuclease and Rad50-ATPase. *Cell*, **105**, 473–485.

Hsieh, P. (2001) Molecular mechanisms of DNA mismatch repair. *Mutat. Res.* **486**, 71–87.

de Jager, M. & Kanaar, R. (2002) Genome instability and Rad50 (S): subtle yet severe. *Genes Dev.* **16**, 2173–2178.

de Jager, M., van Noort, J., van Gent, D.C., Dekker, C., Kanaar, R. & Wyman, C. (2001) Human Rad50/Mre11 is a flexible complex that can tether DNA ends. *Mol. Cell*, **8**, 1129–1135.

de Jager, M., Wyman, C., van Gent, D.C. & Kanaar, R. (2002) DNA end-binding specificity of human Rad50/Mre11 is influenced by ATP. *Nucl Acids Res.* **30**, 4425–4431.

Janićijević, A., Sugawara, K., Shimizu, Y., Hanaoka, F., Wijgers, N., Djurica, M., Hoefijmakers, J.H. & Wyman, C. (2003) DNA bending by the human damage recognition complex XPC-HR23B. *DNA Repair*, **2**, 325–336.

Jiang, H., Xie, Y., Houston, P., Stemke-Hale, K., Mortensen, U.H., Rothstein, R. & Kodadek, T. (1996) Direct association between the yeast Rad51 and Rad54 recombination proteins. *J. Biol. Chem.* **271**, 33181–33186.

- Kanaar, R., Hoeijmakers, J.H. & van Gent, D.C. (1998) Molecular mechanisms of DNA double strand break repair. *Trends Cell. Biol.* **8**, 483–489.
- Kolodner, R.D. & Marsischky, G.T. (1999) Eukaryotic DNA mismatch repair. *Curr. Opin. Genet. Dev.* **9**, 89–96.
- de Laat, W.L., Jaspers, N.G. & Hoeijmakers, J.H. (1999) Molecular mechanism of nucleotide excision repair. *Genes Dev.* **13**, 768–785.
- Mazin, A.V., Bornarth, C.J., Solinger, J.A., Heyer, W.D. & Kowalczykowski, S.C. (2000) Rad54 protein is targeted to pairing loci by the Rad51 nucleoprotein filament. *Mol. Cell.* **6**, 583–592.
- Melby, T.E., Ciampaglio, C.N., Briscoe, G. & Erickson, H.P. (1998) The symmetrical structure of structural maintenance of chromosomes (SMC) and MukB proteins: long, antiparallel coiled coils, folded at a flexible hinge. *J. Cell. Biol.* **142**, 1595–1604.
- van Noort, J., Orsini, F., Eker, A., Wyman, C., de Grooth, B. & Greve, J. (1999) DNA bending by photolysis in specific and non-specific complexes studied by atomic force microscopy. *Nucl. Acids Res.* **27**, 3875–3880.
- van Noort, J., van der Heijden, T., de Jager, M., Wyman, C., Kanaar, R. & Dekker, C. (2003) The coiled-coil of the human Rad50 DNA repair protein contains specific segments of increased flexibility. *Proc. Natl Acad. Sci. USA*, **100**, 7581–7586.
- van Noort, S.J., van der Werf, K.O., Eker, A.P., Wyman, C., de Grooth, B.G., van Hulst, N.F. & Greve, J. (1998) Direct visualization of dynamic protein–DNA interactions with a dedicated atomic force microscope. *Biophys. J.* **74**, 2840–2849.
- Petukhova, G., Stratton, S. & Sung, P. (1998) Catalysis of homologous DNA pairing by yeast Rad51 and Rad54 proteins. *Nature*, **393**, 91–94.
- Petukhova, G., Sung, P. & Klein, H. (2000) Promotion of Rad51-dependent D-loop formation by yeast recombination factor Rdh54/Tid1. *Genes Dev.* **14**, 2206–2215.
- Petukhova, G., Van Komen, S., Vergano, S., Klein, H. & Sung, P. (1999) Yeast Rad54 promotes Rad51-dependent homologous DNA pairing via ATP hydrolysis-driven change in DNA double helix conformation. *J. Biol. Chem.* **274**, 29453–29462.
- Ratcliff, G.C. & Erie, D.A. (2001) A novel single-molecule study to determine protein–protein association constants. *J. Am. Chem. Soc.* **123**, 5632–5635.
- Ristic, D., Wyman, C., Paulusma, C. & Kanaar, R. (2001) The architecture of the human Rad54–DNA complex provides evidence for protein translocation along DNA. *Proc. Natl Acad. Sci. USA*, **98**, 8454–8460.
- Rivetti, C., Guthold, M. & Bustamante, C. (1996) Scanning force microscopy of DNA deposited onto mica: equilibration versus kinetic trapping studied by statistical polymer chain analysis. *J. Mol. Biol.* **264**, 919–932.
- Sancar, A. (1994) Structure and function of DNA photolyase. *Biochemistry*, **33**, 2–9.
- Seitz, E.M., Brockman, J.P., Sandler, S.J., Clark, A.J. & Kowalczykowski, S.C. (1998) RadA protein is an archaeal RecA protein homolog that catalyzes DNA strand exchange. *Genes Dev.* **12**, 1248–1253.
- Strunnikov, A.V. & Jessberger, R. (1999) Structural maintenance of chromosomes (SMC) proteins. Conserved molecular properties for multiple biological functions. *Eur. J. Biochem.* **263**, 6–13.
- Sugasawa, K., Ng, J.M., Masutani, C., Iwai, S., van der Spek, P.J., Eker, A.P., Hanaoka, F., Bootsma, D. & Hoeijmakers, J.H. (1998) *Xeroderma pigmentosum* group C protein complex is the initiator of global genome nucleotide excision repair. *Mol. Cell.* **2**, 223–232.
- Swagemakers, S.M., Essers, J., de Wit, J., Hoeijmakers, J.H. & Kanaar, R. (1998) The human RAD54 recombinational DNA repair protein is a double-stranded DNA-dependent ATPase. *J. Biol. Chem.* **273**, 28292–28297.
- Symington, L.S. (2002) Role of RAD52 epistasis group genes in homologous recombination and double-strand break repair. *Microbiol. Mol. Biol. Rev.* **66**, 630–670.
- Tan, T.L., Essers, J., Citterio, E., Swagemakers, S.M., de Wit, J., Benson, F.E., Hoeijmakers, J.H. & Kanaar, R. (1999) Mouse Rad54 affects DNA conformation and DNA-damage-induced Rad51 foci formation. *Curr. Biol.* **9**, 325–328.
- Van Komen, S., Petukhova, G., Sigurdsson, S., Stratton, S. & Sung, P. (2000) Superhelicity-driven homologous DNA pairing by yeast recombination factors Rad51 and Rad54. *Mol. Cell.* **6**, 563–572.
- Verhoeven, E.E., Wyman, C., Moolenaar, G.F. & Goosen, N. (2002) The presence of two UvrB subunits in the UvrAB complex ensures damage detection in both DNA strands. *EMBO J.* **21**, 4196–4205.
- Verhoeven, E.E., Wyman, C., Moolenaar, G.F., Hoeijmakers, J.H. & Goosen, N. (2001) Architecture of nucleotide excision repair complexes: DNA is wrapped by UvrB before and after damage recognition. *EMBO J.* **20**, 601–611.
- Volker, M., Mone, M.J., Karmakar, P., van Hoffen, A., Schul, W., Vermeulen, W., Hoeijmakers, J.H., van Driel, R., van Zeeland, A.A. & Mullenders, L.H. (2001) Sequential assembly of the nucleotide excision repair factors in vivo. *Mol. Cell.* **8**, 213–224.
- de Vries, E., van Driel, W., Bergsma, W.G., Arnberg, A.C. & van der Vliet, P.C. (1989) HeLa nuclear protein recognizing DNA termini and translocating on DNA forming a regular DNA-multimeric protein complex. *J. Mol. Biol.* **208**, 65–78.
- Wood, R.D. (1999) DNA damage recognition during nucleotide excision repair in mammalian cells. *Biochimie*, **81**, 39–44.
- Wyman, C. & Kanaar, R. (2002) Chromosome organization: reaching out to embrace new models. *Curr. Biol.* **12**, R446–R448.
- Wyman, C., Rombel, I., North, A.K., Bustamante, C. & Kustu, S. (1997) Unusual oligomerization required for activity of NtrC, a bacterial enhancer-binding protein. *Science*, **275**, 1658–1661.
- Xue, Y., Ratcliff, G.C., Wang, H., Davis-Searles, P.R., Gray, M.D., Erie, D.A. & Redinbo, M.R. (2002) A minimal exonuclease domain of WRN forms a hexamer on DNA and possesses both 3′–5′ exonuclease and 5′-protruding strand endonuclease activities. *Biochemistry*, **41**, 2901–2912.
- Yaneva, M., Kowalewski, T. & Lieber, M.R. (1997) Interaction of DNA-dependent protein kinase with DNA and with Ku: biochemical and atomic-force microscopy studies. *EMBO J.* **16**, 5098–5112.

Chapter 3

Homologous recombination-mediated double-strand break repair



Review

Homologous recombination-mediated double-strand break repair

Claire Wyman^{a,b,*}, Dejan Ristic^b, Roland Kanaar^{a,b}^a Department of Radiation Oncology, Erasmus Medical Center-Daniel, PO Box 1738, 3000 DR Rotterdam, The Netherlands^b Department of Cell Biology & Genetics, Erasmus MC, PO Box 1738, 3000 DR Rotterdam, The Netherlands

Available online 24 April 2004

Abstract

Exchange of DNA strands between homologous DNA molecules via recombination ensures accurate genome duplication and preservation of genome integrity. Biochemical studies have provided insights into the molecular mechanisms by which homologous recombination proteins perform these essential tasks. More recent cell biological experiments are addressing the behavior of homologous recombination proteins in cells. The challenge ahead is to uncover the relationship between the individual biochemical activities of homologous recombination proteins and their coordinated action in the context of the living cell.

© 2004 Elsevier B.V. All rights reserved.

Keywords: Homologous; Recombination; DNA double-strand break; Genome; Prokaryotes; Eukaryotes; Holliday junction

Homologous recombination, the exchange of DNA sequence between homologous DNA molecules, is essential for accurate genome duplication and preservation of genome integrity. DNA double-strand breaks (DSBs) and single-stranded gaps are efficient initiators of homologous recombination, which results in their accurate repair using an intact homologous template DNA in the same cell [1]. Decades of genetic and biochemical experiments have resulted in a detailed picture of homologous recombination as practiced by the bacterium *Escherichia coli* which serves as the mechanistic paradigm for comparison of recombination reactions in other organisms. The core of the homologous recombination reaction, homology recognition and DNA strand exchange, is similar between prokaryotes and eukaryotes. However, the eukaryotic homologous recombination reaction is evidently more complex and in many aspects not yet elucidated. With the advance of new fluorescence microscopy techniques, cell biological studies have begun to address the behavior of homologous recombination proteins inside cells. The challenge ahead is to link the understanding of the biochemical mechanisms of homologous recombination with its operation in the context of the living cell. In keeping with the theme of this Special Issue of DNA Repair on the 'Double-Strand Break

Response' we will concentrate on how homologous recombination mediates DSB repair, rather than on its role(s) in underpinning DNA replication [2].

The DNA transactions of homologous recombination serve to identify three basic steps as depicted in Fig. 1: (1) pre-synapsis, preparation of a recombination proficient DNA end; (2) synapsis, formation of a joint molecule between the recombination proficient DNA end and a double-stranded homologous template DNA; (3) post-synapsis and resolution, repair of DNA strands and separation of the recombined DNA molecules. These DNA transactions have to occur in a sequential and coordinated manner for recombination to happen. Recombination also needs to be carefully controlled to avoid partial or inappropriate recombination reactions that will threaten genome stability. The protein machinery responsible for accomplishing these steps in *E. coli* will first be described as it forms the basis for investigations into the mechanism of homologous recombination in other organisms. The RecA recombinase is the key player in homologous recombination as it alone can mediate homology recognition and exchange of DNA strands [3].

The function of the pre-synaptic stage of homologous recombination is to create a proper DNA substrate onto which RecA can assemble in an activated form, as a helical nucleoprotein filament. A broken DNA end is first processed to expose a single-strand overhang with a 3'-end onto which RecA can be loaded (Table 1). DNA unwinding, nucleolytic processing and RecA loading are coordinated through the

* Corresponding author. Tel.: +31-10-4088337; fax: +31-10-4089468.
E-mail address: c.wyman@erasmusmc.nl (C. Wyman).

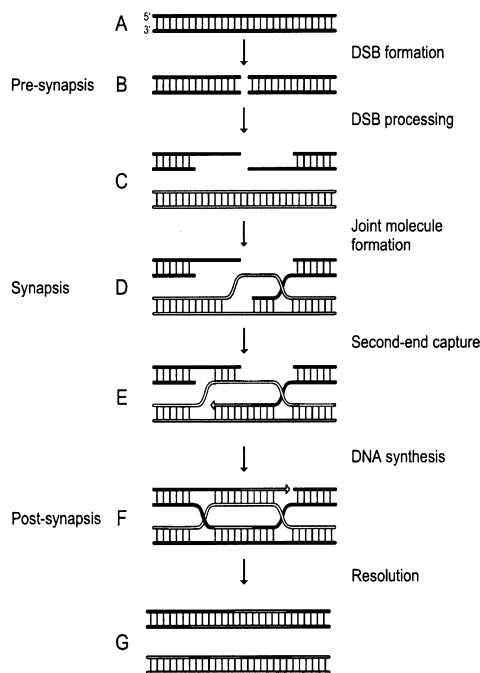


Fig. 1. Schematic representation of DSB-initiated homologous recombination between DNA molecules. Duplex DNAs are indicated by the ladders with the rungs representing base pairs. Pre-synapsis spans stages A–C. Upon DSB formation, the ends are nucleolytically processed, as described in the text, to result in 3' single-stranded tails. The white duplex DNA molecule represents a homologous template DNA. Synapsis, indicated in stages D and E, results when the processed broken DNA forms a joint molecule with the intact homologous repair template DNA using the strand invasion and strand exchange activities of the RecA/Rad51 protein. Post-synapsis, spanning stages E–G, involves the establishment of base pairs between the joint molecule and the second DNA end, the re-synthesis of DNA, and the resolution of Holliday junctions by structure-specific endonucleases. Many possible variations of the model depicted here have been described and can be found in more in-depth reviews [1,43].

action of a single protein complex, RecBCD [4,5]. Alternatively, under certain circumstances, these same steps can be accomplished through the sequential action of a several proteins. A recombination competent DNA end can be produced through unwinding by RecQ, nucleolytic processing by RecJ, after which, RecF, RecO and RecR are needed to load the RecA recombinase [6–8]. The molecular complex formed in pre-synapsis, RecA-coated single-strand DNA, together with a double-strand homologous template DNA are sufficient for the next step in recombination, synapsis. The RecA nucleoprotein filament can effectively mediate homology recognition, strand invasion and strand exchange in the absence of other proteins *in vitro*. In the post-synaptic stage, the joint molecule between the broken DNA and the intact homologous template is a substrate for DNA polymerase and its accessory proteins which re-incorporate missing nucleotides. The recombining molecules can be physically linked through crossed DNA strands in structures known as Holliday junctions. The RuvAB protein

complex is a molecular motor that can branch migrate Holliday junctions which results in extension of heteroduplex DNA between the recombining DNA molecules [9]. The RuvC protein, which interacts with RuvAB, is a Holliday junction resolvase that nicks strands at the junction thereby liberating the recombining partners from each other.

Not all DNA ends or single-stranded regions should be substrates for homologous recombination. Because the recombinase-coated single strand is very efficient at synapsis, unregulated formation of this intermediate could result in inappropriate strand invasion and joint molecule formation leading to genome instability. Control at this step is achieved by the need for specialized enzymes to load RecA onto only those DNA substrates that need recombination for repair. DSBs result in DNA ends that are recognized and processed for homologous recombination repair by the RecBCD complex, which loads RecA onto single-stranded DNA as it is produced which occurs after RecBCD's nuclease activity is attenuated due to its interaction with a special DNA sequence, called a Chi site [10,11]. Other DNA structures resulting from problems in replication that produce gaps bound by Single-Strand Binding (SSB) protein are processed for recombination by the RecF pathway. Here RecF, RecO, and RecR, perhaps as a complex, are needed to displace SSB and replace it with RecA for repair [7,12,13]. The RecF pathway can be made into a DSB repair system, but then requires the helicase and nuclease activities of RecQ and RecJ, respectively [6].

The expectation is that eukaryotes will have molecular machinery that performs functions analogous to those described for homologous recombination-mediated DSB repair in *E. coli*. Intriguingly the only protein component clearly conserved at the amino acid sequence level is the recombinase, RecA in *E. coli* and Rad51 in eukaryotes [14,15]. While other eukaryotic proteins, identified to be important in homologous recombination, are not conserved at the amino acid sequence level, a number of them do have some of the expected biochemical activities. Assembling a complete mechanistic picture of homologous recombination repair in eukaryotes is complicated by the abundance of proteins that can perform some of the required steps and by the absence of identified proteins needed for others.

Although many eukaryotic recombination proteins are predicted to play a role in pre-synapsis, a protein machine such as RecBCD that both processes DNA ends and loads the recombinase has not been described in eukaryotes (Table 1). Biochemically, the Mre11 complex, consisting of the Mre11, Rad50 and NBS1 proteins, is most similar to RecBCD [16] because it has affinity for DNA ends [17,18], nuclease activities [19,20] and apparently can migrate along DNA [21]. The described nuclease activity of the Mre11 complex produces DNA with 5' single-stranded overhangs and not the 3' ends needed for productive synapsis and homologous recombination repair. However, this is also true of RecBCD before its activity is changed at a Chi site [10]. Even though *in vitro* the Mre11 complex has 3'

Table 1
Proteins implicated in the different stages of homologous recombination through biochemical analyses

Stage of homologous recombination	Processes mediated	Proteins	
		<i>E. coli</i>	Eukaryotes ^a
Pre-synapsis (A–C) ^b	Endprocessing	RecBCD, RecQ, RecJ	Mre11 complex
	Negotiating single-stranded DNA	SSB	RPA
	Recombinase loading	RecBCD, RecFOR	Rad52, Rad51 paralogs
	Recombinase nucleo-protein filament stabilization		Rad54
Synapsis (D, E) ^b	Joint molecule formation by strand invasion	RecA	Rad51, Rad54
Post-synapsis (F, G) ^b	Branch migration	RuvAB	Rad54
	Resolution of crossed DNA strands	RuvC	Mus81/Eme1, Rad51C/Xrcc3

See text for more detailed description of activities of the indicated proteins.

^a Some of the protein listed can have additional functions during homologous recombination. In addition, for some of the processes redundant activities are present (see, for example [42]). Furthermore, all stages are likely to require additional proteins not yet identified.

^b Letters refer to stages of homologous recombination shown in Fig. 1.

to 5' exonuclease activity, the kinetics of the appearance of recombinogenic single-stranded DNA with a 3' end is significantly slower in *mre11* mutant yeast cells [22]. In vivo, the activity of Mre11 may be different due to association with yet unidentified components or a modified form of the complex. In addition to its RecBCD-like functions in pre-synapsis, the Mre11 complex also keeps DNA ends in close proximity prior to proper processing, so that they can eventually be efficiently rejoined [17]. In contrast to RecBCD, there is no evidence for simultaneous production of single-stranded DNA and loading of a recombinase by the Mre11 complex. However, the RecF pathway in *E. coli* also illustrates that the same job can be done by a collection of separate proteins. It is possible that in vivo the Mre11 complex works together with other recombination components to coordinate DNA processing and recombinase loading.

There is however no lack of other candidates for the role of helping load Rad51 onto single-stranded DNA to form a functional nucleoprotein filament. The ability to interact in vitro with Rad51 is a property shared by many of the proteins genetically implicated in homologous recombination, including Rad52, Rad54, BRCA2, and the Rad51 paralogs (Rad55/57 in *Saccharomyces cerevisiae* and Rad51B, Rad51C, Rad51D, XRCC2 and XRCC3 in vertebrate cells). Most of these proteins have been called recombination mediators based on their ability in biochemical assays to promote or stabilize Rad51 nucleoprotein filament formation [23]. One important role of mediators is to negotiate between the negative and positive effects of the single-strand DNA binding protein complex RPA on Rad51 polymerization on single-stranded DNA [23,24]. The plethora of Rad51 interacting partners suggest that the mechanism of homologous recombination in eukaryotes is more complicated than in *E. coli*. The multiple interactions influencing Rad51 filament formation and stability do allow for intricate control of homologous recombination in vivo. The in vitro data suggest roles for the recombination mediators in pre-synapsis but do not define their authentic mechanistic functions in vivo or discriminate between their participation in possible (com-

peting) sub-pathways. As is the case in *E. coli* where the RecBCD and RecF pathways are required for pre-synapsis under different circumstances, the recombination mediators that appear to be similar in vitro may be required in specific circumstances in vivo.

The mechanistic anchor to homologous recombination in all organisms is synapsis, consisting of strand invasion and joint molecule formation (Fig. 1D and E). Synapsis requires a recombinase protein assembled into a nucleoprotein filament on the invading single-stranded DNA. Indeed the structure of this nucleoprotein filament is one of the most conserved features of homologous recombination [15]. All current models of DNA synapsis assume that DNA strand exchange occurs within the recombinase nucleoprotein filament. The mechanistic details of this cloaked exchange of partners are not known and their elucidation is the tantalizing goal of ongoing biophysical studies. Sequence comparison and biochemical analyses indicate that Rad51 is the eukaryotic equivalent of the bacterial RecA recombinase [14,15,23,25]. However, there are important differences between these proteins. Efficient assembly of a Rad51 nucleoprotein filament involves the cooperation of several recombination mediators, including Rad52, Rad54 and the Rad51 paralogs [23]. In addition, once formed the Rad51 nucleoprotein filament is less efficient than RecA in joint molecule formation. Some of the “extra” eukaryotic recombination proteins without homologs in bacteria may serve to make Rad51 more RecA-like. One such eukaryotic-specific recombination factor is Rad54. The results of diverse in vitro assays can support roles for Rad54 at all three stages of homologous recombination outlined in Fig. 1 (reviewed in [26]). However, Rad54's biochemical talents, the ability to use ATP energy to translocate along DNA stimulated by a Rad51 filament and double-stranded DNA, can best be exploited at synapsis. Rad54 associated with a Rad51 nucleoprotein filament and homologous double-stranded DNA would translocate along the double-stranded DNA facilitating the location of homologous sequences and or extension of heteroduplex DNA in the joint molecule. Rad54 may also

be needed in eukaryotes to aid synapsis in the context of chromatin [27–29]. So even at this most conserved step of homologous recombination, synapsis, important mechanistic differences exist between eukaryotes and prokaryotes.

Repair of DSBs by homologous recombination is not complete until the product DNA molecules are separated. Because DNA structures with crossed strands are an unavoidable consequence of homologous recombination (Fig. 1D–F) they need to be separated or resolved by structure-specific endonucleases. Bacteria cleave Holliday junctions (Fig. 1F), DNA structures where the four strands of two duplex DNA molecules are crossed, with the RuvC resolvase working in coordination with the RuvAB complex [9]. The search for RuvAB- and RuvC-like machinery in eukaryotes is lively and ongoing. Extracts of mammalian cells are able to perform Holliday junction branch migration and resolution in a manner similar to RuvABC [30,31]. However, the identity of the proteins responsible for this activity has been difficult to determine. Compelling evidence for the involvement of one of the Rad51 paralogs, Rad51C, in this *in vitro* reaction has recently been presented [32]. It cannot yet be determined if Rad51C is (part of) the actual resolvase, or if it is needed to modify other proteins that contribute the actual resolvase activity, or if its presence in the nucleoprotein filament at a junction is needed to recruit the resolvase. The latter possibility is mentioned because other *in vitro* data suggests that the Rad51 paralogs function in pre-synapsis to help form an active nucleoprotein filament. Rad51C is present in several multi-protein complexes in cells [33], which complicates mechanistic analysis of its role in Holliday junction resolution.

However, bona fide functional homologs of RuvC may not be needed to complete homologous recombination in eukaryotes. Both mammals and yeast have structure-specific endonucleases that can cleave Holliday junctions *in vitro*, though they work more efficiently on other DNA structures [34]. It has recently been shown that one of these nucleases, Mus81/Eme1, can resolve homologous recombination products by cleavage of intermediate crossed DNA structure without the need for formation (or resolution) of Holliday junctions [35]. A similar solution can be achieved by the combined action of a helicase, specifically those in the RecQ family, and topoisomerase III [34]. Thus, eukaryotic cells may have more than one way to resolve crossed DNA intermediates and the absence of a RuvABC-like machine should not be too alarming.

The added complexity of homologous recombination in eukaryotes may reflect the need for a variety of mechanistic pathways specialized for different circumstances, such as the need to perform recombination in a multitude of different specialized cell types, the need for the eukaryotic machinery to cope with DNA packaged into chromatin, the need for careful control to avoid ectopic recombination of repetitive DNA sequences, or the need to build up recombination machinery out of multifunctional components that are also used in other aspects of genome metabolism. As outlined above,

biochemical experiments have identified eukaryotic proteins with activities that fit into a homologous recombination mechanism but cannot assure that the isolated proteins do the same thing *in vivo*. In addition, because homologous recombination is coordinated with DNA replication and other complex genome transactions it is difficult to recapitulate the authentic reaction with isolated components.

Studying homologous recombination in living cells does assure that all necessary molecular components are present and presumably functional. However, this approach does not always clarify the mechanistic functions of the proteins involved. The results of two very similar studies reported recently disagree on the order of action of the proteins analyzed and on the step in homologous recombination where they are first required. Both studies used chromatin immuno-precipitation of proteins localized near a site-specific DSB in yeast cells. However, Wolner et al. [36], conclude that Rad54 is needed early in formation of the Rad51 nucleoprotein filament, whereas Sugawara et al. [37], conclude that Rad54 is not needed for Rad51 filament formation but is required only much later for the formation of a strand invasion structure used for DNA synthesis. The reason for the discrepancy in these conclusions is not clear but serves to point out that answering even straightforward mechanistic questions from *in vivo* data is complicated by the multitude of experimental variables that can affect the outcome.

Another approach to study the mechanism of homologous recombination *in vivo* is to follow the dynamics of DNA repair proteins and their substrates in living cells. These methods are now being applied to provide new insight in the mechanisms of homologous recombination repair and the interactions among different aspects of genome metabolism. A number of proteins involved in homologous recombination congregate in response to DNA damage (Fig. 2). GFP-tagged Rad52 was shown to associate with a site-specific DSB in living *S. cerevisiae* cells [38]. In S phase, multiple ionizing radiation-induced DSBs appear to be recruited to repair centers. In mammalian cells, gathering of DSBs is also observed but mostly in G1-phase [39]. The movement of several homologous recombination components, Rad51, Rad52 and Rad54, were followed in S-phase both before and after induction of DNA damage in living mammalian cells [40]. In the absence of DNA damage, the Rad51 protein was present in both a mobile and an immobile fraction whereas all Rad52 and Rad54 were diffusing in the nuclei. Upon DNA damage some Rad51 became stably associated with structures at the site of DNA damage, consistent with formation of a nucleoprotein filament required for homologous recombination. Rad52 and Rad54 transiently associated with sites of DNA damage. Both before and after induction of DNA damage the mobile fractions of Rad52 and Rad54 diffused through the nucleus at different rates, indicating that they are not part of the same pre-assembled holo-complex. These first descriptions of the dynamic features of the recombination proteins have already provided important implications for

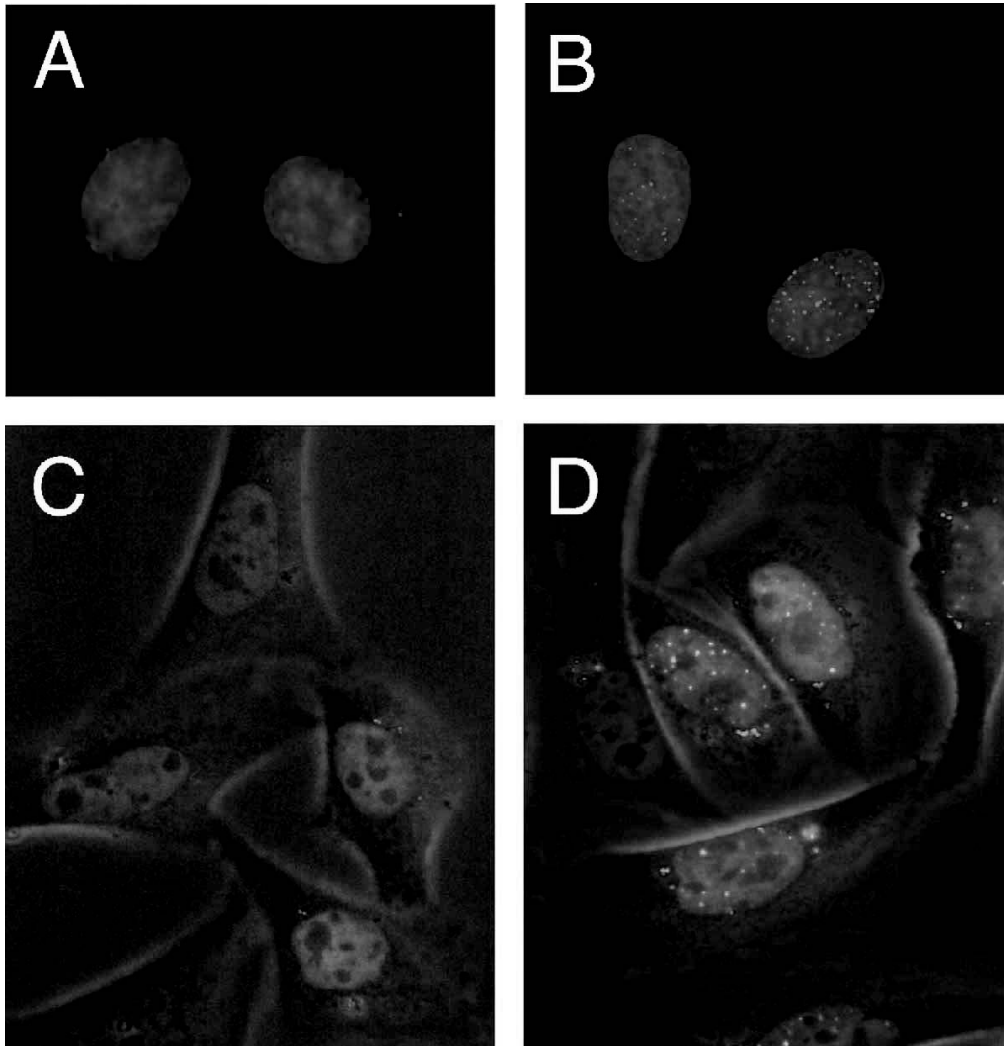


Fig. 2. DNA damage response of mammalian Rad51 and Rad52 proteins at the cellular level. Upon the induction of DSBs the proteins accumulate at sites of DNA damage [38,39,44,45]. The resulting foci are dynamic structures that undergo a continuous association and dissociation of proteins. Each protein has a characteristic residence time in these DNA damage associated structures [40]. (A) DAPI-stained nuclei of primary human fibroblasts before treatment with ionizing radiation. In these fixed cells, the Rad51 protein, stained with antibodies in red, cannot easily be detected. (B) As in (A), except the cells were treated with ionizing radiation. (C) Chinese hamster ovary cells expressing a Rad52-GFP fusion protein. Cells were visualized by a combination of fluorescence and phase-contrast microscopy. (D) As in (C), except the cells were treated with ionizing radiation. Pictures were provided by Jeroen Essers and Lieneke van Veelen.

the mechanism of homologous recombination *in vivo*. First, it is clear that the recombination machinery must be assembled at the site of damage. This is advantageous because it allows flexible use of DNA repair components, exchange of components between different multi-step DNA repair pathways and an increase in the diversity of DNA lesions that can be repaired by a limited number of gene products. Second, the relatively stable interaction of Rad51 and transient interaction of Rad52 and Rad54 at sites of DNA damage likely reflect the affinity of the RAD52 group proteins for

the DSB site. Increased affinity for damaged sites compared to intact DNA ensures that some proteins are immobilized for a longer time at the DSB site, resulting increased local concentration, favoring subsequent interaction of other proteins needed for completing homologous recombination.

Further insight into the authentic mechanism of homologous recombination repair will come from analyzing the behavior of proteins with biochemically characterized mutations to see how these effect *in vivo* performance. One recent study used this approach to test the importance of

interaction between Rad51 and BRCA2 [41]. These investigators also observed two pools of Rad51 in mammalian cells, some freely mobile in the nucleus and some immobile. The immobile pool of Rad51 could be further subdivided into one part that was specifically immobilized in association with BRCA2. Rad51 mutants defective in interaction with BRCA2 were used to show that this pool is specifically mobilized in response to DNA damage caused by replication arrest. This implies a major *in vivo* role of BRCA2 is to control the availability of Rad51, and associates this function with a specific type of DNA damage. It is clear that the technology is in place to sort through the mechanistic possibilities suggested from genetic and biochemical studies of homologous recombination repair in mammalian cells. The issues that we have highlighted here; the authentic roles of many homologous repair proteins, the possibility of multiple pathways depending on the cellular circumstances, the control and coordination of homologous recombination repair with other aspects of genome metabolism, are likely to be elucidated, perhaps in surprising ways, in the not too distant future.

References

- [1] L.S. Symington, Role of RAD52 epistasis group genes in homologous recombination and double-strand break repair, *Microbiol. Mol. Biol. Rev.* 66 (2002) 630–670.
- [2] M.M. Cox, Recombinational DNA repair of damaged replication forks in *Escherichia coli*: questions, *Annu. Rev. Genet.* 35 (2001) 53–82.
- [3] S.L. Lusetti, M.M. Cox, The bacterial RecA protein and the recombinational DNA repair of stalled replication forks, *Annu. Rev. Biochem.* 71 (2002) 71–100.
- [4] S.C. Kowalczykowski, Initiation of genetic recombination and recombination-dependent replication, *Trends Biochem. Sci.* 25 (2000) 156–165.
- [5] G.R. Smith, Homologous recombination near and far from DNA breaks: alternative roles and contrasting views, *Annu. Rev. Genet.* 35 (2001) 243–274.
- [6] S.K. Amundsen, G.R. Smith, Interchangeable parts of the *Escherichia coli* recombination machinery, *Cell* 112 (2003) 741–744.
- [7] K. Morimatsu, S.C. Kowalczykowski, RecFOR proteins load RecA protein onto gapped DNA to accelerate DNA strand exchange: a universal step of recombinational repair, *Mol. Cell* 11 (2003) 1337–1347.
- [8] I. Ivancic-Bace, P. Peharec, S. Moslavac, N. Skrobot, E. Salaj-Smic, K. Brcic-Kostic, RecFOR function is required for DNA repair and recombination in a RecA loading-deficient *recB* mutant of *Escherichia coli*, *Genetics* 163 (2003) 485–494.
- [9] S.C. West, Molecular views of recombination proteins and their control, *Nat. Rev. Mol. Cell. Biol.* 4 (2003) 435–445.
- [10] D.G. Anderson, S.C. Kowalczykowski, The recombination hot spot *chi* is a regulatory element that switches the polarity of DNA degradation by the RecBCD enzyme, *Genes Dev.* 11 (1997) 571–581.
- [11] D.G. Anderson, S.C. Kowalczykowski, The translocating RecBCD enzyme stimulates recombination by directing RecA protein onto ssDNA in a *chi*-regulated manner, *Cell* 90 (1997) 77–86.
- [12] K. Umez, R.D. Kolodner, Protein interactions in genetic recombination in *Escherichia coli*. Interactions involving RecO and RecR overcome the inhibition of RecA by single-stranded DNA-binding protein, *J. Biol. Chem.* 269 (1994) 30005–30013.
- [13] B.L. Webb, M.M. Cox, R.B. Inman, Recombinational DNA repair: the RecF and RecR proteins limit the extension of RecA filaments beyond single-strand DNA gaps, *Cell* 91 (1997) 347–356.
- [14] A. Shinohara, H. Ogawa, T. Ogawa, Rad51 protein involved in repair and recombination in *S. cerevisiae* is a RecA-like protein, *Cell* 69 (1992) 457–470.
- [15] T. Ogawa, X. Yu, A. Shinohara, E.H. Egelman, Similarity of the yeast RAD51 filament to the bacterial RecA filament, *Science* 259 (1993) 1896–1899.
- [16] G.A. Cromie, J.C. Connelly, D.R. Leach, Recombination at double-strand breaks and DNA ends: conserved mechanisms from phage to humans, *Mol. Cell* 8 (2001) 1163–1174.
- [17] M. de Jager, J. van Noort, D.C. van Gent, C. Dekker, R. Kanaar, C. Wyman, Human Rad50/Mre11 is a flexible complex that can tether DNA ends, *Mol. Cell* 8 (2001) 1129–1135.
- [18] L. Chen, K. Trujillo, W. Ramos, P. Sung, A.E. Tomkinson, Promotion of Dnl4-catalyzed DNA end-joining by the Rad50/Mre11/Xrs2 and Hdf1/Hdf2 complexes, *Mol. Cell* 8 (2001) 1105–1115.
- [19] T.T. Paull, M. Gellert, The 3' to 5' exonuclease activity of Mre 11 facilitates repair of DNA double-strand breaks, *Mol. Cell* 1 (1998) 969–979.
- [20] T.T. Paull, M. Gellert, Nbs1 potentiates ATP-driven DNA unwinding and endonuclease cleavage by the Mre11/Rad50 complex, *Genes Dev.* 13 (1999) 1276–1288.
- [21] M. de Jager, C. Wyman, D.C. van Gent, R. Kanaar, DNA end-binding specificity of human Rad50/Mre11 is influenced by ATP, *Nucleic Acids Res.* 30 (2002) 4425–4431.
- [22] S.E. Lee, J.K. Moore, A. Holmes, K. Umez, R.D. Kolodner, J.E. Haber, *Saccharomyces Ku70*, *mre11/rad50* and RPA proteins regulate adaptation to G2/M arrest after DNA damage, *Cell* 94 (1998) 399–409.
- [23] P. Sung, L. Krejci, S. Van Komen, M.G. Sehorn, Rad51 recombinase and recombination mediators, *J. Biol. Chem.* 278 (2003) 42729–42732.
- [24] T. Sugiyama, S.C. Kowalczykowski, Rad52 protein associates with replication protein A (RPA)-single-stranded DNA to accelerate Rad51-mediated displacement of RPA and presynaptic complex formation, *J. Biol. Chem.* 277 (2002) 31663–31672.
- [25] P. Baumann, S.C. West, Role of the human RAD51 protein in homologous recombination and double-stranded-break repair, *Trends Biochem. Sci.* 23 (1998) 247–251.
- [26] T.L. Tan, R. Kanaar, C. Wyman, Rad54, a Jack of all trades in homologous recombination, *DNA Repair (Amst)* 2 (2003) 787–794.
- [27] A. Alexeev, A. Mazin, S.C. Kowalczykowski, Rad54 protein possesses chromatin-remodeling activity stimulated by the Rad51–ssDNA nucleoprotein filament, *Nat. Struct. Biol.* 10 (2003) 182–186.
- [28] V. Alexiadis, J.T. Kadonaga, Strand pairing by Rad54 and Rad51 is enhanced by chromatin, *Genes Dev.* 16 (2002) 2767–2771.
- [29] M. Jaskelioff, S. Van Komen, J.E. Krebs, P. Sung, C.L. Peterson, Rad54p is a chromatin remodeling enzyme required for heteroduplex DNA joint formation with chromatin, *J. Biol. Chem.* 278 (2003) 9212–9218.
- [30] A. Constantinou, A.A. Davies, S.C. West, Branch migration and Holliday junction resolution catalyzed by activities from mammalian cells, *Cell* 104 (2001) 259–268.
- [31] A. Constantinou, X.B. Chen, C.H. McGowan, S.C. West, Holliday junction resolution in human cells: two junction endonucleases with distinct substrate specificities, *Embo J.* 21 (2002) 5577–5585.
- [32] Y. Liu, J.Y. Masson, R. Shah, P. O'Regan, S.C. West, RAD51C is required for Holliday junction processing in mammalian cells, *Science* 303 (2004) 243–246.
- [33] J.Y. Masson, M.C. Tarsounas, A.Z. Stasiak, A. Stasiak, R. Shah, M.J. McIlwraith, F.E. Benson, S.C. West, Identification and purification of two distinct complexes containing the five RAD51 paralogs, *Genes Dev.* 15 (2001) 3296–3307.

- [34] W.D. Heyer, K.T. Ehmsen, J.A. Solinger, Holliday junctions in the eukaryotic nucleus: resolution in sight? *Trends Biochem. Sci.* 28 (2003) 548–557.
- [35] F. Osman, J. Dixon, C.L. Doe, M.C. Whitby, Generating crossovers by resolution of nicked Holliday junctions: a role for Mus81–Eme1 in meiosis, *Mol. Cell* 12 (2003) 761–774.
- [36] B. Wolner, S. van Komen, P. Sung, C.L. Peterson, Recruitment of the recombinational repair machinery to a DNA double-strand break in yeast, *Mol. Cell* 12 (2003) 221–232.
- [37] N. Sugawara, X. Wang, J.E. Haber, In vivo roles of Rad52, Rad54, and Rad55 proteins in Rad51-mediated recombination, *Mol. Cell* 12 (2003) 209–219.
- [38] M. Lisby, U.H. Mortensen, R. Rothstein, Colocalization of multiple DNA double-strand breaks at a single Rad52 repair centre, *Nat. Cell Biol.* 5 (2003) 572–577.
- [39] J.A. Aten, J. Stap, P.M. Krawczyk, C.H. van Oven, R.A. Hoebe, J. Essers, R. Kanaar, Dynamics of DNA double-strand breaks revealed by clustering of damaged chromosome domains, *Science* 303 (2004) 92–95.
- [40] J. Essers, A.B. Houtsmuller, L. van Veelen, C. Paulusma, A.L. Nigg, A. Pastink, W. Vermeulen, J.H. Hoeijmakers, R. Kanaar, Nuclear dynamics of RAD52 group homologous recombination proteins in response to DNA damage, *EMBO J.* 21 (2002) 2030–2037.
- [41] D.S. Yu, E. Sonoda, S. Takeda, C.L. Huang, L. Pellegrini, T.L. Blundell, A.R. Venkitaraman, Dynamic control of Rad51 recombinase by self-association and interaction with BRCA2, *Mol. Cell* 12 (2003) 1029–1041.
- [42] A. Fujimori, S. Tachiiri, E. Sonoda, L.H. Thompson, P.K. Dhar, M. Hiraoka, S. Takeda, Y. Zhang, M. Reth, M. Takata, Rad52 partially substitutes for the Rad51 paralog XRCC3 in maintaining chromosomal integrity in vertebrate cells, *EMBO J.* 20 (2001) 5513–5520.
- [43] F. Paques, J.E. Haber, Multiple pathways of recombination induced by double-strand breaks in *Saccharomyces cerevisiae*, *Microbiol. Mol. Biol. Rev.* 63 (1999) 349–404.
- [44] T. Miyazaki, D.A. Bressan, M. Shinohara, J.E. Haber, A. Shinohara, In vivo assembly and disassembly of Rad51 and Rad52 complexes during double-strand break repair, *Embo J.* (2004), in press.
- [45] A. Hauptner, S. Dietzel, G.A. Drexler, P. Reichart, R. Krucken, T. Cremer, A.A. Friedl, G. Dollinger, Microirradiation of cells with energetic heavy ions, *Radiat. Environ. Biophys.* 42 (2004) 237–245.

Chapter 4

Rad52 and Ku bind to different DNA structures produced early in double-strand break repair



Rad52 and Ku bind to different DNA structures produced early in double-strand break repair

Dejan Ristic¹, Mauro Modesti¹, Roland Kanaar^{1,2} and Claire Wyman^{1,2,*}

¹Department of Cell Biology and Genetics, Erasmus MC and ²Department of Radiation Oncology, Erasmus MC-Daniel, PO Box 1738, 3000 DR Rotterdam, The Netherlands

Received July 16, 2003; Revised and Accepted July 22, 2003

ABSTRACT

DNA double-strand breaks are repaired by one of two main pathways, non-homologous end joining or homologous recombination. A competition for binding to DNA ends by Ku and Rad52, proteins required for non-homologous end joining and homologous recombination, respectively, has been proposed to determine the choice of repair pathway. In order to test this idea directly, we compared Ku and human Rad52 binding to different DNA substrates. However, we found no evidence that these proteins would compete for binding to the same broken DNA ends. Ku bound preferentially to DNA with free ends. Under the same conditions, Rad52 did not bind preferentially to DNA ends. Using a series of defined substrates we showed that it is single-stranded DNA and not DNA ends that were preferentially bound by Rad52. In addition, Rad52 aggregated DNA, bringing different single-stranded DNAs in close proximity. This activity was independent of the presence of DNA ends and of the ability of the single-stranded sequences to form extensive base pairs. Based on these DNA binding characteristics it is unlikely that Rad52 and Ku compete as 'gatekeepers' of different DNA double-strand break repair pathways. Rather, they interact with different DNA substrates produced early in DNA double-strand break repair.

INTRODUCTION

The toxicity of DNA double-strand breaks in eukaryotic cells is reflected in the multiplicity of pathways to repair them. Double-strand break repair follows one of two general mechanistic routes, non-homologous end joining or homologous recombination (1). These two distinct mechanisms necessarily require distinct sets of proteins. Proteins specifically involved in homologous recombination were originally defined as products of genes belonging to the *RAD52* epistasis group in *Saccharomyces cerevisiae* (2). In human cells these include the homologous gene products: Rad51, Rad52, Rad54, XRCC2, XRCC3, Rad51B, Rad51C, Rad51D, as well as a complex including Rad50, Mre11 and Nbs1. Proteins

specifically involved in non-homologous end joining include the Ku70/80 heterodimer (hereafter referred to as Ku), DNA-PK catalytic subunit (DNA-PKcs) and the XRCC4-ligaseIV complex (3). The complex of Rad50, Mre11 and Xrs2 (the yeast equivalent of Nbs1) also plays a role in non-homologous end joining in *S.cerevisiae* (3,4).

Any double-strand break repair reaction must necessarily begin with recognition of DNA ends. For non-homologous end joining this is likely to be accomplished by Ku. Ku is a structure-specific DNA binding protein. It requires a free end for binding but can then migrate along DNA (5,6). The mechanism of DNA end-binding and inward translocation became clear with the solution of the atomic level structure of Ku. A co-crystal of Ku bound to DNA revealed that the protein forms a ring with DNA passing through it (7). Biochemical analysis suggests that DNA end-binding by Ku initiates a cascade of molecular events that leads to joining of the broken DNA ends. In this scenario, DNA-PKcs joins an end-bound Ku (8,9) which then leads to synapsis of the DNA ends (10). After processing to produce ligatable ends, if necessary, the XRCC4-ligaseIV complex completes the repair of the break (11).

A DNA end that will eventually be repaired by homologous recombination must be specifically processed to expose a single-stranded 3' overhang. It is not clear if this end processing is the first step of homologous recombination repair or if some homologous recombination-specific protein first binds an unprocessed DNA end. Homologous recombination proteins that have been described to bind DNA ends include the Rad50-Mre11 complex and Rad52. The Rad50-Mre11 complex can bind to linear and circular DNA but assembles large oligomers only on linear DNA (12). The formation of Rad50-Mre11 oligomers on DNA with different end structures is modulated by ATP binding. ATP binding increases the preference for Rad50-Mre11 oligomer formation on DNA with 3' overhangs (13). Rad50-Mre11 oligomers can tether DNA molecules and this could function at an early stage in double-strand break repair, perhaps a stage common to both non-homologous end joining and homologous recombination, to keep ends in close proximity for further processing (12).

Rad52 can also bind DNA ends; however, the importance of Rad52 to double-strand break repair goes beyond initial DNA end binding. *In vitro*, Rad52 has been shown to bind to both single-stranded and double-stranded DNA (14). Rad52 interacts with both RPA and Rad51, proteins also required for

homologous recombination. Due to these interactions, Rad52 is described as a mediator in the formation of Rad51-directed formation of joint molecules between the broken DNA end and the double-stranded template DNA (15–19). Rad52 aggregates DNA and promotes annealing of complementary single strands (20). The full-length human protein forms heptameric rings alone and when bound to DNA (14,21). The DNA binding domain of Rad52 crystallized as an undecameric ring and its atomic level structure was solved (22,23). Single-stranded DNA modeled onto the undecameric ring structure has the bases exposed and available for pairing (23). The precise register with which some single-stranded DNA substrates bind to Rad52 and Rad52 protection of DNA ends from nuclease digestion have been interpreted to indicate a specific mechanistic role for Rad52 in double-strand break repair that requires its binding to DNA ends (24,25). This has led to the prominent proposal that Rad52 is the ‘gatekeeper’ of homologous recombination (25,26). In this model, the binding of Rad52 to DNA ends precludes non-homologous end joining and begins a cascade of events culminating in repair by homologous recombination.

A competition between Ku and Rad52 for DNA end binding has been suggested to provide a mechanistic switching point between repair by non-homologous end joining and homologous recombination (25,26). We wanted to test the interesting prediction that Ku and Rad52 compete for binding to DNA ends. The binding of Ku to DNA and the binding of Rad52 to DNA have been described using a variety of techniques but not directly compared with any of them. Notably, many Rad52–DNA binding studies are done *in vitro* in conditions with relatively low concentrations of monovalent cations and lacking magnesium ions (14,24,25,27). These factors can have a dramatic effect of DNA–protein interactions and these conditions are very different from those used in Ku–DNA binding studies. In order to understand the relative DNA binding properties of these two proteins, Ku and Rad52, we have compared their interactions with a variety of DNA substrates under the same conditions. Using scanning force microscopy (SFM; also called atomic force microscopy) to visualize DNA–protein complexes we could simultaneously determine the percentage of DNA bound by protein and the position at which the protein was bound. In this way we could define DNA features preferentially bound by Rad52 and Ku, showing that these proteins bind to different DNA structures and do not compete for binding to similar structures.

MATERIALS AND METHODS

DNA substrates

Plasmid pDERI1, used in this study, is a 1821 bp derivative of pUC19 (28). Substrates with blunt ends and short 5′ or 3′ overhangs were made by linearization of pDERI1 with ScaI, BsaI or PvuI digestion, respectively. Singly nicked plasmid was obtained by digesting supercoiled pDERI1 (17 µg/ml) with DNase I (1 µg/ml) in a 30 µl reaction mixture containing 20 mM Tris–HCl (pH 7.5), 50 mM NaCl, 10 mM MgCl₂ and 360 µg/ml ethidium bromide. The reaction was carried out at 30°C for 30 min and stopped by the addition of a 0.1 vol of stop solution containing 5% (w/v) SDS, 50 mM EDTA, 30 µg/ml proteinase K and incubation at 65°C for 30 min.

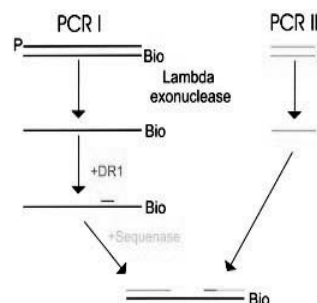


Figure 1. Schematic representation of the steps in synthesis of the DNA substrate with an internal single-stranded gap. The 810 bp PCR I DNA, shown in black at the left, formed the basis for building up the complete product. It was first digested with lambda exonuclease III to produce the bottom strand, to which oligo DR1, red, was hybridized and used as a primer for synthesis of double-stranded DNA, blue, toward one end. The 313 bp PCR II DNA, shown in green at the right, was identical in sequence to the first 313 bp of PCR I but has a 5′ phosphate on the opposite strand as PCR I. Digestion of PCR II with lambda exonuclease left a 313 nt single-stranded DNA complementary to the PCR I bottom strand. Upon annealing, this resulted in the final product with blunt ends and an internal 200 nt single-stranded gap.

DNA was purified by extraction with phenol and phenol/chloroform (1:1, v/v), precipitated with ethanol and dissolved in H₂O (glass-distilled; Sigma).

Relaxed covalently closed DNA was prepared by treatment of plasmid pDERI1 with calf-thymus topoisomerase I (Amersham). Reaction mixtures of 30 µl contained 1 µg of DNA, 35 mM Tris–HCl (pH 8.0), 72 mM KCl, 5 mM MgCl₂, 5 mM DTT, 5 mM spermidine, 0.01% bovine serum albumin and 1.5 U topoisomerase I and were incubated at 37°C for 1 h. The reaction was stopped by the addition of 0.1 vol of stop solution containing 5% (w/v) SDS, 50 mM EDTA, 30 µg/ml proteinase K and incubated at 65°C for 30 min. After extraction with phenol and phenol/chloroform, DNA was purified over a GFX™ column (Amersham).

Substrates with a long 5′ overhang were produced as follows: plasmid pDERI1 was cut with XmnI and treated with a pre-determined saturating amount of *Escherichia coli* exonuclease III (10 U/µg DNA) for 20 min at 20°C in a 75 µl reaction mixture containing 66 mM Tris–HCl (pH 8.0) and 0.66 mM MgCl₂ (44 µg of DNA, 440 U exoIII). Exonuclease treatment produced 5′ single-stranded tails with an average length of 200 nt as determined by measuring the contour length of the remaining double-stranded DNA from SFM images. Subsequent digestion of DNA with long 5′ tails with AlwNI produced a substrate with a long 5′ tail at one end and a short restriction site overhang at the other end (6 nt 3′).

Linear DNA with a gap was made as follows (see schematic outline in Fig. 1): using the *URA3* gene from *S.cerevisiae* as template DNA, an 810 bp PCR fragment was produced using primer U3 which was 5′ phosphorylated (GAAGGAAGAAGAAGGAAGGAGC) and primer Bio 5′ which was 5′ biotinylated (TTTCCCGGGGGGCCCGGGTCTACTGTTGACCC). The PCR product was purified on a GFX™ column (Amersham). The DNA strand with a 5′-phosphate was digested by λ exonuclease (5 U/µg DNA). The reaction was carried out at 37°C for 1 h and stopped by heat

inactivation (95°C for 10 min). The resulting single-stranded DNA was dialyzed against TE buffer and hybridized with oligonucleotide primer DR1 (AGCGGTTTGAAGCAGG-CGGCGG anneals to position 526–548 of the PCR I bottom strand, see Fig. 1). Primer DR1 was extended for 30 min at 37°C in a reaction containing Sequenase™ DNA polymerase Version 2.0 (Amersham), 40 mM Tris-HCl pH 7.5, 20 mM MgCl₂, 200 μM dNTPs and 50 mM NaCl. The partially double-stranded linear DNA produced with a long 3′ overhang was purified on a GFX™ column. A second PCR fragment of 313 bp, identical to the part of the 810 bp fragment described above, was produced using primer U3 (GAAGGAAGAAGGAAGGAGC) and primer B313 which was 5′ phosphorylated (TTTGTAGTAAACAAATTTGGGACC). The PCR product was purified on a GFX™ column, before incubation with λ exonuclease (5 U/μg DNA) as described above, in order to digest the phosphorylated strand. The resulting single-stranded DNA was hybridized with partially double-stranded 810 nt long linear DNA with a long 3′ overhang produced as described above. The resulting linear DNA, with a 213 nt gap between 313 and 283 bp of double-stranded DNA with blunt ends, was resolved on a 2% agarose gel and purified from gel with a GFX™ column.

Proteins and DNA-binding reactions

Ku70/80 (Ku80, Ku70-his tag) was produced in baculovirus-infected Sf21 cells and purified as described (29). The human Rad52 protein was produced in *E. coli* FB810 carrying pET28a-hRad52 (30) and purified as described (16), with the following modification: a Ni²⁺-NTA agarose column (Qiagen) was used for the first purification step, followed by a MonoQ column (Pharmacia). Protein purity was checked by SDS-PAGE and peak fractions with Rad52 were stored at –80°C.

Complexes of proteins and DNA were prepared in reaction mixtures (10 μl final volume) containing 24 μM DNA (concentration of nucleotides), 90 nM protein, 20 mM HEPES-KOH (pH 7.4), 30 mM KCl, 1 mM DTT and, if present, 10 mM MgCl₂. Reactions were carried out at 37°C for 15 min and then placed on ice. For SFM imaging, reaction mixtures were diluted 15–30 times in deposition buffer (5 mM HEPES-KOH pH 7.8, 5 mM MgCl₂) and deposited on freshly cleaved mica. After 30 s, the mica was rinsed with H₂O (glass distilled; Sigma) and dried with a stream of filtrated air. Images were obtained on a NanoScope IIIa or NanoScope IV (Digital Instruments; Santa Barbara, CA) operating in tapping mode in air with a type E scanner using silicon Nanotip cantilevers (Nanoprobe).

RESULTS

In order to compare Ku and Rad52 binding to different features of DNA we constructed a variety of defined substrates with the same sequence and length but different structure (shown schematically in Fig. 2). Linear DNA, 1.8 kb in length, with either blunt ends or short 3′ or 5′ single-stranded overhang ends was produced by restriction digestion of plasmid pDERI1. DNA with long 5′ single-stranded overhangs was produced from the same plasmid by digestion with a restriction enzyme followed by limited digestion with *E. coli* exonuclease III. Relaxed covalently closed circular and singly

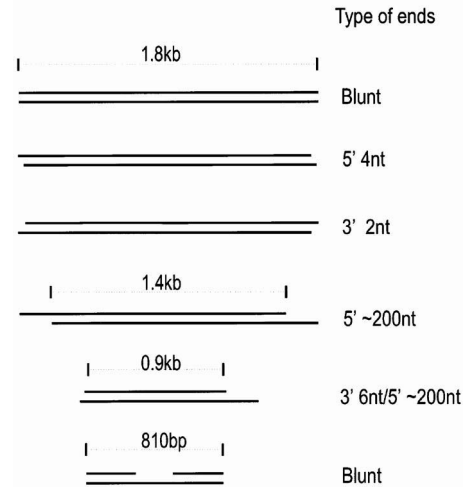


Figure 2. Diagram of the DNA substrates used in this study. The length as well as type of ends for each DNA is indicated. All but the substrate with the internal 213 nt gap were derived from 1.8 kb plasmid pDERI1. The substrate with the internal 213 nt gap was derived from the *S.cerevisiae* URA3 gene.

nicked circular forms of plasmid pDERI1 were also produced. A substrate with a defined central single-stranded gap, whose sequence is not the same as plasmid pDERI1, was also produced. Binding reactions with Ku and Rad52 were performed under the same conditions with respect to buffer components and molar amounts of protein and DNA. Importantly, the binding reactions analyzed by SFM did not contain a vast molar excess of protein as is common in binding reactions analyzed by biochemical methods. The DNA concentration was chosen to result in deposition of a sufficient density of molecules for convenient analysis. The concentration of protein was kept to a slight molar excess over DNA fragments in order to visualize complexes without prior purification away from free protein. All of the DNA-protein binding reactions were done with DNA concentrations of 24 μM with respect to nucleotides and protein concentrations of 90 nM Rad52 monomers or Ku70/80 heterodimers. This is equivalent to an ~14-fold molar excess of protein over DNA molecules for the 1.8 kb substrates and an ~6-fold molar excess of protein over DNA molecules for the 810 bp gapped substrate.

From the SFM images we determined the percentage of DNA molecules bound by protein for each of the different DNA substrates. The results for the 1.8 kb pDERI1-derived DNA substrates are summarized in Table 1. These DNA substrates had either no ends or interruptions, a single nick, blunt ends, short single-stranded overhang ends or long single-stranded ends. Rad52 binding reactions were done in two different conditions, one without magnesium ions for comparison with the most previous published studies and one with the same buffer, including magnesium ions, used for Ku-DNA binding (see Materials and Methods for details). As expected, Ku showed preferential binding to linear DNA with a similar percentage of linear DNA bound by Ku, 28–37% of DNA bound by protein, independent of the DNA end structure.

Table 1. Percentage of different DNA substrates bound by protein

DNA substrate	Ku	Rad52 – Mg ²⁺	Rad52 + Mg ²⁺
Linear blunt	28.5 (1180)	26.7 (409)	8.9 (190)
Linear 2 nt 3'	27.7 (1014)	48.5 (330)	19.8 (304)
Linear 4 nt 5'	34.0 (113)	24.4 (522)	17.4 (172)
Linear 200 nt 5'	36.6 (175)	25.7 (678)	18.5 (427)
Circle relaxed	8.8 (512)	29.6 (412)	12.5 (331)
Circle nicked	6.7 (430)	24.0 (58)	16.7 (102)

The percentage of DNA molecules bound by protein is listed for each reaction. The number in parenthesis is the total number of DNA molecules counted. Binding reactions with Rad52 were done in buffers without or with magnesium ions. The number of molecules counted was pooled from several independent experiments. No significant inter-experiment differences were noted.

Much less of the circular DNA, 7–9%, was bound by Ku. In contrast, Rad52 bound a similar percentage of all DNA substrates irrespective of the presence of an end. There was an ~2-fold preference for binding to DNA with a short 3' single-stranded overhang (see Discussion). When Rad52 binding

reactions were done in the same buffer used for Ku binding reactions, which most notably differed in the presence of magnesium ions, the percentage of protein-bound DNA dropped for all substrates. Again, under these conditions there was no evidence for Rad52 preferentially binding to DNA substrates with ends. The percentage of DNA bound by protein was even a bit higher for circular DNA than for some of the linear substrates. There were, however, distinct qualitative differences in the protein–DNA complexes formed by Rad52 on the different DNA substrates. Rad52 is presumed to function as a large DNA-bound oligomer. Notably, large DNA-bound Rad52 oligomers only formed on the DNA with a long single-stranded end (Fig. 3A). Rad52 bound to all other DNA substrates as small complexes, presumably monomeric in size (Fig. 3B).

For all binding reactions with linear DNA, the position of the DNA-bound proteins was also analyzed. The percentage of protein located at an end or at an internal position for the various substrates is summarized in Table 2. As is well known from other studies, Ku requires an end for DNA association but does not remain bound to ends. Here also we observed

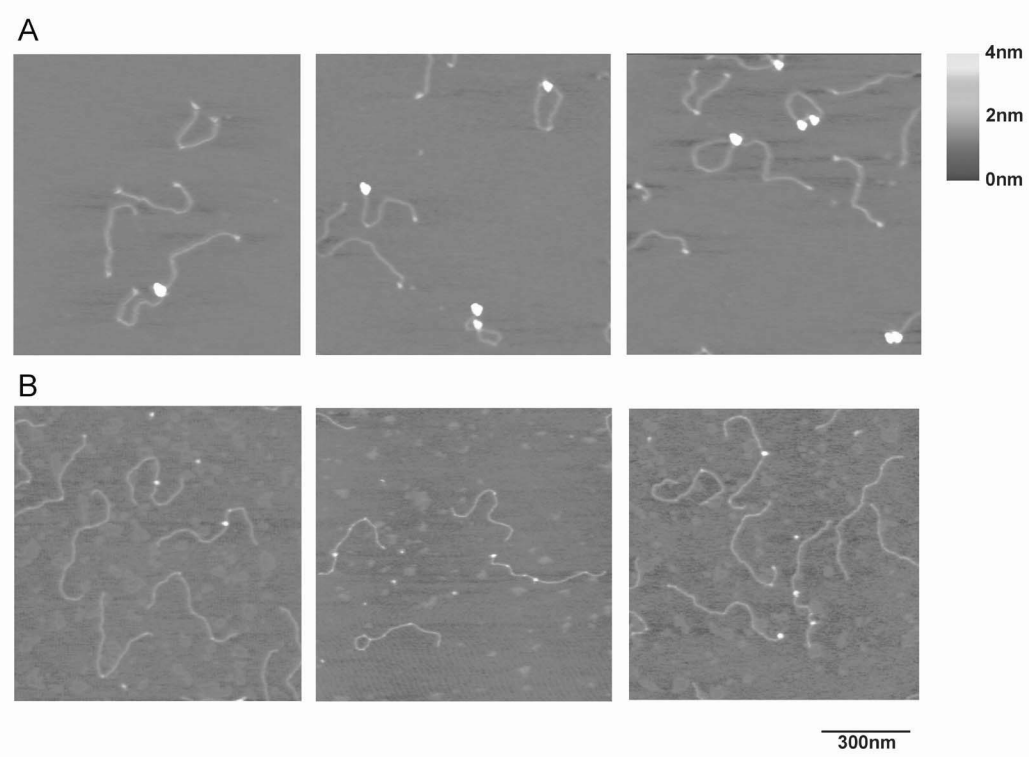


Figure 3. Human Rad52 forms large oligomers on long single-stranded DNA. (A) SFM images showing large Rad52 complexes formed in binding reactions including DNA with long single-stranded ends. The long single-stranded DNA ends not bound by protein appear as a small knob at the end of the substrate. (B) SFM images showing small Rad52 complexes formed in binding reactions including DNA with blunt ends (left), short 5' overhang ends (middle) and short 3' overhang ends (right). The scale bar indicates 300 nm in the X and Y dimensions and height is represented by color as shown by the bar at the right.

Table 2. Percentage of DNA–protein complexes with protein bound at an end

DNA substrate	Ku	Rad52 – Mg ²⁺	Rad52 + Mg ²⁺
Linear blunt	6.0 (336)	18.2 (109)	5.9 (17)
Linear 2 nt 3′	11.0 (281)	24.8 (160)	28.3 (60)
Linear 4 nt 5′	14.3 (38)	29.0 (127)	26.7 (30)
Linear 200 nt 5′	88.2 (64)	100.0 (174)	100.0 (79)

The percentage of DNA–protein complexes that have protein bound to an end is listed for each binding reaction. Data is from the same experiments as presented in Table 1. The total number of DNA–protein complexes for each data point is given in parenthesis.

only 6–14% of DNA-bound protein present at an end if it was blunt or a short single-stranded overhang. There was no difference in the size or structure of Ku located at DNA ends or at internal positions. The observation that most of the DNA-bound Ku remained at an end on the substrate with long single-stranded overhangs was at least in part due to the appearance of single-stranded DNA in these SFM experiments. Presumably due to irregular secondary structure and a very short persistence length, the single-stranded DNA appeared as a small knob at the end of the remaining double-stranded segment (e.g. see the protein-free DNA ends in Fig. 3A and protein-free DNA with a single-stranded gap in Fig. 5B). Thus, protein bound to any position along the single-stranded DNA appeared to be at an end of the double-stranded DNA segment. It is also possible that translocation of Ku along single-stranded DNA is inhibited by irregular DNA secondary structure.

DNA-bound Rad52 had no general preference for an end position on DNA with blunt or short single-stranded DNA ends, either in the presence or absence of magnesium ions (Table 2). In the presence of magnesium ions, ~20–30% of the protein–DNA complexes had Rad52 bound to a DNA end. However, if a long single-strand overhang was available, all of the Rad52 was found bound to the DNA ends. As mentioned above, the Rad52 structures on the long single-stranded DNA ends were also very different from those bound to double-stranded DNA. All of the Rad52 bound to long single-stranded DNA was in the form of large oligomers (Fig. 3A). Direct competition experiments were also done in which either Ku or Rad52 was combined with a mixture of DNA substrates; nicked circular, linear blunt-ended and linear with one long single-stranded end (Fig. 4). When presented with this choice of DNA substrates, the results were similar to those obtained with the DNA substrates used one at a time (Table 3). Ku was bound almost exclusively to the linear DNA substrates with more protein remaining at an end on the DNA with a long single-stranded overhang. Rad52 was found exclusively on the DNA with a long single-stranded end in large oligomeric complexes.

We wished to determine which feature of the DNA structure was most important for Rad52 binding, the molecular end or the single-stranded nature. For this purpose, we produced DNA substrates with different combinations of end structures and single-stranded regions. These substrates had either two blunt ends and an internal single-stranded gap or one end with a 6 nt single-stranded overhang and one end with a long, ~200 nt, single-stranded overhang (Fig. 5). Binding reactions

with Ku or Rad52 were performed in the same buffer conditions, those including magnesium ions, and the location of the bound protein on the DNA determined. These results, presented as the percentage of DNA–protein complexes with protein bound at different locations, single-stranded or double-stranded regions at an end or internal position, are summarized in Table 4. Here also, Rad52 was bound exclusively to the single-stranded region, independent of the presence of a DNA end. As expected, most of the Ku had migrated to internal positions on the DNA. Again, an increased percentage of Ku was found at the single-stranded end, which may indicate that Ku is less able to translocate over long stretches of single-stranded DNA.

Rad52 has been described to have a single-stranded DNA annealing activity (20), it promotes the annealing of complementary DNAs and large Rad52 complexes have been visualized joining DNAs with long single-stranded regions (27). We also observed multiple DNA molecules joined within large Rad52 protein complexes; 42% of the protein-bound DNA with long single-stranded ends was in complexes including more than one DNA molecule (Fig. 5A). In some cases, the protein complexes joining two or more DNA molecules were obviously larger than those formed on a single DNA molecule (e.g. see Figs 3A and 5B). However, from these images we cannot determine if multiple DNAs were captured by a Rad52 oligomer or if Rad52 oligomers bound to different DNAs aggregated. In either case, single-stranded DNAs were brought into close proximity, which would presumably favor base pairing if that were possible. In our experiments, the different single-stranded DNA molecules to which Rad52 bound were identical and not complementary, demonstrating that extensive base-pairing interactions are not important for Rad52-induced DNA aggregation. Importantly, DNA ends were not required as Rad52-induced DNA aggregation was observed with a similar frequency with the internally gapped substrate, 30% of the protein-bound DNA was in complexes including more than one DNA molecule (Fig. 5B).

DISCUSSION

We have directly compared the ability of Ku and Rad52 to bind to DNA substrates with different end structures. Instead of a comparable binding preference for the same DNA structures, which would be required if these proteins compete in binding to broken DNA ends, we observe that Ku and Rad52 preferentially bound to different DNA structures. As expected, Ku bound to DNA with a free end. Rad52, however, had no apparent preference for binding to DNA ends above internal double-stranded positions on DNA. Rad52 did preferentially bind to single-stranded DNA and notably formed large oligomers on long single-stranded DNA independent of end or internal location on DNA fragments. We did not attempt mixing both proteins with a given DNA substrate. In SFM images, objects are distinguished by their size and shape. We would expect Rad52 monomers to appear smaller than a Ku heterodimer. However, Rad52 is known to form multimers, which would likely be larger than Ku. Based on size alone, it would be impossible to determine if a DNA-bound complex consisted of Rad52 multimers or a combination of Rad52 and Ku. However, because we did not observe

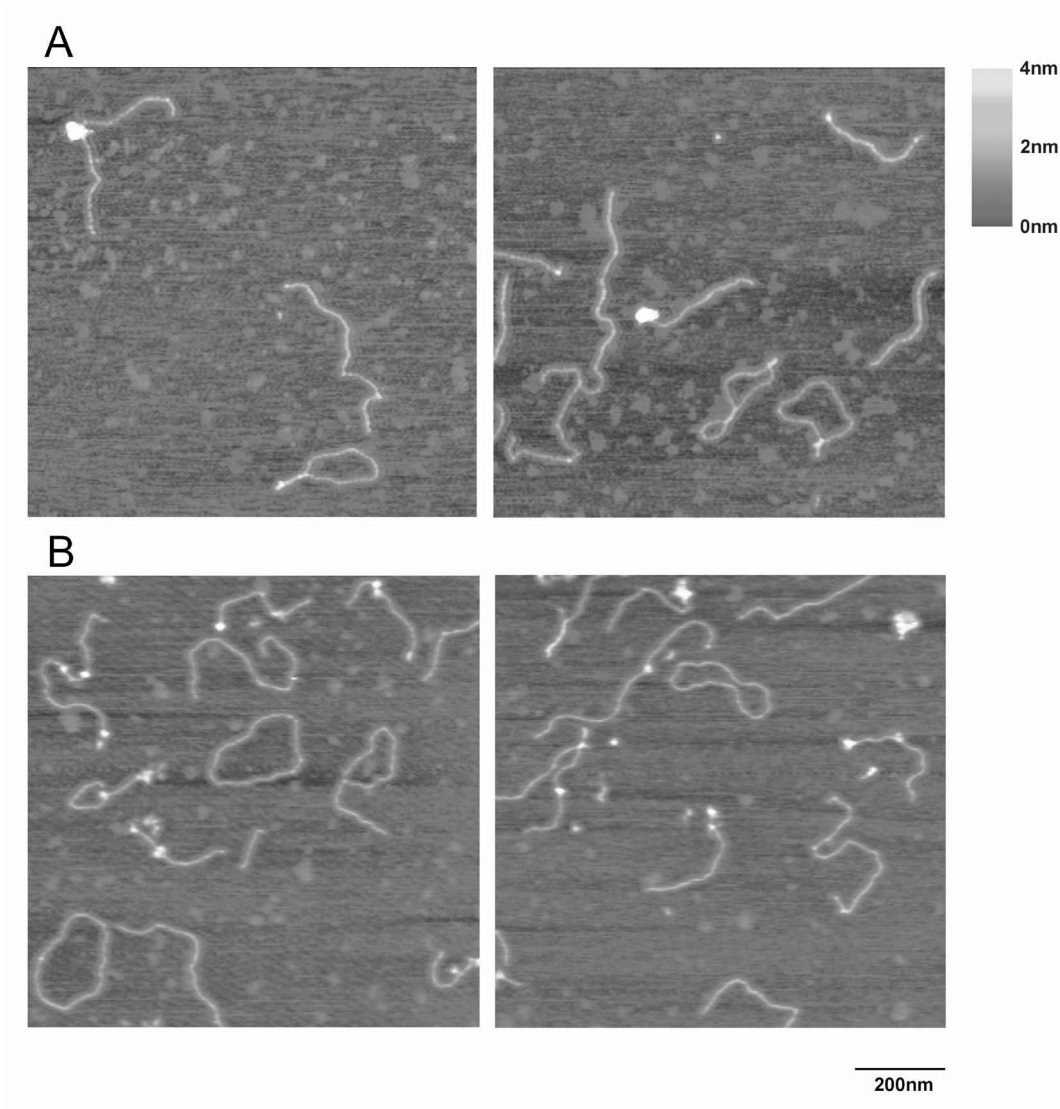


Figure 4. Competition for binding to a mixture of DNA substrates by human Rad52 or Ku. (A) SFM images from binding reactions including Rad52 and a mixture of 1.8 kb nicked circular DNA, 1.8 kb linear blunt-ended DNA and 0.9 kb DNA with a 200 nt single-stranded end. Rad52 bound exclusively to the long single-stranded DNA as large oligomers. (B) SFM images from binding reactions including Ku and the same mixture of DNA substrates as in (A). Ku bound almost exclusively to the linear DNA substrates independent of the end structure. The scale bar indicates 200 nm in the *X* and *Y* dimensions and height is represented by color as shown by the bar at the right.

any preference for Rad52 binding to DNA ends in the absence of Ku, any observable change in Rad52 binding to DNA ends would likely be positive, indicating cooperative activity rather than competition.

Given the binding characteristics we have observed it seems highly unlikely that there is a competition between Ku and Rad52 for binding to the same broken DNA. Thus, these two

proteins probably do not function as a molecular switching point between the non-homologous end joining and the homologous recombination repair pathways. Ku associates with DNA via ends and Rad52 associates with single-stranded DNA. The choice of double-strand break repair via either non-homologous end joining or homologous recombination may in part be determined by the structure of the end at a DNA break.

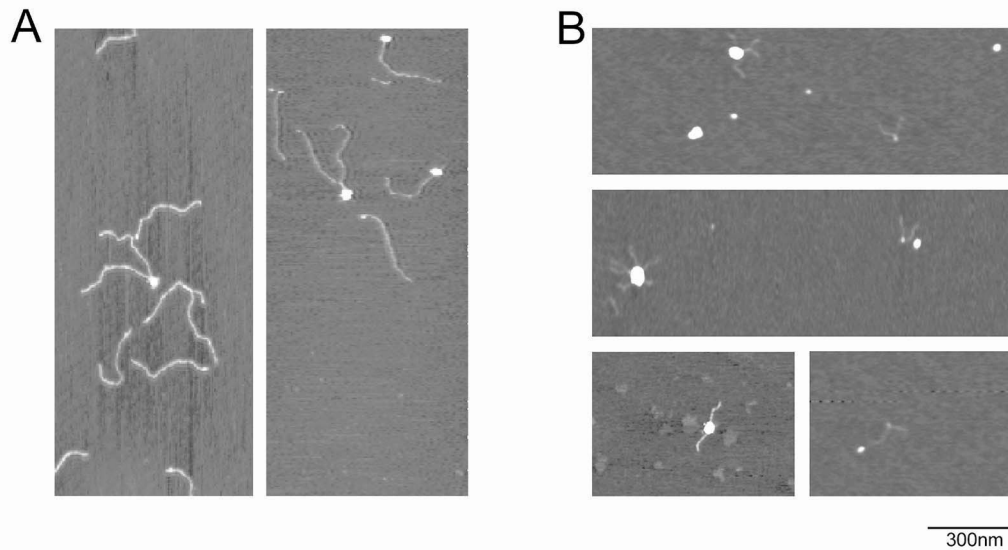


Figure 5. Human Rad52 complexes often aggregate single-stranded DNA. (A) SFM images from binding reactions including Rad52 and DNA with one long single-stranded end. Large Rad52 oligomers form on the single-stranded end of the DNA and often aggregate more than one DNA molecule. (B) SFM images from binding reactions including Rad52 and DNA with a central single-stranded gap. Large Rad52 oligomers form on the central single-stranded region of this DNA and often aggregate more than one DNA molecule. The scale bar indicates 300 nm in the *X* and *Y* dimensions, height ranges from 0 to 4 nm and is represented by color (red to yellow as in the scale bars of Figs 3 and 4).

Table 3. Competition between different DNA substrate for binding Rad52 or Ku

DNA substrate	Percentage of complexes formed on different DNA substrates	
	Rad52	Ku
Linear blunt	0 (0/94, 736)	61 (146/240, 395)
Linear 200 nt 5'	100 (94/94, 276)	39 (93/240, 259)
Circle nicked	0 (0/94, 146)	0.4 (1/240, 74)

The percentage of protein–DNA complexes on the different DNA substrates is listed. In parenthesis is the number of DNA–protein complexes on the given substrate over the total number of DNA–protein complexes, and the total number of DNA molecules counted for each substrate.

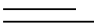

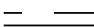

For instance, two DNA ends produced by breaking a chromosome can be effectively joined by non-homologous end joining. However, end joining would be impossible, and homologous recombination would be required, for repairing single DNA ends that occur when DNA damage is encountered during replication (31). Factors, such as the point in the cell cycle at which a DNA break occurs and the availability of a homologous partner for repair, are also likely to influence the choice of pathway used for repair of a double-strand break (32).

The preference for binding to long stretches of single-stranded DNA by Rad52 suggests that nucleolytic processing to form long single-stranded regions at a DNA break precedes Rad52 binding in the homologous recombination mechanism.

The Rad52 monomers that bind to short single-stranded DNA ends may also be mechanistically important, though most models of Rad52 function involve large DNA-bound oligomers (19,24,26,33). It is interesting to note that the only DNA end that was preferentially bound by human Rad52 in our experiments was a short 3' overhang, though this preference is diminished in binding reactions including magnesium ions. One striking feature of Rad52 binding to single-stranded DNA is the apparent specific phasing with respect to the end of some substrates (24). This would require a specific interaction at an end to initiate the phasing for which our results with short 3' overhangs may provide some evidence. The preference for binding to a 3' end is also interesting because double-strand break repair by homologous recombination requires joint molecule formation by a single-stranded DNA with a 3' overhang. The preferential binding of Rad52 to 3' ends provides an intriguing entry point for further analysis of the role of this protein in homologous recombination.

The *in vitro* activities described for Rad52 can be accommodated in at least two mechanistic pathways of homology-dependent DNA repair, homologous recombination and single-strand annealing. The Rad52-mediated aggregation of single-stranded DNA that we observed here, and previously described by others (25,27), is obviously consistent with a role in single-strand annealing. However, because the aggregation of single-stranded DNA did not require either complementary sequences or DNA ends, the relevance of *in vitro* annealing to *in vivo* repair mechanisms remains to be proven. The importance of Rad52 for homologous recombination is

Table 4. Location of protein bound to DNA with a terminal or central single-stranded region

Protein	Schematic of substrates	Single-stranded end	Blunt end	Single-stranded internal	Double-stranded internal
Ku		25	5	NA	70
Rad52		100	0	NA	0
Ku		NA	10.4	19.8 (+22.8) ^a	47 (+22.8) ^a
Rad52		NA	0	100	0

The percentage of DNA-protein complexes with protein located at the indicated position is listed for each binding reaction. All binding reactions were done in the presence of magnesium ions. The gapped DNA has a 213 nt single-stranded region between 283 and 313 bp of duplex DNA. Of this DNA substrate, 31.3% was bound by protein in a reaction containing Ku. Of the gapped substrate, 19.1% was bound by protein in a reaction containing Rad52. NA, not applicable.

^aOf the DNA bound by Ku, 22.8% had protein at multiple sites, both single-stranded internal and double-stranded internal positions.

underscored by its interactions with several proteins involved in the process. *In vitro*, a careful balance between RPA, Rad51 and Rad52 is needed for optimal joint molecule formation (15,17,33,34). We expect that direct imaging experiments will help elucidate the way Rad52, RPA and Rad51 act together with DNA to eventually produce Rad51 filaments active in joint molecule formation.

We often observed single-stranded DNAs joined by Rad52 oligomers. In some cases the size of the protein complexes aggregating DNA appeared larger than those formed on a single DNA molecule [e.g. Fig. 5B and examples in Van Dyck *et al.* (27)] implying that aggregation occurred via interaction of multiple DNA-bound Rad52 complexes. However, in other cases the DNA was aggregated by Rad52 complexes that were no larger than those formed on single DNA molecules (e.g. Fig. 5A). This raises the possibility that additional DNA molecules could be captured by a DNA-bound Rad52 oligomer. The model of DNA bound to a Rad52 oligomer based on the atomic level structure places the DNA in a large groove encircling the complex (23). The proposed DNA binding groove is an iteration of identical DNA binding domains of Rad52 monomers and does not *a priori* require complete occupancy by a single DNA. The possibility that multiple DNA molecules could bind to a Rad52 oligomer suggests a function in keeping different DNA molecules in close proximity, to favor annealing of complementary sequences if present. In addition, this may allow for dynamic rearrangement of the single-stranded DNAs if they can exchange positions among the identical binding sites of the complex. Describing the dynamic interactions between Rad52 and single-stranded DNA will be essential to understanding the mechanistic role of this protein in DNA double-strand break repair.

ACKNOWLEDGEMENTS

We thank Cecile Beerens for assistance in protein purification. This study was supported by grants from The Netherlands Organization for Scientific Research (NWO), The Dutch Cancer Society (KWF) and the Association for International Cancer Research (AICR).

REFERENCES

1. Kanaar, R., Hoeijmakers, J.H. and van Gent, D.C. (1998) Molecular mechanisms of DNA double strand break repair. *Trends Cell Biol.*, **8**, 483–489.
2. Symington, L.S. (2002) Role of RAD52 epistasis group genes in homologous recombination and double-strand break repair. *Microbiol. Mol. Biol. Rev.*, **66**, 630–670.
3. Critchlow, S.E. and Jackson, S.P. (1998) DNA end-joining: from yeast to man. *Trends Biochem. Sci.*, **23**, 394–398.
4. D'Amours, D. and Jackson, S.P. (2002) The Mre11 complex: at the crossroads of DNA repair and checkpoint signalling. *Nature Rev. Mol. Cell Biol.*, **3**, 317–327.
5. de Vries, E., van Driel, W., Bergsma, W.G., Arnberg, A.C. and van der Vliet, P.C. (1989) HeLa nuclear protein recognizing DNA termini and translocating on DNA forming a regular DNA-multimeric protein complex. *J. Mol. Biol.*, **208**, 65–78.
6. Paillard, S. and Strauss, F. (1991) Analysis of the mechanism of interaction of simian Ku protein with DNA. *Nucleic Acids Res.*, **19**, 5619–5624.
7. Walker, J.R., Corpina, R.A. and Goldberg, J. (2001) Structure of the Ku heterodimer bound to DNA and its implications for double-strand break repair. *Nature*, **412**, 607–614.
8. Dynan, W.S. and Yoo, S. (1998) Interaction of Ku protein and DNA-dependent protein kinase catalytic subunit with nucleic acids. *Nucleic Acids Res.*, **26**, 1551–1559.
9. Lieber, M.R. (1999) The biochemistry and biological significance of nonhomologous DNA end joining: an essential repair process in multicellular eukaryotes. *Genes Cells*, **4**, 77–85.
10. DeFazio, L.G., Stansel, R.M., Griffith, J.D. and Chu, G. (2002) Synapsis of DNA ends by DNA-dependent protein kinase. *EMBO J.*, **21**, 3192–3200.
11. Jones, J.M., Gellert, M. and Yang, W. (2001) A Ku bridge over broken DNA. *Structure*, **9**, 881–884.
12. de Jager, M., van Noort, J., van Gent, D.C., Dekker, C., Kanaar, R. and Wyman, C. (2001) Human Rad50/Mre11 is a flexible complex that can tether DNA ends. *Mol. Cell*, **8**, 1129–1135.
13. de Jager, M., Wyman, C., van Gent, D.C. and Kanaar, R. (2002) DNA end-binding specificity of human Rad50/Mre11 is influenced by ATP. *Nucleic Acids Res.*, **30**, 4425–4431.
14. Van Dyck, E., Hajibagheri, N.M., Stasiak, A. and West, S.C. (1998) Visualisation of human Rad52 protein and its complexes with hRad51 and DNA. *J. Mol. Biol.*, **284**, 1027–1038.
15. Sung, P. (1997) Function of yeast Rad52 protein as a mediator between replication protein A and the Rad51 recombinase. *J. Biol. Chem.*, **272**, 28194–28197.
16. Benson, F.E., Baumann, P. and West, S.C. (1998) Synergistic actions of Rad51 and Rad52 in recombination and DNA repair. *Nature*, **391**, 401–404.
17. New, J.H., Sugiyama, T., Zaitseva, E. and Kowalczykowski, S.C. (1998) Rad52 protein stimulates DNA strand exchange by Rad51 and replication protein A. *Nature*, **391**, 407–410.

18. Shinohara, A. and Ogawa, T. (1998) Stimulation by Rad52 of yeast Rad51-mediated recombination. *Nature*, **391**, 404–407.
19. Gasior, S.L., Olivares, H., Ear, U., Hari, D.M., Weichselbaum, R. and Bishop, D.K. (2001) Assembly of RecA-like recombinases: distinct roles for mediator proteins in mitosis and meiosis. *Proc. Natl Acad. Sci. USA*, **98**, 8411–8418.
20. Mortensen, U.H., Bendixen, C., Sunjevaric, I. and Rothstein, R. (1996) DNA strand annealing is promoted by the yeast Rad52 protein. *Proc. Natl Acad. Sci. USA*, **93**, 10729–10734.
21. Stasiak, A.Z., Larquet, E., Stasiak, A., Muller, S., Engel, A., Van Dyck, E., West, S.C. and Egelman, E.H. (2000) The human Rad52 protein exists as a heptameric ring. *Curr. Biol.*, **10**, 337–340.
22. Kagawa, W., Kurumizaka, H., Ishitani, R., Fukai, S., Nureki, O., Shibata, T. and Yokoyama, S. (2002) Crystal structure of the homologous-pairing domain from the human Rad52 recombinase in the undecameric form. *Mol. Cell*, **10**, 359–371.
23. Singleton, M.R., Wentzell, L.M., Liu, Y., West, S.C. and Wigley, D.B. (2002) Structure of the single-strand annealing domain of human RAD52 protein. *Proc. Natl Acad. Sci. USA*, **99**, 13492–13497.
24. Parsons, C.A., Baumann, P., Van Dyck, E. and West, S.C. (2000) Precise binding of single-stranded DNA termini by human RAD52 protein. *EMBO J.*, **19**, 4175–4181.
25. Van Dyck, E., Stasiak, A.Z., Stasiak, A. and West, S.C. (1999) Binding of double-strand breaks in DNA by human Rad52 protein. *Nature*, **398**, 728–731.
26. Haber, J.E. (1999) DNA repair. Gatekeepers of recombination. *Nature*, **398**, 665–667.
27. Van Dyck, E., Stasiak, A.Z., Stasiak, A. and West, S.C. (2001) Visualization of recombination intermediates produced by RAD52-mediated single-strand annealing. *EMBO Rep.*, **2**, 905–909.
28. Ristic, D., Wyman, C., Paulusma, C. and Kanaar, R. (2001) The architecture of the human Rad54–DNA complex provides evidence for protein translocation along DNA. *Proc. Natl Acad. Sci. USA*, **98**, 8454–8460.
29. Ono, M., Tucker, P.W. and Capra, J.D. (1994) Production and characterization of recombinant human Ku antigen. *Nucleic Acids Res.*, **22**, 3918–3924.
30. de Jager, M., Dronkert, M.L., Modesti, M., Beerens, C.E., Kanaar, R. and van Gent, D.C. (2001) DNA-binding and strand-annealing activities of human Mre11: implications for its roles in DNA double-strand break repair pathways. *Nucleic Acids Res.*, **29**, 1317–1325.
31. Cromie, G.A., Connelly, J.C. and Leach, D.R. (2001) Recombination at double-strand breaks and DNA ends: conserved mechanisms from phage to humans. *Mol. Cell*, **8**, 1163–1174.
32. Takata, M., Sasaki, M.S., Sonoda, E., Morrison, C., Hashimoto, M., Utsumi, H., Yamaguchi-Iwai, Y., Shinohara, A. and Takeda, S. (1998) Homologous recombination and non-homologous end-joining pathways of DNA double-strand break repair have overlapping roles in the maintenance of chromosomal integrity in vertebrate cells. *EMBO J.*, **17**, 5497–5508.
33. Sugiyama, T. and Kowalczykowski, S.C. (2002) Rad52 protein associates with replication protein A (RPA)-single-stranded DNA to accelerate Rad51-mediated displacement of RPA and presynaptic complex formation. *J. Biol. Chem.*, **277**, 31663–31672.
34. McIlwraith, M.J., Van Dyck, E., Masson, J.Y., Stasiak, A.Z., Stasiak, A. and West, S.C. (2000) Reconstitution of the strand invasion step of double-strand break repair using human Rad51 Rad52 and RPA proteins. *J. Mol. Biol.*, **304**, 151–164.

Chapter 5

The architecture of the human Rad54–DNA complex provides evidence for protein translocation along DNA



The architecture of the human Rad54–DNA complex provides evidence for protein translocation along DNA

Dejan Ristic^{*†}, Claire Wyman^{*†}, Coen Paulusma^{*}, and Roland Kanaar^{*‡§}

^{*}Department of Cell Biology and Genetics, Center for Biomedical Genetics, Erasmus University Rotterdam, PO Box 1738, 3000 DR Rotterdam, The Netherlands; and [†]Department of Radiation Oncology, University Hospital Rotterdam/Daniel, PO Box 5201, 3008 AE Rotterdam, The Netherlands

Proper maintenance and duplication of the genome require accurate recombination between homologous DNA molecules. In eukaryotic cells, the Rad51 protein mediates pairing between homologous DNA molecules. This reaction is assisted by the Rad54 protein. To gain insight into how Rad54 functions, we studied the interaction of the human Rad54 (hRad54) protein with double-stranded DNA. We have recently shown that binding of hRad54 to DNA induces a change in DNA topology. To determine whether this change was caused by a protein-constrained change in twist, a protein-constrained change in writhe, or the introduction of unconstrained plectonemic supercoils, we investigated the hRad54–DNA complex by scanning force microscopy. The architecture of the observed complexes suggests that movement of the hRad54 protein complex along the DNA helix generates unconstrained plectonemic supercoils. We discuss how hRad54-induced superhelical stress in the target DNA may function to facilitate homologous DNA pairing by the hRad51 protein directly. In addition, the induction of supercoiling by hRad54 could stimulate recombination indirectly by displacing histones and/or other proteins packaging the DNA into chromatin. This function of DNA translocating motors might be of general importance in chromatin metabolism.

Recombination between homologous DNA molecules is important for maintenance and faithful duplication of the genome (1–4). Homologous recombination is a major pathway for the accurate repair of DNA double-strand breaks (DSBs) that arise from exposure to exogenous DNA-damaging agents such as ionizing radiation, which is commonly used in antitumor therapies. Furthermore, homologous recombination processes programmed DSB intermediates during meiosis. Finally, homologous recombination plays a major role in reestablishing DNA replication forks that are stalled or have collapsed because of the presence of spontaneous or induced DNA damage in one of the template strands of the DNA double helix (5–12).

Extensive genetic and biochemical experiments have revealed that DSB repair mediated by homologous recombination in yeast, chicken, and mammalian cells occurs through the close cooperation of the *RAD52* group of proteins, including Rad51, Rad52, and Rad54 (13, 14). A key member of this group is the Rad51 protein. Rad51 protomers assemble a nucleoprotein filament on the single-stranded DNA tails that form at the break site. This filament pairs with homologous double-stranded DNA, resulting in a joint molecule. Joint molecules are pivotal intermediates in recombination because they allow the broken DNA to use the intact homologous double-stranded DNA as a repair template (15). The Rad52 and Rad54 proteins serve as accessory factors in Rad51-mediated joint molecule formation. The details of the molecular mechanisms through which Rad52 and Rad54 stimulate joint molecule formation are not well understood. Rad52 has been shown to increase the rate of annealing of complementary single-stranded DNA molecules, to bind to

DNA ends, to stimulate homologous pairing by Rad51, and to overcome the inhibitory effect of the single-stranded DNA-binding protein RPA on Rad51 nucleoprotein filament formation (16–22). Rad54 can interact with Rad51 (23–26) and has ATPase activity (27, 28). Importantly, the ATPase activity of Rad54 specifically requires the presence of double-stranded DNA. It is not active in the presence of single-stranded DNA (27, 28). This cofactor specificity is opposite to that of Rad51 (29). Because the initial substrate of Rad51 during homologous recombination is single-stranded DNA (13), it is likely that the substrate for Rad54 is the double-stranded homologous repair template.

To understand how the Rad54 protein assists Rad51 during joint molecule formation we have investigated the interaction of the human Rad54 (hRad54) protein with double-stranded DNA. We have recently demonstrated that binding of hRad54 to double-stranded DNA induces a change in the topology of the DNA (26), as is also observed for yeast Rad54 homologues (30–33). In the topological experiments, singly nicked plasmid DNA is incubated with hRad54 protein. Subsequently, the nick is closed by the addition of DNA ligase. The ligation will fix any change in linking number (ΔLk) in the DNA that is induced by protein binding. Lk describes the number of times that the two strands of the DNA double helix wind around each other. Lk is a topological parameter of double-stranded DNA that is made up of two geometrical parameters, twist (Tw) and writhe (Wr) (34). Tw and Wr give information about the shape of the DNA. The local winding of the two strands of the double helix is described by Tw , whereas Wr describes the number of times that the axis of the double helix winds around itself. The relationship between these three parameters is expressed by the equation $Lk = Tw + Wr$ (35). Therefore, to mechanistically interpret the ΔLk induced by hRad54 binding it is necessary to determine whether protein binding changes Tw or Wr .

One well-characterized class of proteins that has the ability to change the Lk of DNA is topoisomerases (36–38). Topoisomerases induce a ΔLk by a strand passage mechanism because these enzymes can break and rejoin DNA strands. In contrast, no strand breakage and rejoining activity has been detected for hRad54 (26). Therefore, the ΔLk measured by the assay described above could be caused by the hRad54 protein constraining either Tw or Wr . Protein-constrained ΔTw and ΔWr result

This paper results from the National Academy of Sciences colloquium, "Links Between Recombination and Replication: Vital Roles of Recombination," held November 10–12, 2000, in Irvine, CA.

Abbreviations: ΔLk , change in linking number; SFM, scanning force microscopy; Tw , twist; Wr , writhe; ATP- γ S, adenosine 5'-[γ -thio]triphosphate.

[†]D.R. and C.W. contributed equally to this work.

[§]To whom reprint requests should be addressed. E-mail: kanaar@gen.fgg.eur.nl.

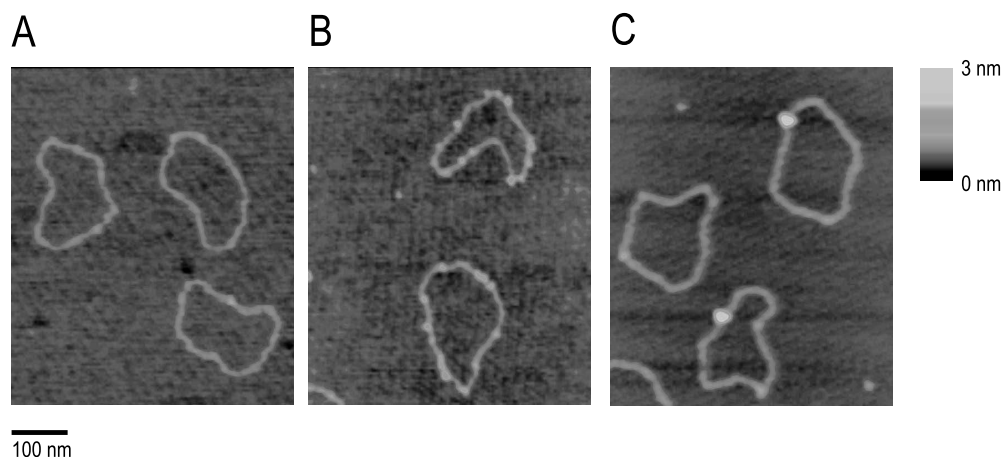


Fig. 1. SFM images of nicked circular DNA molecules in the absence or presence of hRad54. The images were processed only by flattening to remove background slope and are presented as top views. All images show an area of 500 nm \times 500 nm, zoomed in from 2- μ m \times 2- μ m scans. The z dimension is indicated by color as shown on the bar at the right. (A) DNA molecules without hRad54. (B) hRad54–DNA complexes formed in the absence ATP. (C) hRad54–DNA complexes formed in the presence of ATP.

from very different DNA-binding modes of the protein and therefore imply a different function for hRad54 in homologous recombination. For example, proteins induce a ΔW_r by wrapping the DNA around their surface. A classical example of such a binding mode is provided by the nucleosome (39). This mode of DNA binding is not restricted to general architectural proteins, because it has also been found to occur with a protein involved in modulating DNA supercoiling (40) and DNA damage recognition (41). Proteins can induce a ΔT_w by stretching the helix in a protein-stabilized filament. An example of this binding mode is provided by the *Escherichia coli* RecA protein, the central homologous pairing and strand exchange protein in homologous recombination (42–44). The two different binding modes are not easily distinguished by biochemical assays. However, they will result in architecturally different DNA–protein complexes, and therefore the binding modes can be distinguished if the complexes are imaged directly. A protein-constrained ΔL_k caused by decreasing T_w will be evident by an extensive protein filament formed on the DNA and an increase in the contour length of the resulting complex relative to unbound DNA. A ΔL_k due to wrapping of DNA around proteins will not result in an extensive region of DNA covered by protein but will cause a decrease in contour length of the DNA–protein complexes relative to naked DNA. Alternatively, the ΔL_k measured in the topological assay could be due to the introduction of unconstrained supercoils in the plasmid by a protein translocation mechanism (45). In our assay, this would require the formation of specific DNA–protein complexes that create topologically separate domains. Any relevant change in the structure of the DNA–protein complexes will have to occur in the presence of ATP because ATP hydrolysis by hRad54 is required for the ΔL_k induction (26). With analysis of these parameters in mind, we chose to investigate the structure of DNA–protein complexes formed between hRad54 and circular DNA molecules by scanning force microscopy (SFM).

Materials and Methods

DNA Substrates. Substrate DNA plasmids used in this study were pTrcHisB (Invitrogen) and pDERII. Plasmid pDERII was generated by deletion of the *Spl*–*SapI* fragment from plasmid pUC19, resulting in a plasmid 1,821 bp in length. Singly nicked plasmid DNA was produced in a 30- μ l reaction mixture containing 0.5 μ g of DNA, 20 mM Tris-HCl (pH 7.5), 50 mM NaCl, 10 mM MgCl₂, 360 μ g/ml ethidium bromide, and 1 μ g/ml

DNase I at 30°C for 30 min. The reaction was stopped by the addition of 0.1 vol of 5% (wt/vol) SDS/50 mM EDTA/30 μ g/ml proteinase K and subsequent incubation at 65°C for 30 min. DNA was purified by extraction with phenol and phenol/chloroform (1:1, vol/vol), precipitated with ethanol, and dissolved in 10 mM Tris-HCl (pH 8.0)/1 mM EDTA. Linear DNA substrates were made by digestion of plasmid pTrcHisB (Invitrogen) with *EcoRV* and *NcoI*, followed by isolation of the 732-bp and 3,672-bp DNA fragments from a 1.0% agarose gel.

Proteins and DNA-Binding Reactions. The hRad54 protein was produced in baculovirus-infected Sf21 cells and purified as described (27). In addition, a mutant version of hRad54 was purified that contained a single amino acid substitution at position 189. The invariant lysine residue in the Walker A nucleotide-binding motif was changed to an alanine residue by using site-specific mutagenesis. This protein is referred to as hRad54^{K189A}. hRad54^{K189A} had no detectable DNA-dependent ATPase activity. Given the sensitivity of the ATPase assay, the ATPase activity of the mutant protein must be reduced by more than 50-fold compared with the wild-type protein (data not shown). The Ku70/80 heterodimer was produced and purified as described and was the generous gift of M. Modesti (46). *E. coli* RNA polymerase was purchased from Boehringer Mannheim.

Protein–DNA complexes were prepared by addition of the hRad54 and hRad54^{K189A} protein preparations to DNA substrates. Reaction mixtures (10 μ l final volume) were assembled by mixing hRad54 or hRad54^{K189A} (up to final concentrations of 0.34 μ M) and DNA (76 μ M; concentration in nucleotides) in buffer containing 20 mM Hepes-KOH (pH 7.4), 20 mM KCl, 5 mM MgCl₂, and 2 mM ATP or 2 mM adenosine 5'-[γ -thio]triphosphate (ATP γ S). After incubation at 30°C for 10 min, glutaraldehyde was added to a final concentration of 0.1%, followed by additional incubation at 30°C for 10 min. Experiments done without glutaraldehyde fixation showed the same type of DNA protein complexes as observed with glutaraldehyde, but in general fewer complexes and more naked DNA were observed. The Ku70/80 heterodimer was incubated with the 732-bp linear DNA fragment in 10- μ l reaction mixtures containing 75 ng of Ku 70/80 (50 nM), 270 ng of DNA substrate (81 μ M), 50 mM Hepes-KOH (pH 8.0), 100 mM KCl, 10 mM MgCl₂, and 1 mM DTT. Incubations were carried out at 37°C for 20 min. *E. coli* RNA polymerase was bound to the 3,672-bp DNA fragment in a 20- μ l reaction mixture containing 250 ng of RNA

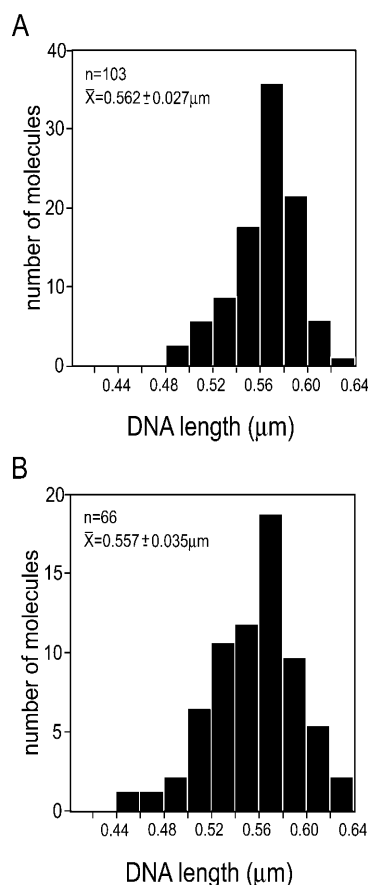


Fig. 2. Histograms of DNA contour length measured from molecules with or without bound hRad54. hRad54–DNA complexes were formed in the presence of ATP. All DNA length measurements were from images collected from one deposition of molecules from one reaction mixture. The top left of each panel shows the number of DNA molecules measured, their average contour length, and standard deviation. (A) Contour length of DNA molecules without bound protein. (B) Contour length of DNA molecules with bound hRad54.

polymerase (55 nM), 200 ng of DNA fragment (30 μM), 30 mM Hepes-KOH (pH 7.4), 100 mM NaCl, 10 mM MgCl₂, and 0.5 mM DTT. Incubations were at 37°C for 15 min, followed by addition of glutaraldehyde to a final concentration of 0.1% and an additional incubation at 37°C for 15 min.

SFM. Reaction mixtures were diluted 15- to 30-fold in deposition buffer, consisting of 5 mM Hepes-KOH (pH 7.5) and 5 mM MgCl₂. Within 15 sec a 10- to 15-μl drop was placed onto freshly cleaved mica. After 30 sec the mica surface was washed with H₂O (glass-distilled, Sigma), followed by drying with a stream of filtered air. For the simultaneous deposition of protein–DNA complexes from different binding reactions, the separate reaction mixtures were combined at the dilution step. The nucleoprotein complexes were imaged in air at room temperature and humidity by using a NanoScope IIIa (Digital Instruments, Santa Barbara, CA) operating in the tapping mode with a type E scanner. Silicon tips (Nanoprobes) were obtained from Digital Instruments. DNA length and the size of protein complexes on DNA were measured from NanoScope images imported into IMAGE SXM 1.62 (National Institutes of Health IMAGE version modified by Steve Barrett, Surface Science Research Centre, Univ. of Liverpool, Liverpool, U.K.). DNA contours were

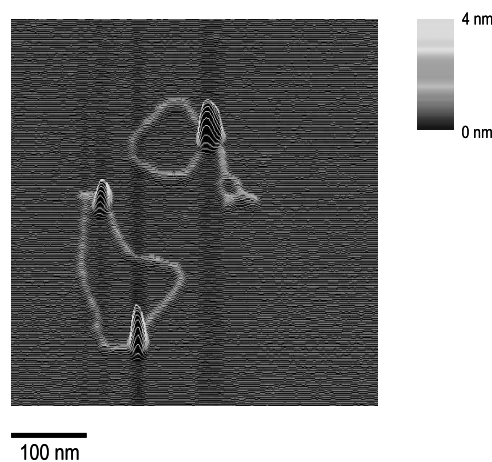


Fig. 3. SFM image of hRad54–DNA complexes formed in the presence of ATP. The image is presented as line plot at a 60° viewing angle to emphasize topography. Height is indicated by color as shown on the bar at the right. One plasmid has a hRad54 complex bound at the junction of relaxed and supercoiled domains. The other plasmid has two hRad54 complexes bound.

manually traced. In the case of DNA–protein complexes, contour length was traced as the shortest possible DNA path through the bound protein. The volume of DNA-bound protein complexes was determined as described (47). Briefly, the object was manually traced and its area and average height were measured, and a background volume of the same traced area at an adjacent position including DNA was subtracted. Volume measurements are given in arbitrary units because they are used only to compare the relative sizes of objects.

Results

Visualization of hRad54–DNA Complexes by SFM. Complexes between DNA and hRad54 were formed by incubating the protein with a singly nicked, circular DNA substrate. Reaction mixtures were deposited on mica and imaged by SFM. In the absence of protein, the majority (80–85%) of DNA molecules looked like a relaxed circle with uniform height (Fig. 1A). The remaining circles had some DNA crossings or small regions where two double-stranded regions were next to each other, which is typical of DNA prepared in this manner for SFM (C.W., unpublished observation). In the absence of ATP, hRad54 bound to DNA as small complexes with several on each DNA circle (Fig. 1B). Addition of ATP to the binding reaction resulted in a dramatic change both in frequency and in size of hRad54–DNA complexes. The DNA-bound protein now formed much larger complexes with only one or sometimes two on each DNA circle (Fig. 1C). In neither case were protein-coated filaments of any kind observed. Thus, it appears likely that hRad54 does not alter DNA topology by inducing a ΔTw through constraining the DNA double helix in a protein filament.

hRad54 Binding Does Not Induce DNA Wrapping. To determine whether hRad54 binding resulted in ΔWr by wrapping of DNA around the large protein complexes formed in the presence of ATP, we measured the contour length of the DNA. Histograms of contour length for DNA alone and DNA bound by large protein complexes are shown in Fig. 2A and B, respectively. On the basis of the size of hRad54 and the stiffness of DNA, we would expect a minimum wrap of about 60 bp of DNA or loss of about 20 nm in length per complex to introduce each ΔLk of –1 or +1, depending on the handedness of the wrapping. Thus, according to this model significant length changes should occur to account for the large ΔLk seen in the topological assays in

Table 1. Correlation of hRad54 ATP hydrolysis activity and observation of hRad54-anchored supercoiled domains

Protein	Nucleotide	No. of protein-DNA complexes	No. of protein complexes anchoring DNA domains	Percentage of complexes anchoring DNA domains
hRad54	ATP	496	52	10.5
hRad54	ATP γ S	100	3	3
hRad54 ^{K189A}	ATP	217	0	<0.5

which topoisomers with a ΔLk of up to -23 have been resolved (26). However, the data presented in Fig. 2 show that there is no difference in either the mean DNA length or the distribution of DNA lengths in the presence or absence of bound large hRad54 complexes. Thus, it appears that hRad54 does not alter DNA topology by introducing ΔWt through DNA wrapping.

Supercoiled Domains Anchored by the hRad54 Protein. The SFM experiments did reveal some intriguing complexes formed between hRad54 and DNA in the presence of ATP. Occasionally we observed a large hRad54 complex anchoring the junction between relaxed and apparently plectonemically supercoiled domains of the plasmid (Fig. 3). To determine whether the structures with hRad54 anchoring a supercoiled domain were a relevant representation of hRad54 activity on DNA, we correlated the occurrence of these structures with the ability to hydrolyze ATP. In similar SFM experiments either ATP was replaced by the slowly hydrolyzable ATP analogue ATP γ S or the wild-type hRad54 protein was replaced by hRad54^{K189A}, a mutant defective in ATP hydrolysis (27) (data not shown). The number of DNA-protein complexes in which the protein anchors a supercoiled domain was counted and calculated as a percentage of the total number of protein-bound DNA molecules observed (Table 1). While the structures indicative of domain anchoring were 10.5% of the total protein-bound DNA for wild-type hRad54 in the presence of ATP, they were only 3% when ATP was replaced with ATP γ S. It should be noted that wild-type hRad54 has some residual activity in topological assays in the presence of ATP γ S (26). The difference was even more

dramatic when hRad54^{K189A} was used. Both the frequency of DNA-bound protein and the size of the complexes formed by this mutant were the same in the presence and absence of ATP. Most of the DNA-bound complexes appeared to be the same size as those formed by the wild-type protein in the presence of ATP. Although compared with wild-type protein significantly more of the total DNA was bound by protein (about 90% of DNA molecules compared with 15–20% for wild-type hRad54 in the presence of either ATP or ATP γ S), the protein was never observed to anchor a supercoiled DNA domain. Thus, our results show a direct correlation between ATP hydrolysis, the ability to induce a ΔLk , and the appearance of protein complexes anchoring a plectonemically supercoiled domain.

Multimeric State of hRad54 Bound to DNA. We believe that the hRad54 complexes bound to DNA in the presence of ATP are the functional form(s) of this protein (see *Discussion*). These complexes were much larger than those bound to DNA in the absence of ATP. We wished to estimate the size of the presumptive functional form of hRad54 from our SFM images. Because of the well-known distortions in the absolute dimensions of biomolecules imaged by SFM (48, 49), it is necessary to measure the volume of the protein of interest, as well as proteins of known size from the same deposition with the same tip. The approximate size of the unknown complex is then determined by comparison to the standards (47). In this way, we can estimate the size of the protein complexes bound to DNA, even if there is more than one complex per DNA molecule, a measurement that would not be possible with biochemical methods. Three separate protein-DNA complexes, *E. coli* RNA polymerase (450 kDa) bound to a long linear DNA (3,672 bp), Ku70/80 heterodimer (155 kDa) bound to a short linear DNA (732 bp), and hRad54 (87.8-kDa monomers) bound to singly nicked circular DNA (1,821 bp) in the presence of ATP, were prepared and mixed together for a single deposition. Fig. 4 shows a field containing these three protein-DNA complexes; it is obvious that the hRad54 complex is much larger than the Ku heterodimer and nearly the same size as RNA polymerase. An average volume for the different DNA-bound proteins was determined from over 100 individual complexes of each kind. In one experiment the average volume of the hRad54 complexes was close to that of RNA polymerase, indicative of a molecular mass of about 450 kDa or slightly above five 87.8-kDa hRad54 monomers. In two other experiments the average volume of the hRad54 complexes was between that of Ku70/80 and RNA polymerase at a value corresponding to approximately three hRad54 monomers. There is large variation in these volume measurements, partially because of the inaccuracies in SFM dimensions of biomolecules. For the hRad54 complexes the variation between experiments is possibly caused by variation in the population of complexes with different sizes. We have no unbiased way of sorting the DNA-bound complexes that are not anchoring a supercoiled domain. The Rad54 complexes anchoring a supercoiled domain do appear larger than the isolated complexes (see Fig. 3). However, there were not enough of them in the experiments with size standards to determine a significant average volume. Although this is only an estimation of molecular

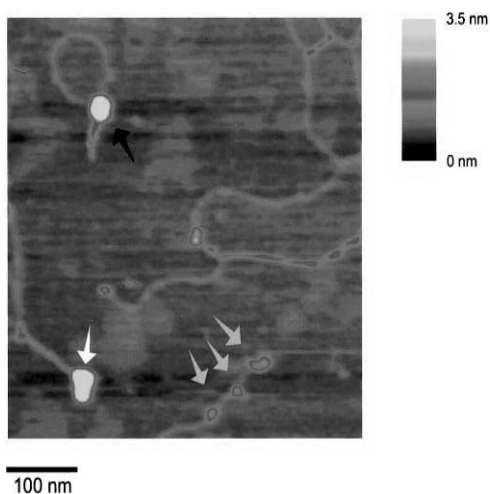


Fig. 4. Comparison of the size of large hRad54 complexes bound to DNA in the presence of ATP and proteins of known size. SFM image of a mixture of hRad54, RNA polymerase, and Ku70/80 bound to the different DNA substrates. Upper left, circular DNA-hRad54 complex (hRad54 monomer is 87.8 kDa); lower left, RNA polymerase (450 kDa) bound to a long linear DNA (partially shown); lower middle, three Ku70/80 heterodimers (155 kDa) bound to a short linear DNA.

mass, the active form of hRad54 bound to DNA is at least a trimer and possibly as large as a hexamer.

Discussion

Rad54 belongs to a superfamily of proteins that includes known helicases but could more generally be described as DNA-translocating motors (50). The detailed mechanism(s) by which proteins use the energy of ATP hydrolysis to track along the DNA helix and accomplish work such as strand separation, supercoiling, and possibly chromatin remodeling is not well understood. Rad54 belongs to the Swi2/Snf2 subfamily on the basis of its amino acid sequence. Rad54 has double-stranded DNA-dependent ATPase activity but, like other members of this family, it has not been demonstrated to have any strand displacement activity (27, 28). We have recently demonstrated that hRad54 can use the energy of ATP hydrolysis to change the topology of DNA (26). As classical topoisomerase activity, involving breakage, passage, and rejoining of DNA strands, could not be demonstrated for hRad54, we hypothesized that the observed changes in DNA topology might result from hRad54 constrained changes in DNA Tw or Wr. We used SFM to distinguish between the protein–DNA structures that would have induced changes in DNA Tw and those that would have induced changes in DNA Wr. We observed neither protein filaments on DNA that would have constrained Tw nor protein-induced DNA length changes that would have accompanied changes in Tw or Wr. Instead, in conditions where DNA topology is altered, we observed single large hRad54 protein complexes anchoring supercoiled DNA domains. We believe these structures result from interaction between two DNA-bound hRad54 complexes and movement of one of them. We will now discuss how these structures may arise and, in light of other information on the function of Rad54, how this activity fits into a recombination reaction.

Proteins that move along DNA by tracking the helix can introduce supercoiling if certain conditions are met (45). There has to be significant effective frictional torque to prevent the protein from freely rotating around the DNA in order for movement alone to cause supercoiling, positive ahead of movement and negative behind (Fig. 5). It has recently been suggested that yeast Rad54 movement induces unconstrained supercoils in DNA (31, 32). However, the Rad54 protein alone tracking along the helix, even as part of the large complexes observed here in the presence of ATP, would not cause DNA supercoiling because the protein would be free to rotate around the DNA double helix axis as it moved. In contrast, if two DNA-bound hRad54 complexes interact and one of them moves along the helix, rotation of the protein relative to the DNA is prevented and supercoils will accumulate both ahead and behind the movement. The observation that the hRad54 complexes anchoring supercoiled DNA domains appear larger than those bound simply to other positions on the plasmid (Fig. 3) implies that proteins bound at two sites initially interact to form these structures. In our case such an association of DNA-bound hRad54 complexes would divide the plasmid into two domains. Because the DNA is singly nicked, one domain will contain a nick, whereas the other will contain two covalently closed DNA strands. When the protein complex translocates along the helix, the nicked domain will not accumulate any supercoiling because the strands are free to rotate around each other. On the other hand, the domain containing the covalently closed strands will become supercoiled (Fig. 5C). This is how we interpret the origin of the type of complex shown in Fig. 3. This mechanism predicts that both negative and positive supercoils would be produced, depending on the random occurrence of the nick in the domain either ahead or behind the moving proteins. Indeed the topological experiment, also performed on singly nicked plasmids, did show that hRad54 introduced both negative and positive

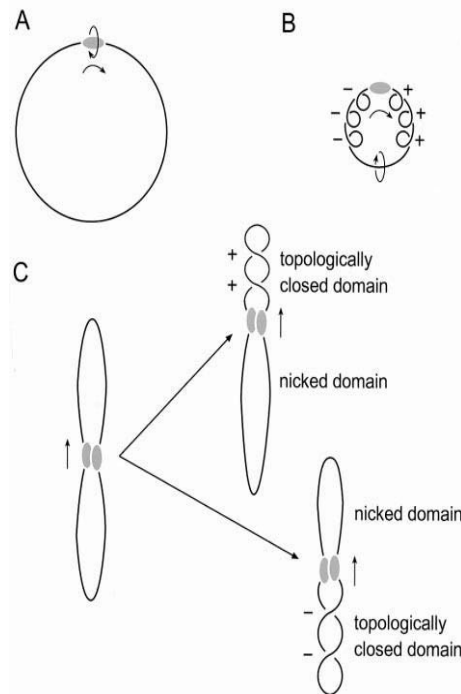


Fig. 5. Model for generation of supercoiling by hRad54 translocation along DNA. The hRad54 complex and plasmid DNA are indicated by the shaded oval and black line, respectively. (A) Movement of the hRad54 complex by tracking along the helical path of DNA is indicated by the arrows. When the complex is free to rotate around the DNA, no change in supercoiling will be induced in the plasmid DNA. (B) When the hRad54 complex tracks along the helix, while being prevented from rotating around the DNA, positive supercoils will arise ahead of the protein complex and negative supercoils behind it. These supercoils can freely distribute along the plasmid and therefore they will cancel each other out. (C) The interaction of two hRad54 complexes on a plasmid will divide the plasmid into two domains. Because the plasmid is singly nicked, one domain will contain a nick, whereas the other contains two covalently closed DNA strands. Depending on the position of the nick relative to the movement of the protein complex along the DNA, topoisomers containing either negative or positive supercoils will result after ligation of the nick.

supercoils into plasmids (26). Thus, if free rotation of DNA and protein is prevented, hRad54 can use the energy of ATP hydrolysis to supercoil DNA domains.

In our experiments hRad54 is most likely prevented from rotating around the helix as it moves because of interaction with another hRad54 complex on the same plasmid. This is probably not how this protein works *in vivo*. On the small plasmid we used hRad54 complexes tethered by chance to the same DNA molecule are in very high local concentration, possibly allowing even nonspecific interactions. The activity of Rad54 relevant to homologous recombination is as an accessory factor, along with Rad52, in promoting Rad51-mediated joint molecule formation. Specific interaction between hRad54 and hRad51 has been demonstrated biochemically (23, 26). More interestingly, it has recently been demonstrated that the ATPase activity of yeast Rad54 and its activity in altering DNA topology are both stimulated by the Rad51–single-stranded DNA filament (31, 33). Physical association with and activation of Rad54 by the Rad51–single-stranded DNA filament would have two very favorable consequences for the mechanism of homologous recombination. The filament would favor interaction with homologous double-stranded DNA, thereby targeting Rad54 to the correct chromosomal location for activity. In addition, Rad54 attached to a

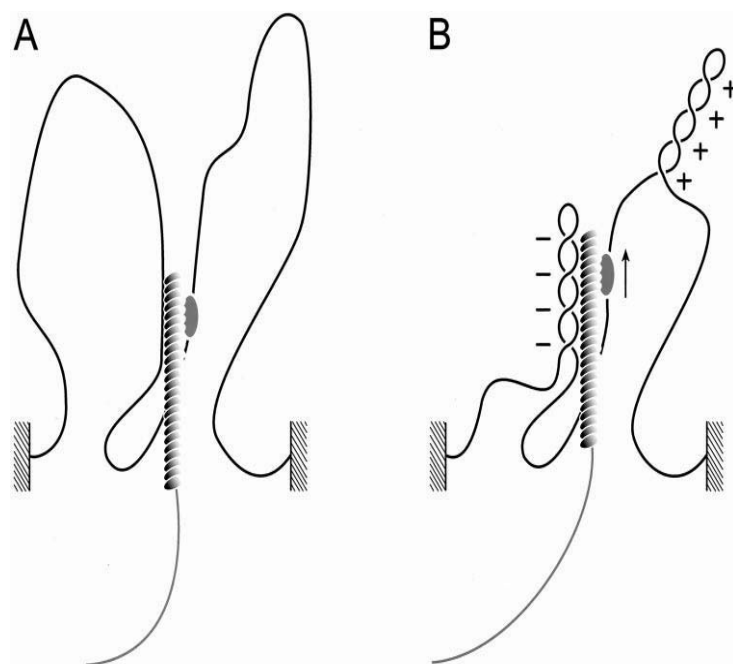


Fig. 6. Model for stimulation of Rad51-mediated joint molecule formation by Rad54 translocation. A chromosomal domain is indicated by the black line connecting the hatched areas. The Rad54 protein complex is represented by the shaded oval, and it is shown to interact with the Rad51 nucleoprotein filament that is assembled on the broken DNA indicated in gray (A, before hRad54 translocation). This interaction will provide the frictional torque that prevents the Rad54 complex from rotating around the DNA as it tracks along the helix. In this way, movement of the Rad54 complex along the DNA (B, after hRad54 translocation) will generate negative and positive supercoils into the domains divided by the Rad54 complex. See text for details on how this process might stimulate Rad51-mediated joint molecule formation.

Rad51 filament that is itself part of a broken chromosome would provide more than sufficient frictional torque to prevent rotation of Rad54 along the target DNA helix and thus create differentially supercoiled domains ahead and behind the moving Rad54 (Fig. 6). The negative supercoiling created behind the protein could promote joint molecule formation. This is because negative supercoiling will promote unpairing of the target DNA (31, 34) and thereby facilitate the hybridization of the incoming single-stranded DNA in the filament. Furthermore, one could also envision Rad54 at the end of a Rad51–single-stranded DNA filament effectively threading the filament into the target duplex by dragging it along as it tracks the helix.

In addition, Rad54-induced superhelical stress in the target DNA may function to displace histones and/or other proteins packaging the DNA into chromatin and inhibiting recombination. This function of DNA-translocating motors may be of general importance in chromatin metabolism. The archetypal chromatin remodeling factor, yeast SWI/SNF, as well as others, has recently been shown to induce superhelical stress in DNA (51). This ability to change DNA topology has also been shown to be required for SWI/SNF chromatin remodeling activity (52). The ability of hRad54 to induce topological stress in the target chromosome may also disrupt chromatin structure, making it accessible for Rad51 nucleoprotein filament invasion.

It would be very interesting to know more about the structure of these protein complexes that use the energy of ATP hydrolysis to translocate along DNA. Structural details that would reveal how these protein machines grasp DNA strands and move are currently very limited. The available information indicates there is a subclass of helicases that are hexameric rings, some of which are known to encircle DNA (50). Our SFM images cannot resolve the path of the DNA as either going through a protein structure or simply covered by

a protein on top of it. However, the images do show a clear difference in the size of hRad54 complexes bound to DNA in the presence and absence of ATP. Our estimate of the size of these large complexes is that they are at least trimers and may be as large as hexamers. Although hexamers might be expected, either trimers or hexamers could produce similar functional structures. For example, the DNA polymerase processivity factors from prokaryotes and eukaryotes form nearly identical six-lobed rings around DNA while one is a trimer of two-lobed subunits and the other dimer of three-lobed subunits (53). Clearly an accurate answer to the question of the multimeric state of active hRad54 requires additional experiments such as negative stain electron microscopy and image reconstruction. We have at least identified the type of protein complexes formed on DNA that should be the subjects for further analysis.

Using SFM, we were able to detect hRad54 in complex structures with DNA. The images simultaneously revealed that, in the presence of ATP, the protein complexes were large and could anchor a supercoiled DNA domain. These two pieces of information together suggested a mechanism for hRad54 DNA supercoiling that we had not initially considered. It now seems likely the role of hRad54 in recombination is to induce superhelical torsion in the target DNA. This superhelical torsion may result in melting of the target duplex (31), removal of nucleosomes from the target, or both of these. We anticipate that such direct imaging combined with biochemistry will continue to provide interesting insights into the mechanism of action of the hRad54 in the context of a hRad51–single-stranded DNA filament and interactions of this structure with target DNA and chromatin.

This work was supported by grants from the Dutch Cancer Society (NKB/KWF) and the Netherlands Organization for Scientific Research (NWO). We thank Mauro Modesti for purified Ku70/80.

1. Haber, J. E. (2000) *Trends Genet.* **16**, 259–264.
2. Morrison, C. & Takeda, S. (2000) *Int. J. Biochem. Cell Biol.* **32**, 817–831.
3. Thompson, L. H. & Schild, D. (1999) *Biochimie* **81**, 87–105.
4. Karran, P. (2000) *Curr. Opin. Genet. Dev.* **10**, 144–150.
5. Kogoma, T. (1997) *Microbiol. Mol. Biol. Rev.* **61**, 212–238.
6. Kuzminov, A. (1995) *Mol. Microbiol.* **16**, 373–384.
7. Marians, K. J. (2000) *Curr. Opin. Genet. Dev.* **10**, 151–156.
8. Kowalczykowski, S. C. (2000) *Trends Biochem. Sci.* **25**, 165–173.
9. Rothstein, R., Michel, B. & Gangloff, S. (2000) *Genes Dev.* **14**, 1–10.
10. Haber, J. E. (1999) *Trends Biochem. Sci.* **24**, 271–275.
11. Flores-Rozas, H. & Kolodner, R. D. (2000) *Trends Biochem. Sci.* **25**, 200–204.
12. Cox, M. M., Goodman, M. F., Kreuzer, K. N., Sherratt, D. J., Sandler, S. J. & Marians, K. J. (2000) *Nature (London)* **404**, 37–41.
13. Baumann, P. & West, S. C. (1998) *Trends Biochem. Sci.* **23**, 247–251.
14. Kanaar, R., Hocijmakers, J. H. & van Gent, D. C. (1998) *Trends Cell Biol.* **8**, 483–489.
15. Pâques, F. & Haber, J. E. (1999) *Microbiol. Mol. Biol. Rev.* **63**, 349–404.
16. Sung, P. (1997) *J. Biol. Chem.* **272**, 28194–28197.
17. New, J. H., Sugiyama, T., Zaitseva, E. & Kowalczykowski, S. C. (1998) *Nature (London)* **391**, 407–410.
18. Benson, F. E., Baumann, P. & West, S. C. (1998) *Nature (London)* **391**, 401–404.
19. Van Dyck, E., Stasiak, A. Z., Stasiak, A. & West, S. C. (1999) *Nature (London)* **398**, 728–731.
20. Shinohara, A. & Ogawa, T. (1998) *Nature (London)* **391**, 404–407.
21. Mortensen, U. H., Bendixen, C., Sunjevaric, I. & Rothstein, R. (1996) *Proc. Natl. Acad. Sci. USA* **93**, 10729–10734.
22. Reddy, G., Golub, E. I. & Radding, C. M. (1997) *Mutat. Res.* **377**, 53–59.
23. Golub, E. I., Kovalenko, O. V., Gupta, R. C., Ward, D. C. & Radding, C. M. (1997) *Nucleic Acids Res.* **25**, 4106–4110.
24. Clever, B., Interthal, H., Schmuckli-Maurer, J., King, J., Sigrist, M. & Heyer, W.-D. (1997) *EMBO J.* **16**, 2535–2544.
25. Jiang, H., Xie, Y., Houston, P., Stemke-Hale, K., Mortensen, U. H., Rothstein, R. & Kodadek, T. (1996) *J. Biol. Chem.* **271**, 33181–33186.
26. Tan, T. L., Essers, J., Citterio, E., Swagemakers, S. M., de Wit, J., Benson, F. E., Hocijmakers, J. H. & Kanaar, R. (1999) *Curr. Biol.* **9**, 325–328.
27. Swagemakers, S. M., Essers, J., de Wit, J., Hocijmakers, J. H. & Kanaar, R. (1998) *J. Biol. Chem.* **273**, 28292–28297.
28. Petukhova, G., Stratton, S. & Sung, P. (1998) *Nature (London)* **393**, 91–94.
29. Baumann, P., Benson, F. E. & West, S. C. (1996) *Cell* **87**, 757–766.
30. Petukhova, G., Van Komen, S., Vergano, S., Klein, H. & Sung, P. (1999) *J. Biol. Chem.* **274**, 29453–29462.
31. Van Komen, S., Petukhova, G., Sigurdsson, S., Stratton, S. & Sung, P. (2000) *Mol. Cell* **6**, 563–572.
32. Petukhova, G., Sung, P. & Klein, H. (2000) *Genes Dev.* **14**, 2206–2215.
33. Mazin, A. V., Bornarth, C. J., Solinger, J. A., Heyer, W. D. & Kowalczykowski, S. C. (2000) *Mol. Cell* **6**, 583–592.
34. Cozzarelli, N. R., Boles, T. C. & White, J. H. (1990) in *DNA Topology and Its Biological Effects*, eds. Cozzarelli, N. R. & Wang, J. C. (Cold Spring Harbor Lab. Press, Plainview, NY), pp. 139–215.
35. White, J. H. (1969) *Am. J. Math.* **91**, 693–728.
36. Champoux, J. J. (1994) *Adv. Pharmacol.* **29A**, 71–82.
37. Cozzarelli, N. R. (1980) *Science* **207**, 953–960.
38. Berger, J. M. & Wang, J. C. (1996) *Curr. Opin. Struct. Biol.* **6**, 84–90.
39. Travers, A. & Klug, A. (1987) *Nature (London)* **327**, 280–281.
40. Kirkegaard, K. & Wang, J. C. (1981) *Cell* **23**, 721–729.
41. Verhoeven, E. E. A., Wyman, C., Moolenaar, G. F., Hocijmakers, J. H. J. & Goosen, N. (2001) *EMBO J.* **20**, 601–611.
42. Stasiak, A., Di Capua, E. & Koller, T. (1981) *J. Mol. Biol.* **151**, 557–564.
43. Conley, E. C. & West, S. C. (1990) *J. Biol. Chem.* **265**, 10156–10163.
44. Cunningham, R. P., Shibata, T., DasGupta, C. & Radding, C. M. (1979) *Nature (London)* **281**, 191–195.
45. Liu, L. F. & Wang, J. C. (1987) *Proc. Natl. Acad. Sci. USA* **84**, 7024–7027.
46. Ono, M., Tucker, P. W. & Capra, J. D. (1994) *Nucleic Acids Res.* **22**, 3918–3924.
47. Wyman, C., Rombel, I., North, A. K., Bustamante, C. & Kustu, S. (1997) *Science* **275**, 1658–1661.
48. Bustamante, C., Keller, D. & Yang, G. (1993) *Curr. Opin. Struct. Biol.* **3**, 363–372.
49. Van Noort, S. J. T., van der Werf, K. O., de Grooth, B. G., van Hulst, N. F. & Greve, J. (1997) *Ultramicroscopy* **64**, 117–127.
50. West, S. C. (1996) *Cell* **86**, 177–180.
51. Havas, K., Flaus, A., Phelan, M., Kingston, R., Wade, P. A., Lilley, D. M. J. & Owen-Hughes, T. (2000) *Cell* **103**, 1133–1142.
52. Gavin, I., Horn, P. J. & Peterson, C. L. (2001) *Mol. Cell* **7**, 97–104.
53. Wyman, C. & Botchan, M. (1995) *Curr. Biol.* **5**, 334–337.

Chapter 6

ATP hydrolysis affects stability of hRad51 nucleoprotein filaments



ATP hydrolysis affects stability of hRad51 nucleoprotein filaments

Dejan Ristić¹, Mauro Modesti¹, Thijn van der Heijden², John van Noort², Cees Dekker², Roland Kanaar^{1,3}, Claire Wyman^{1,3}

¹ Department of Cell Biology and Genetics, Erasmus MC, University Medical Center Rotterdam, the Netherlands

² Kavli Institute of Nanoscience, Delft University of Technology, The Netherlands

³ Department of Radiation Oncology, Erasmus MC-Daniel, Rotterdam, The Netherlands

ABSTRACT

Homologous recombination, the exchange of strands between homologous DNA molecules, is a universal aspect of genome metabolism needed to repair DNA double strand breaks, to ensure proper replication and chromosome segregation and to create genetic diversity. The defining mechanistic steps of homologous recombination are homology search, strand invasion and joint molecule formation. These reactions are catalyzed by a class of proteins called recombinases, including bacterial RecA, the RadA homologs in archaea and the Rad51 homologs in eukaryotes. The catalytic core of these reactions is the recombinase protein assembled into a helical nucleoprotein filament on the invading DNA. We described the effect of reaction conditions that influence *in vitro* recombination on the structure of human Rad51 nucleoprotein filaments by directly observing and characterizing filaments with scanning force microscopy. In all cases conditions that enhance *in vitro* recombination activity result in regular and stable filaments on dsDNA with elongated DNA. In addition, human Rad51 filaments are irregular and apparently unstable in the presence of ATP. Disassembly of filaments immobilized on mica was followed over time revealing that protein disassociation occurs all over the filament with no directionality or end effects. Preliminary single molecule dynamic studies of human Rad51 filament assembly and disassembly also showed that stable filaments formed in conditions that favour *in vitro* strand exchange reactions. As well, the kinetics of filament disassembly followed in solution in real time indicated disassociation of human Rad51 protomers from many points at once not coordinately from an end of the filament.

INTRODUCTION

Homologous recombination, the exchange of strands between homologous DNA molecules, is a universal aspect of genome metabolism needed to repair DNA double strand breaks, to ensure proper replication and chromosome segregation and to create genetic diversity. The defining mechanistic step of homologous recombination is called synapsis and consists of strand invasion and joint molecule formation. The DNA transactions of synapsis involve recognition of regions of sequence homology between the recombining partners and the exchange of base paired partner strands. These reactions are catalyzed by a class of proteins called recombinases, typified by bacterial RecA, and including the RadA homologs in archaea and the Rad51 homologs

in eukaryotes. Synapsis requires a striking molecular machine, the recombinase proteins assembled into a helical nucleoprotein filament on the invading DNA. Current models of DNA synapsis assume that strand exchange occurs within the recombinase nucleoprotein filament. The mechanistic details of homology search and the exchange of DNA partners are currently obscure but must require dynamic rearrangements of the nucleoprotein filament components, DNA and the recombinase proteins.

The nucleoprotein filaments formed by bacterial RecA were first observed more than two decades ago (Dunn et al., 1982; Stasiak et al., 1982; Flory et al., 1982). This filament structure is more conserved than the recombinase proteins themselves. Recombinases from organisms representing all three kingdoms assemble on both single-stranded and double-stranded DNA into very similar filaments despite the limited conservation among their amino acid sequences (Yu et al., 2001; Seitz et al., 1998). Though they have similar structures, only the filaments formed on single stranded DNA represent the active form needed to promote synapsis. Filaments formed on double stranded DNA would occur at a later stage in the strand exchange reaction. The recombinase nucleoprotein filaments are all right handed helical structures in which DNA is stretched to about 1.5 times its B-form length. It has been suggested that the function of the recombinase proteins is to stabilize this form of DNA, which is an intrinsic recombinogenic DNA structure (Yu et al., 2004). The recombinase-DNA filaments are in many aspects very dynamic structures. Assembly of a filament on DNA from monomers in solution and their eventual disassociation are necessarily dynamic processes. Once formed the filaments are also remarkably flexible. The variation in helical pitch observed among filaments formed in different conditions and along segments of the same filament imply that dynamic rearrangements occur even once a filament is formed (Yu et al., 2001; Conway et al., 2004). Several lines of evidence suggest that the DNA within the filament is also dynamic. For instance, in single molecule dynamic measurements, the stiffness of RecA filaments formed on double-stranded DNA was not much greater than the stiffness of filaments formed on single-stranded DNA, possibly indicating that only one strand of DNA is tightly bound to the protein in the filament (Hegner et al., 1999). The recent crystal structure of a Rad51 filament formed in the presence of single-stranded DNA does not show clear density for the DNA. One explanation given for the unresolved DNA structure is that the DNA has a variety of conformations or is actually mobile in the crystal filaments (Conway et al., 2004). This lack of DNA density and the various estimates of Rad51 to DNA base pair binding ratios suggest that different protomers in the filament can bind DNA at different stoichiometries.

The source of conformational dynamics of the recombinases and their functional filaments lies in their ability to bind and hydrolyze ATP. The recombinases share a highly conserved ATPase domain based on their amino acid sequences and atomic structures. The status of bound nucleotide cofactors influences DNA binding for both RecA and Rad51, though in subtly different ways for the recombinases from different organisms. Formation of stable extended RecA filaments on single-stranded DNA requires ATP or ATP γ S (Kowalczykowski, 1991). Human Rad51 binds to DNA in the absence or presence of nucleotide cofactors (Kim et al., 2002; De Zutter et al., 1999; Tomblin et al., 2002III) and is reported to form filaments on DNA in variety of conditions including the presence of ATP, ATP γ S, or the transition state analog ADP + AlF $_4^-$ (Yu et al., 2001; Liu et al., 2004). However, the structure of the filaments

formed differs depending on the specific cofactor bound (Yu et al., 2001). Whereas *S. cerevisiae* Rad51 protein binds to single-stranded and double-stranded DNA well only in the presence of ATP, and not in the presence of ADP, ATP γ S or AMP-PNP (Namsaraev et al., 1998; Zaitseva et al., 1999).

Conversely, ATP hydrolysis by the recombinases is dependent on their interaction with DNA, with single-stranded DNA stimulating the activity more strongly than double-stranded DNA (Cox, 2003; Tomblin et al., 2002). However the mechanistic role of ATP hydrolysis in recombinase function remains enigmatic. ATP hydrolysis is dispensable for RecA and Rad51 catalyzed *in vitro* recombination reactions, which assess the pre-synaptic and synaptic stages of recombination, including homology search, strand invasion and joint molecule formation. Complete *in vivo* recombination however does require ATP hydrolysis by the recombinase. RecA mutants that cannot hydrolyze ATP are phenotypically *rec⁻* in *E. coli* (Konola et al., 1994). In *S. cerevisiae*, ATPase defective Rad51 rescues only some of the phenotype of a Rad51 deletion (Sung et al., 1996). In mammalian cells expression of an ATPase defective Rad51 had a dominant negative phenotype in several recombination and DNA repair assays (Starl et al., 2002). There are at least two distinct functions suggested for ATP hydrolysis by RecA. One proposal is that ATP hydrolysis is coupled to subunit exchange along the filament to correct discontinuities (Kowalczykowski et al., 1995; Rehrauer et al., 1993; Menetski et al., 1990). Alternatively it is suggested that coordinated ATP hydrolysis along a filament causes DNA strand rotations that are needed for strand exchange over long distances or to bypass non-homologous sequences (Cox, 1994; Bedale et al., 1996; Kim et al., 1992; Kim et al., 1992; Jain et al., 1994; Shan et al., 1997). Because homologous recombination in eukaryotes requires a host of proteins in addition to Rad51 acting together, ATP hydrolysis by Rad51 may also function to modulate and coordinate the required protein-protein interactions.

The *in vitro* recombination function of the eukaryotic recombinases are sensitive to a number of reaction conditions suggested to affect protein or filament conformation related to ATP binding (Liu et al., 2004; Yu et al., 1992; Yu et al., 2001). The formation of a recombination competent nucleoprotein filament in all cases requires a bound nucleotide cofactor. The recent atomic structure of a yeast Rad51 filament formed in active conditions revealed that the ATPase active site is at the junction of two Rad51 protomers and the conformation at this interface alternates along the filament (Conway et al., 2004). Thus bound nucleotide cofactors are located at structurally important junctions in the Rad51 filament, as had also been predicted by modeling the active RecA filament (VanLoock et al., 2003). The effect of specific *in vitro* conditions on recombination activity differ for yeast and human Rad51, as is also the case for the effect of specific nucleotide cofactors on DNA binding and filament formation. For human Rad51, the protein we study, *in vitro* strand exchange activity is markedly stimulated by addition of ammonium sulfate or substitution of calcium for magnesium in reactions including ATP (Sigurdsson et al., 2001; Bugreev et al., 2004). We described the effect of reaction conditions that influence *in vitro* recombination on the structure of human Rad51 nucleoprotein filaments by directly observing and characterizing filaments with scanning force microscopy (SFM, also called AFM). In all cases conditions that enhance *in vitro* recombination activity result in regular and stable filaments with elongated DNA. In addition, human Rad51 filaments are irregular

and apparently unstable in the presence of ATP. Disassembly of filaments immobilized on mica was followed over time revealing that protein disassociation occurs all over the filament with no directionality or end effects. Single molecule dynamic studies of human Rad51 filament assembly and disassembly also showed that stable filaments formed in conditions that favor *in vitro* strand exchange reactions. As well, the kinetics of filament disassembly followed in solution in real time indicated disassociation of human Rad51 protomers from many points at once not coordinately from an end of the filament.

MATERIALS AND METHODS

DNA substrates

Substrate double-stranded DNA used in this study was made by linearisation of pDER11 (Ristic et al., 2001). Digestion of this plasmid with *ScaI* produced 1821 bp blunt ended linear double-stranded DNA. The oligonucleotide, 90-mer, 5'-CGGGTGTCTCGGGGCTGGCTTAAGTATGCGGCATCAGAGCAGATTGTACTGAGAGTGCACCATATGCGGTGTGAAATACCGCACAGATGCGT was purchased from Sigma-Aldrich. 810 nt single-stranded DNA was made by lambda exonuclease digestion of a double-stranded PCR product with only one 5' phosphate. PCR primers, U3 which was 5' phosphorylated (5'-GAAGGAAGAACGAAGGAAGGAGC) and primer Bio 5 which was 5' biotinylated (5'-TTTCCCGGGGGGCCCCGGGTTCTATACTGTTGACCC), were used to amplify an 810 bp segment of the *S.cerevisiae*_URA3 gene. The PCR product was purified by phenol : chloroform : iso-amyl alcohol (25:24:1) extraction, followed by ethanol precipitation. The DNA strand with the 5' phosphate was digested by lambda exonuclease (5 U/ μ g DNA) at 37°C for 1 h. Digestion was stopped by the addition of 0.1 vol of stop solution containing 5% (w/v) SDS, 50 mM EDTA, 30 mg/ml proteinase K and incubation at 65°C for 30 min. The resulting single-stranded DNA was resolved on a 1.5% agarose gel and purified from a gel by with GFX™ column (Amersham).

The DNA substrate with a long single-stranded 5' overhangs was produced as previously described (Ristic et al., 2003).

For the magnetic tweezers experiments, pSFV1 (Invitrogen) was cleaved with *SpeI* and *XhoI*, resulting in a 8-kb linear fragment, which was ligated to two 700-bp PCR fragments, each containing \approx 180 biotin- or digoxigenin-modified UTP bases. The biotin-modified PCR fragment was pretreated with SAP to dephosphorylate the 5' end. The resulted construct therefore will have at least a single nick near one end attached to the magnetic bead to ensure a torsionally unconstrained DNA molecule.

Rad51 purification

The human Rad51 protein was over-expressed in *E. coli*. Cells were lysed in high salt. The clarified lysate was treated with polyetylenimine. After a second clarification, Rad51 was recovered by (NH₄)₂ SO₄ salting-out and the resuspended pellet was purified by heparin-sepharose chromatography followed by MonoQ chromatography.

The protein was dialyzed against 300 mM KCl, 20 HEPES-NaOH (pH 7.8), 1 mM EDTA, 2 mM DTT, 10 % glycerol and stored at -80°C .

Scanning Force Microscopy

Human Rad51-DNA complexes were formed in 10 μl reactions containing 7.5 μM DNA (concentration in nucleotides), 2.5 μM Rad51, 25mM HEPES-KOH (pH7.5), 5mM MgCl_2 or CaCl_2 , 2mM ATP, ADP or AMPPNP, 30mM KCl. Reactions were incubated at 37°C for 1 h and then placed on ice. When indicated, additional treatment with 200mM $(\text{NH}_4)_2\text{SO}_4$ at 37°C for 10 min was performed prior to putting reactions on ice.

For imaging, reactions were diluted 15-fold in deposition buffer (10mM HEPES-KOH pH 7.5, MgCl_2) and deposited on freshly cleaved mica. After about 30 s, the mica was washed with water (glass distilled; SIGMA) and dried in a stream of filtered air.

For study of complex disassembly on mica, human Rad51-DNA complexes were formed as described above including treatment with $(\text{NH}_4)_2\text{SO}_4$. Reactions were deposited on mica, excess buffer was removed and replaced with a buffer containing 25mM HEPES-KOH (pH7.5), 5mM MgCl_2 , 2mM ATP and 30mM KCl. The human Rad51-DNA complexes were incubated on mica at 19°C for 1, 5 or 30 min and then washed and dried as described above.

Images were obtained on a NanoScope IIIa and NanoScope IV SFM (Digital Instruments; Santa Barbara, CA) operating in tapping mode in air with a type E scanner. Silicon Nanotips were from Digital Instruments (Nanoprobes).

The length of nucleoprotein filaments was measured from NanoScope images imported into IMAGE SXM 1.62 (NIH-IMAGE version modified by Steve Barrett, Surface Science Research Centre, Univ. of Liverpool, Liverpool, U.K.). The filament contours were traced manually. For the irregular filaments the contours were traced as a path through the highest point along the nucleoprotein filaments.

Magnetic Tweezers

The magnetic tweezers setup used has been described (Noort *et al.* PNAS 2004, 101, 6969-6974). The force applied to the bead was calculated by quantifying thermal motion of the DNA-tethered bead and substituting it into equipartition theorem. Using image processing a position accuracy of 5-nm in 3 dimensions was obtained. To exclude thermal drift, all positions were measured relative to a polystyrene bead fixed to the bottom of the flow cell.

Flow cell

Polystyrene beads, as well as DNA constructs carrying at one end a magnetic bead, were anchored to the bottom of a flow cell as described (Noort *et al.* PNAS 2004, 101, 6969-6974). The force-extension curves were used to identify attachment of single DNA molecules. After conformation of the correct contour and persistence lengths, experiments were started by addition of hRad51. All measurements were carried out at 25°C .

hRad51/DNA reactions

The experimental buffer used in the present experiments was 25 mM Hepes (pH 7.5), 5 mM MgCl_2 and 25 mM KCl. hRad51 and ATP then were injected into the flow cell in this buffer while maintaining the DNA tether at a constant force. hRad51 (dis)assembly was monitored through measurement of the height of the magnetic bead.

RESULTS

The structure of nucleoprotein filaments formed by the human recombinase Rad51 was analyzed by SFM imaging. In this way we assess not only if the protein binds to DNA under the conditions tested but also directly observe the architecture of the resulting protein-DNA complexes. Significantly, sample preparation did not include any fixative agents in order to allow the observation of possibly dynamic structures. This also results in capturing the variety of structures present in a reaction mixture at the time they attach to the surface for observation as opposed to capturing structures that include all interactions that may occur during the time a fixative agent is present.

Filaments were formed on linear double-stranded DNA in order to measure DNA extension under the different conditions used. Nucleoprotein filaments formed in the presence of ATP on both single-stranded and double-stranded DNA were irregular and varied in length (figure 1B). In order to assess DNA extension in the filaments, the contour length of the filaments was measured by tracing a path through the highest points along the complex. This is compared to the contour length of DNA molecules in the absence of protein. All length measurements are displayed as distributions in histograms. The length of the filaments formed in the presence of ATP indicated that many of the DNA molecules were not significantly extended in these complexes (Figure 2C). The filaments with lengths significantly shorter than the 1.8 kbp DNA added were due to contaminating short DNA fragments that were eliminated in subsequent experiments. Dramatically different filaments formed in the presence of the non-hydrolysable ATP analog AMP-PNP (Figure 1A). Compared to the filaments formed in the presence of ATP, there were almost no filaments with intermediate lengths between that of the bare 1.8 kbp fragment and the fully extended length. These filaments were regular and (apart from the filaments formed on the small contaminating DNA) had a uniform length indicating extension of the DNA to about 1.5 times that of a B-form helix (Figure 2B).

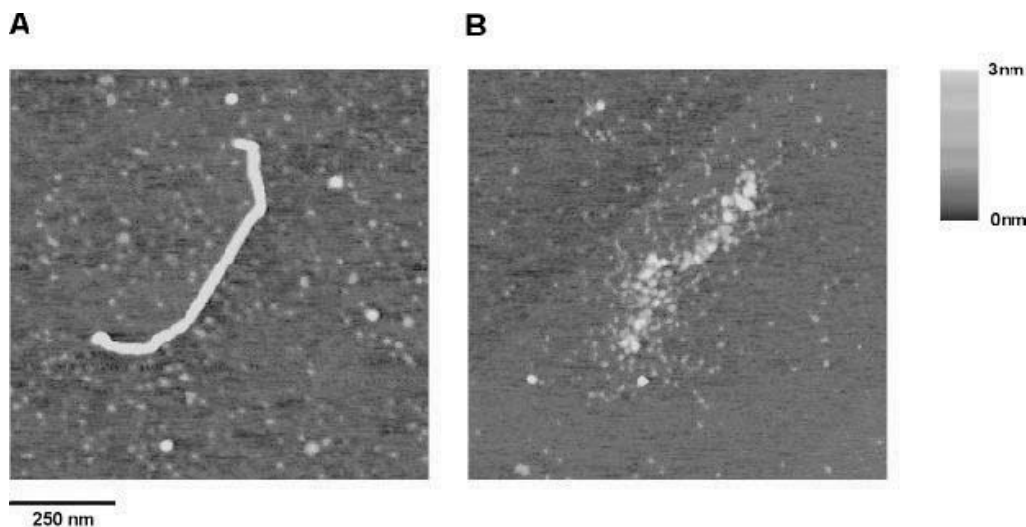


Figure 1. Effect of nucleotide cofactors on the structure of Rad51-dsDNA filament. Height is indicated by color as shown on the bar at the right. (A) Rad51 filament formed on dsDNA in the presence of AMPPNP and MgCl_2 (B) Rad51 filament formed on dsDNA in the presence of ATP and MgCl_2

In vitro strand exchange reactions catalyzed by Rad51 are stimulated by specific conditions such as the addition of ammonium sulfate to a reaction including ATP and Mg^{2+} (Sigurdsson et al., 2001) or the substitution of Ca^{2+} for Mg^{2+} in an ATP containing reaction (Bugreev et al., 2004). Filaments were formed as for *in vitro* strand exchange reactions, by addition of protein and nucleotide cofactor to DNA followed by addition of ammonium sulfate (Sigurdsson et al., 2001). These filaments appeared similar to those formed in the presence of AMP-PNP without ammonium sulfate, regular and elongated relative to naked DNA (Figure 3A and 4B, here in the absence of contaminating small DNA fragments). Filaments formed in the presence of ATP and treated with ammonium sulfate were also regular in appearance (Figure 3B) and elongated, with a length distribution centered near the fully extended form (Figure 4C). The substitution of Ca^{2+} for Mg^{2+} in an ATP containing reaction resulted in regular filaments (Figure 5A) with uniform length elongated 1.5 times relative to naked DNA (Figure 5B).

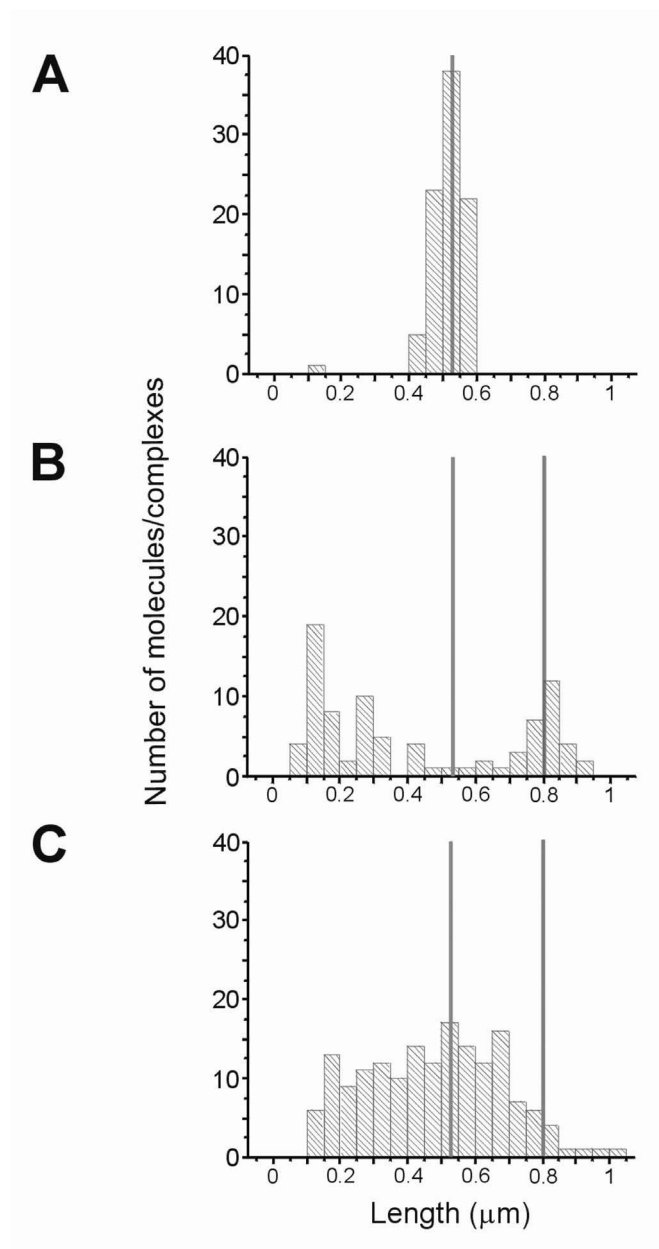


Figure 2. Histograms of contour length of DNA and Rad51 filaments formed with different nucleotide cofactors. Blue and green line represent expected length for naked DNA and for 1.5 times extended DNA in nucleoprotein filaments respectively (A) Contour length of naked DNA. (B) Contour length of Rad51 filaments formed in the presence of AMPPNP and MgCl_2 . (C) Contour length of Rad51 filaments formed in the presence of ATP and MgCl_2

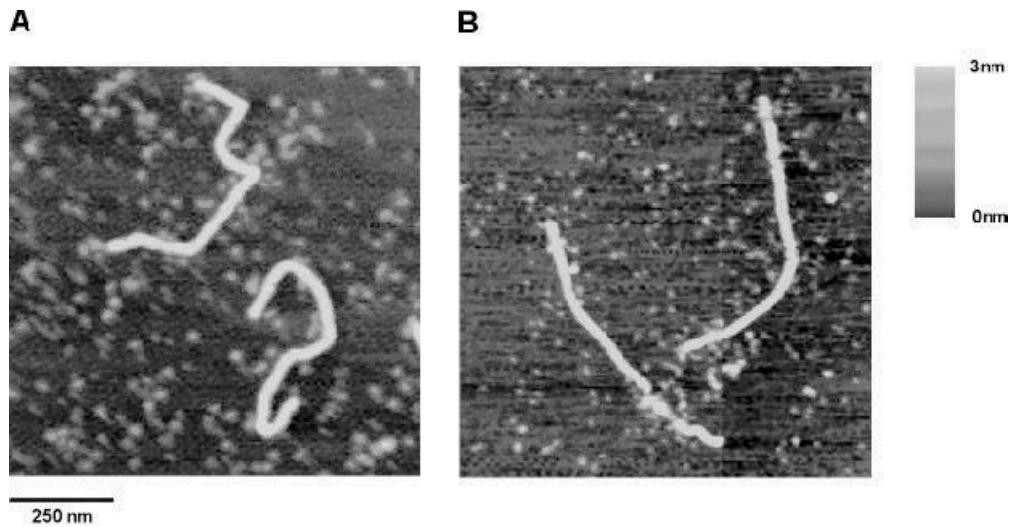


Figure3. Effect of ammonium sulfate on the structure of Rad51-dsDNA filament. (A) Rad51 filament on dsDNA was formed in the presence of AMPPNP and MgCl₂ without additional treatment with ammonium sulfate. (B) Rad51 filament on dsDNA formed in the presence of ATP and MgCl₂. Additional treatment with ammonium sulfate was performed as described in Materials and Methods.

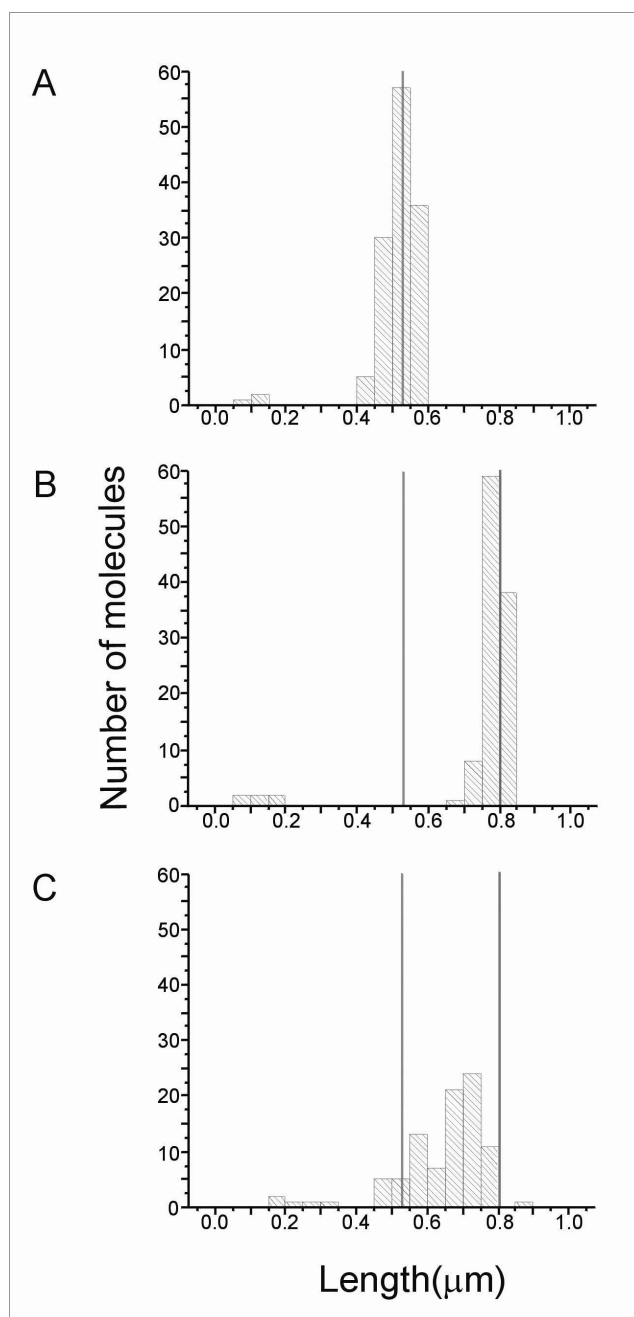


Figure 4. Effect of ammonium sulfate on the DNA extension in Rad51-dsDNA filaments. The expected length for naked DNA and 1.5 time extended DNA are marked with blue and green lines respectively. (A) Contour length of naked DNA. (B) Contour length of Rad51 filaments formed in the presence of AMPNP and MgCl₂. (C) Contour length distribution of Rad51 filaments formed in the presence of ATP and MgCl₂ and additionally treated with ammonium sulfate before deposition on mica.

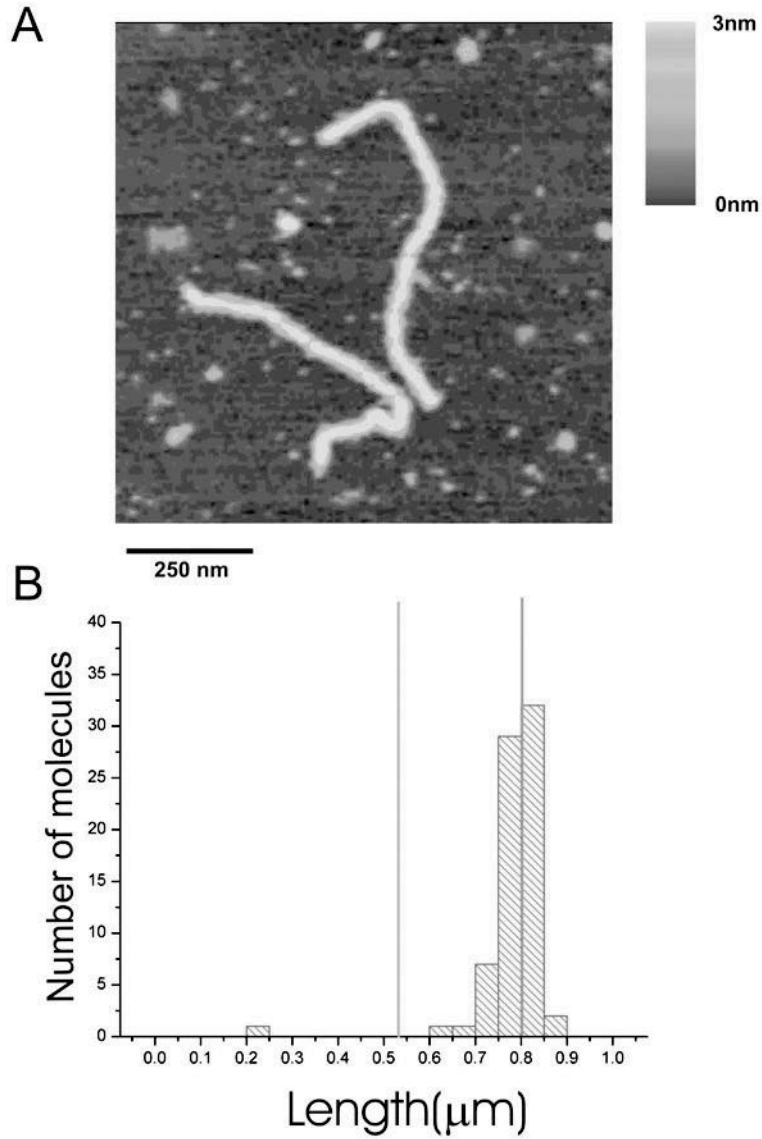


Figure5. SFM image and contour length distribution of Rad51-dsDNA filaments formed in the presence of ATP and CaCl_2 . (A) Two Rad51-dsDNA filaments formed in reaction with ATP and CaCl_2 . (B) Contour length distribution of Rad51-dsDNA filaments formed in the presence of ATP and CaCl_2 . Blue and green lines indicate expected length for naked DNA and for 1.5 time extended DNA respectively.

ATP hydrolysis is required *in vivo* for Rad51 function in homologous recombination (Stark et al., 2002) and we observed that filaments formed in the presence of ATP were very irregular. The irregular structure of these filaments and the broad distribution of their lengths suggested that they might be dynamic, with active exchange of free and DNA bound Rad51 along the filament. In order to test if this was the case we characterized the transition from regular to irregular filaments. Because ammonium sulfate does not significantly inhibit the ATPase activity of human Rad51 (Tomblin et al., 2002; Ristić data not shown) but does result in the formation of regular filaments, we reasoned that removing ammonium sulfate would provide an experimental tool to control the transition from regular to irregular filaments. For this purpose filaments were formed between human Rad51 and double-stranded DNA in conditions including ATP and Mg^{2+} , followed by addition of ammonium sulfate as before. After deposition onto mica excess buffer was removed and replaced with a buffer lacking ammonium sulfate and human Rad51. The filaments deposited on mica were incubated in this buffer for varying times before washing and drying as usual for SFM observation. As can be seen in Figure 6, incubation without ammonium sulfate for 1, 5 and 30 minutes resulted in increasing disorder along the filaments, apparent loss of protein from DNA and eventually completely protein-free DNA. Filament length also decreased over this time indicating that DNA extension is not maintained as the filaments become irregular (Figure 7). In contrast to RecA (Bork et al., 2001), human Rad51 disassociation from the filaments did not occur from one end but apparently from many sites along the filament. The effect of ammonium sulfate on stability of the human Rad51 filaments was specific and not a general effect of ionic strength of the buffer. Maintaining ionic strength by substitution of KCl for ammonium sulfate did not stabilize the filaments, irregular filaments appeared just as in the absence of ammonium sulfate or when it was removed without additional salt (Figure 8 A, B). Though human Rad51 binds to DNA in the presence of ADP, irregular filaments were also formed when ADP was used as a cofactor (Figure 8C).

The experiments incubating filaments on mica suggested that filaments disassembled over the course of about 30 min by disassociation of human Rad51 from many points along the filament. It is notable that the human Rad51 protein in filaments bound to mica appeared to retain activity it had in solution, the same irregular filaments appear on mica after removal of ammonium sulfate as had been trapped by deposition from solution reactions including ATP. However it was not possible to follow these apparent dynamics directly and we could not exclude possible effects of the surface on this reaction and its apparent kinetics.

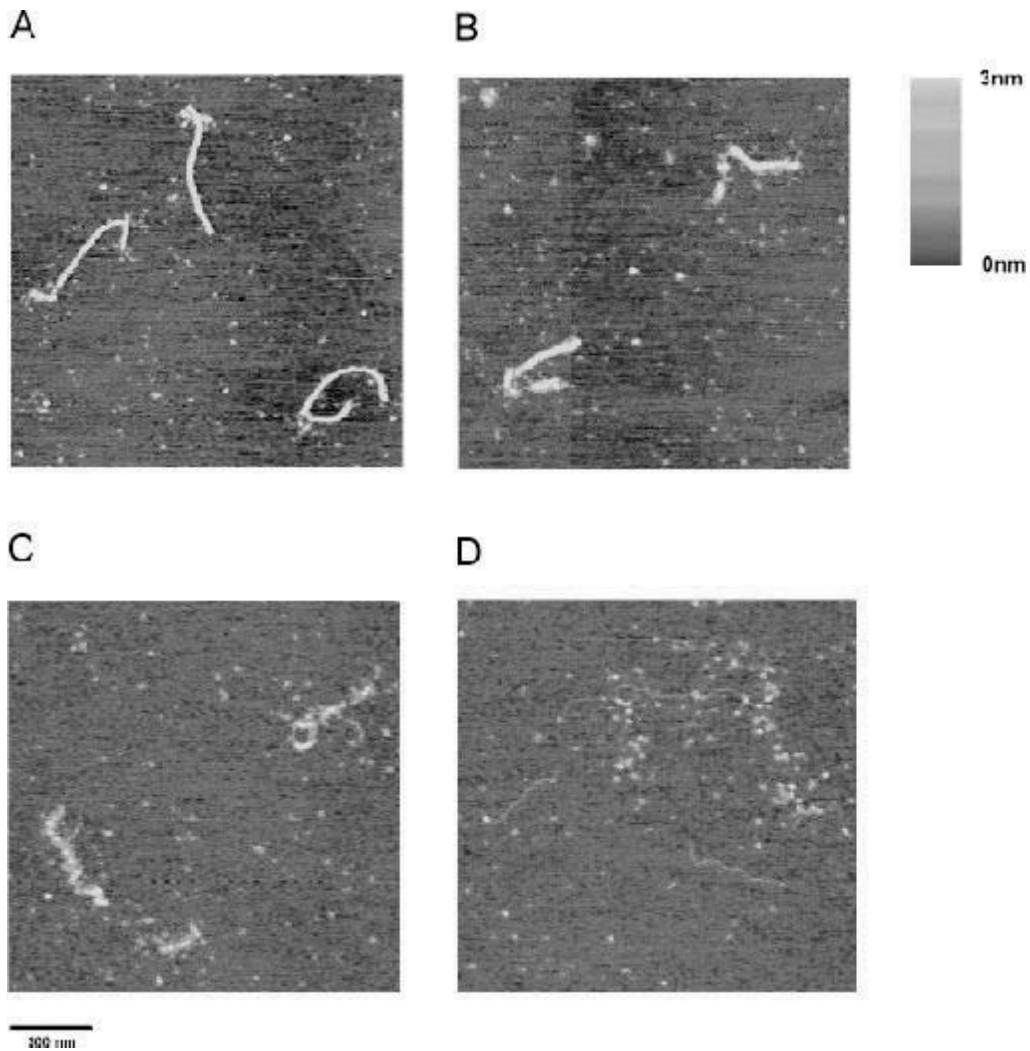


Figure 6. SFM visualization of Rad51-dsDNA filament disassembly. Rad51-dsDNA complexes are formed, disassembled and analyzed as described in Materials and Methods. (A) Rad51-dsDNA filaments formed in the reaction with ATP and $MgCl_2$. Nucleoprotein filaments are treated with ammonium sulfate before deposition. Rad51-dsDNA filaments were visualized after 1 minute (B), 5 minutes (C) and 30 minutes (D) of disassembly on mica.

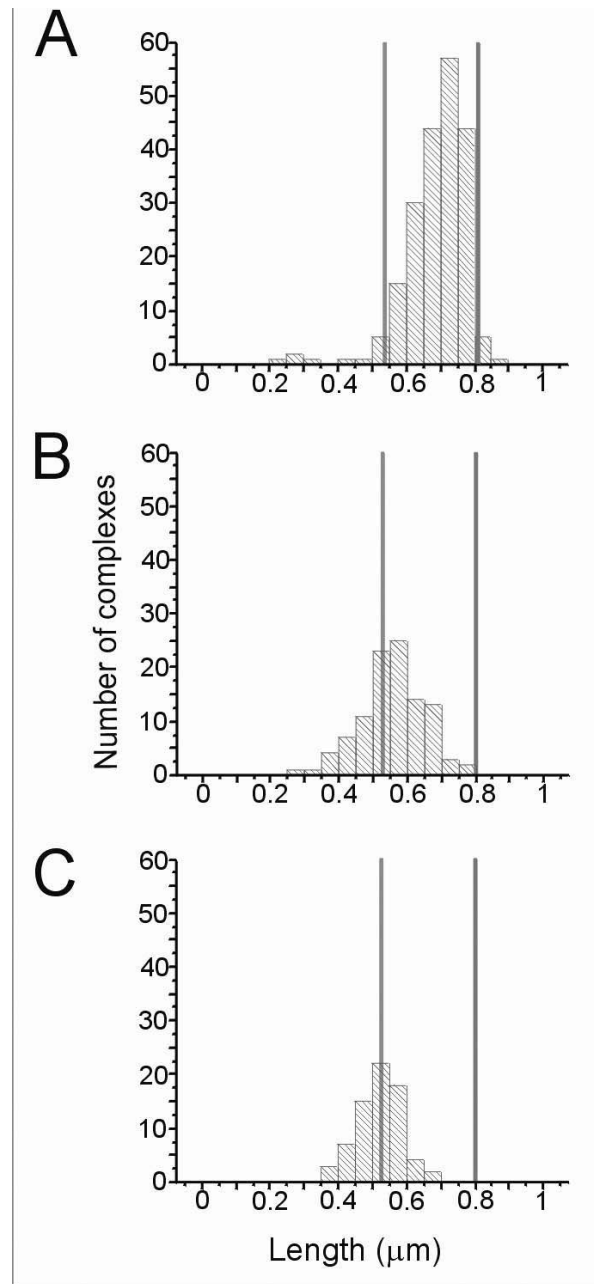


Figure 7. Histograms of Rad51-dsDNA filaments contour length decrease during nucleoprotein filaments disassembly on mica. DNA path was traced through the highest points along the filaments. Contour length of filaments was measure before start (A), after 1 minute (B) and after 5 minutes (C) of the disassembly on mica.

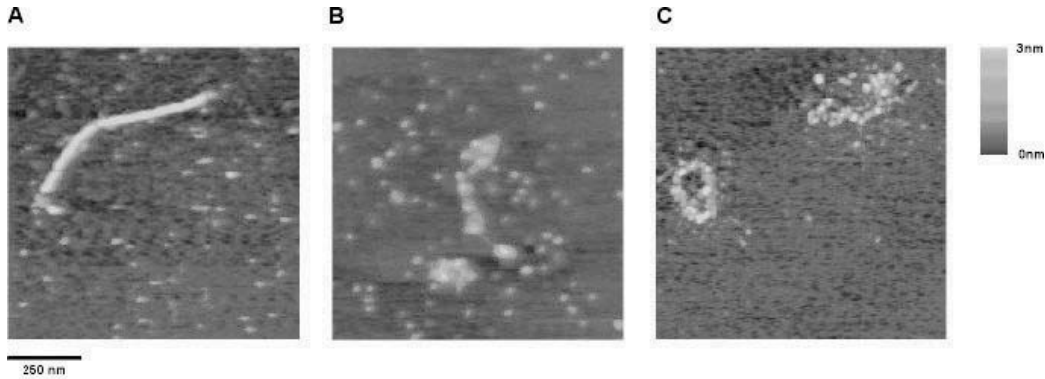


Figure 8. Effect of KCl or ADP on stability of Rad51-dsDNA filaments. Rad51-dsDNA filaments are formed in the presence of ATP (A and B) or ADP (C) and MgCl_2 . Additional treatment with 200 mM ammonium sulfate resulted in regular filaments (A). Treatment with 200 mM KCl instead ammonium sulfate did not stabilized filaments (B). Irregular filaments were also formed in reaction with ADP as cofactor (C).

In order to avoid the surface effects and study the dynamics directly, we followed human Rad51 filament assembly and disassembly on single DNA molecules held in magnetic tweezers. A double stranded DNA molecule was tethered between a surface and a magnetic bead such that the position of the bead and the force exerted upon it could be manipulated and recorded. In the experiments reported nicked DNA was used resulting in a torsionally unconstrained magnetic bead/DNA construct. At a constant force, enough to extend the DNA but not distort its structure, the assembly of a Rad51 filament on this DNA will increase the length of the tethered molecule. Assembly (or disassembly) of the filament is followed in real time by recording changes in the height of the magnetic bead. Upon addition of buffer containing human Rad51, ATP and Mg^{2+} , filaments assembly was very fast. The dynamics of this process could not be followed when 830 nM Rad51 was added to the flow cell as DNA was detected in its fully extended state as soon as the mechanical noise from flushing in protein containing buffer subsided (Figure 9A). At lower levels of Rad51, 166 nM added to the flow cell, the dynamics of filament assembly could be followed however a fully extended filament was not formed (Figure 9B). Both the fast assembly (830 nM Rad51) and the slow assembly (166 nM Rad51) reactions were measured in several independent experiments (3 and 11 respectively) showing very similar times courses.

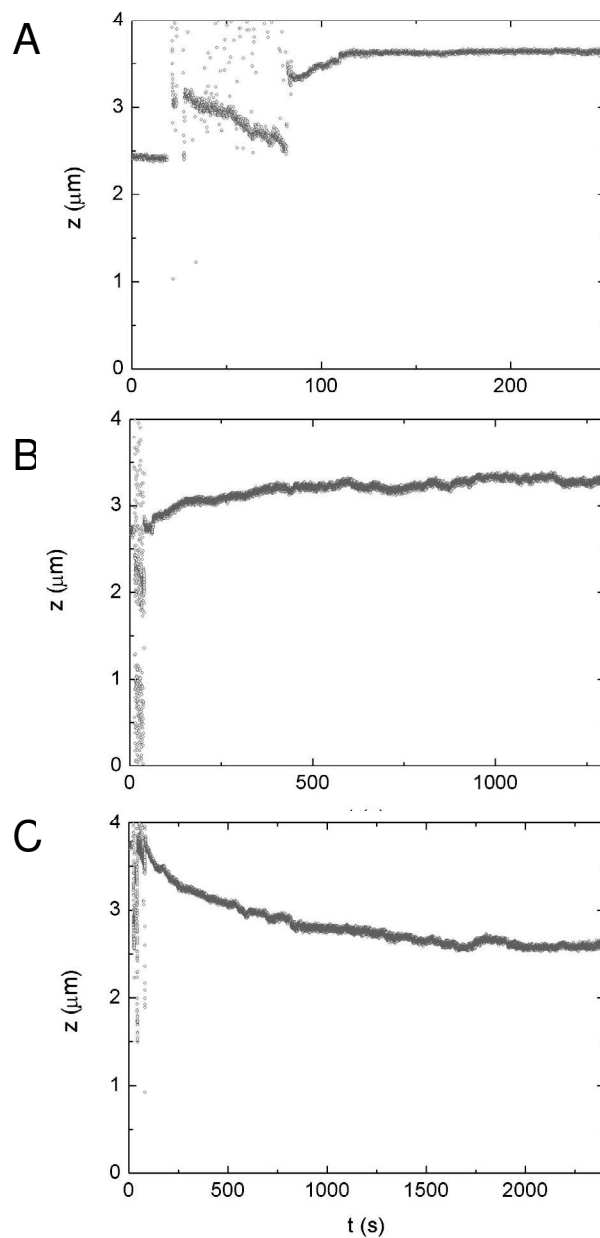


Figure9. Assembly and disassembly of Rad51-dsDNA filaments followed in a real time in magnetic tweezers. The DNA tether was held at a constant force of 1 pN. (A) Fast assembly of filament in reaction with 830 nM Rad51. Fully extended filaments were formed during flushing in protein containing buffer. (B) Slow polymerization of nucleoprotein filaments in reaction containing 166 nM Rad51. (C) Filament disassembly. The disassembly reaction was initiated by removing Rad51 and ATP from the flow cell.

The sigmoidal shape of the curve describing DNA elongation vs. time in the presence of 166 nM Rad51 indicates that the limiting step in filament assembly is not a slow DNA binding or nucleation events followed by rapid growth of a filament (Figure 9B). Rather it appears that nucleation events of Rad51 binding to DNA can occur at multiple sites, the frequency of which is determined by the concentration of free Rad51 (complete quantitative analysis of these and other tweezers experiments to be published elsewhere). Filaments formed in these conditions, continuous presence of hRad51 and ATP, remained stable and elongated, within the detection limits of the tweezers, for several hours. Length changes of a magnitude up to 10 nanometers or with a frequency greater than 30 Hz were within the spatial and temporal noise for Z detection at the force used. Addition of ammonium sulfate after the formation of filaments did not affect their elongation. However, addition of ammonium sulfate together with Rad51 prevented any obvious filament formation, as was also observed in SFM imaging of these reactions (data not shown). As observed by SFM, elongated filaments were formed when Rad51 was added to the flow cell together with AMP-PNP or with ATP and Ca^{2+} instead of Mg^{2+} (data not shown).

Disassembly of filament formed in the presence of ATP was followed after replacing the buffer in the flow cell with one that lacked ATP and Rad51. The bead height, representing end-to-end distance of the tethered molecule decreased over the course of 50 min to the original length of naked DNA. The exponential decay of this curve indicated that filament disassociation did not occur from one end or a single point, but that Rad51 disassociated from many points all over the filament. As expected from the SFM imaging experiments, Rad51 filaments treated with ammonium sulfate or formed with ATP and Ca^{2+} did not disassociate (observed for several hours to over night) when the buffer was replaced with one lacking Rad51 and ATP. These single molecule dynamic measurements of filament disassembly in solution confirmed the snap shot SFM images of filament disassembly on mica.

DISCUSSION

Formation of a regular protein filament with extended DNA is a required step in current models of homologous recombination. We observe that the human recombinase Rad51 forms regular filament with extended double-stranded DNA in the conditions that promote an efficient *in vitro* strand exchange reaction. It has recently been reported that joint molecule formation by hRad51 also occurs efficiently in the presence of AMP-PNP (Bugreev et al., 2004), further extending the correlation between regular filament formation and *in vitro* activity. The common feature of the conditions that favor regular filaments and *in vitro* activity of human Rad51 is an ATP bound conformation of the protein. The regular filament form appears to be trapped when ATP, or a structural mimic, is bound but not hydrolyzed. AMP-PNP is a chemical analog of ATP that can bind to but is not hydrolyzed by ATPases such as Rad51. Substituting Ca^{2+} for Mg^{2+} in reactions involving human Rad51 results in a reduced ATPase rate that maintains human Rad51 in an ATP bound form (Bugreev et al., 2004). It is likely that the effect of ammonium sulfate is also to mimic an ATP bound form of human Rad51. Although ammonium sulfate does not inhibit the ATPase activity of hRad51 (Tomblin et al., 2002; Ristić data not shown) it probably does influence the ATPase active site. Both an archeal recombinase *PfRad51* (Shin et al.,

2003) and yeast Rad51 (Conway et al., 2004), crystallized in the presence of ATPγS have a sulfate ion (presumably scavenged from the crystallization solution), not a nucleotide bound, at their active sites. Either the bound sulfate ion alone or in the presence of ADP could induce the same protein conformation as bound ATP that is needed to assemble regular stable filaments.

The implication of filament stability only in the presence of bound ATP is that once ATP is hydrolyzed and ADP is bound, human Rad51 is no longer able to form stable regular filaments on DNA. Indeed we observed that human Rad51 did form filaments in the presence of ADP, but the structures formed were very irregular. The importance of nucleotide cofactors for filament structure and stability is clear in the atomic structure models of Rad51 and *Methanococcus voltae* RadA filaments (Conway et al., 2004; Wu et al., 2004 respectively). In these two structures the ATPase active site is at the junction of adjacent monomers in a filament. In the *Methanococcus voltae* filament structure the AMP-PNP nucleotide is clearly resolved as a bridge between adjacent RadA monomers. It is easy to imagine that hydrolysis of ATP would, in simple terms, break this bridge or change the conformation of the adjacent recombinase monomers so that the subunit interface becomes less stable.

The human Rad51 filaments we observed appeared dynamic in the presence of ATP. Regular filaments have been reported by others in these conditions (Benson et al., 1994, Liu et al., 2004) but only after fixation which could have trapped otherwise dynamic protein in a regular structure. The irregularity we observed was not limited to an end or a few places along the filaments. Filaments formed on DNA with ATP and ammonium sulfate were regular and stable even though ATP was efficiently hydrolyzed in these conditions. Upon ammonium sulfate wash out the filaments disassembled, again from many points and not just from one end. In the single molecule experiments, with excess human Rad51 and ATP in solution there was no net decrease in length detected at the force applied. The broader distribution and shorter lengths of filaments formed in the presence of ATP in SFM images represented a snap shot of the state of the molecules at the time of immobilization. This variation may not be detected as length changes in the magnetic tweezers because they are transient and in rapid transition with fully bound extended forms. When ATP and Rad51 were removed or when ammonium sulfate was washed out of the buffer in single molecule experiments the filaments got shorter with a time course that also indicated disassembly from many points.

Filament disassembly is likely to be as important as assembly in authentic recombination reactions *in vivo*. The steps of recombination represented in *in vitro* assays do not require ATP hydrolysis by the recombinase (Bugreev et al., 2004). However ATPase activity is needed *in vivo* for recombinase function and recombination activity. *In vitro* assays for recombinase functions usually follow the production of a joint molecule intermediate where homologous single stranded and double stranded DNA molecules become joined or exchange base pairing partners. The DNA products are analyzed after deproteination, which eliminates any differences among the reactions with respect to disassociation of the recombinases after the DNA product formed. However recombination *in vivo* does not stop at joint molecule formation. To complete the process other proteins need to access the joint molecule to extend the invading strand sequences by polymerization or extend the heteroduplex by holiday junction migration and eventually to complete the process by resolution of

the recombined molecules. A recombinase filament covering the joint molecule is likely to inhibit these processes. Indeed, a dynamic RecA filament, capable of hydrolyzing ATP, is required for *in vitro* recombination coupled replication of *E. coli* (Xu et al., 2002). This is an essential recombination process in both prokaryotes and eukaryotes (Cox et al., 2000).

The filaments we have analyzed were formed on double stranded DNA which is not the form required to initiate recombination but represent an intermediate after joint molecule formation. It is at this stage that filament disassembly is expected to be required *in vivo*. We demonstrated that hRad51 filament disassembly occurred when ATP was hydrolyzed and presumably the protein conformation was no longer able to maintain a stable elongated structure.

These results raise several questions concerning mechanism and the control of recombination in human (mammalian) cells. The recombination reaction that can be completed by RecA alone in bacteria requires a host of protein in eukaryotes, often called recombination mediators (Sung et al., 2003; Wyman et al., 2004). In Mammals these additional factors including a group of proteins known as Rad51 paralogs because of their limited sequence similarity to Rad51. Some of the additional factors may function to identify DNA in need of homologous recombination thereby promoting and stabilizing appropriately formed filaments on single stranded DNA. For instance it has been suggested that one of the paralogs, hXRCC2 is an ADP/ATP exchange factor for hRad51 that would help maintain hRad51 in an ATP bound state in stable filaments (Shim et al., 2004). The transition to unstable and disassembling filaments after joint molecule formation is also a step where regulation and control are required and could be provided by the recombination mediators.

ACKNOWLEDGMENTS

This work was supported by grants from the Dutch Organization for Scientific Research (NWO) and The Dutch Cancer Society (KWF)

REFERENCES

1. Bedale, W.A. and M. Cox, *Evidence for the coupling of ATP hydrolysis to the final (extension) phase of RecA protein-mediated DNA strand exchange*. J Biol Chem, 1996. **271**(10): p. 5725-5732.
2. Benson, F.E., A. Stasiak, and S.C. West, *Purification and characterization of the human Rad51 protein, an analogue of E. coli RecA*. Embo J, 1994. **13**(23): p. 5764-5771.
3. Bork, J.M., M.M. Cox, and R.B. Inman, *RecA protein filaments disassemble in the 5' to 3' direction on single-stranded DNA*. J Biol Chem, 2001. **276**(49): p. 45740-45743.
4. Bugreev, D.V. and A.V. Mazin, *Ca²⁺ activates human homologous recombination protein Rad51 by modulating its ATPase activity*. Proc Natl Acad Sci U S A, 2004. **101**(27): p. 9988-9993.
5. Conway, A.B., et al., *Crystal structure of a Rad51 filament*. Nat Struct Mol Biol, 2004. **11**(8): p. 791-796.
6. Cox, M.M., *Why does RecA protein hydrolyse ATP?* Trends Biochem Sci, 1994. **19**(5): p. 217-222.
7. Cox, M.M., *The bacterial RecA protein as a motor protein*. Annu Rev Microbiol, 2003. **57**: p. 551-577.
8. Cox, M.M., et al., *The importance of repairing stalled replication forks*. Nature, 2000. **404**(6773): p. 37-41.

9. De Zutter, J.K. and K.L. Knight, *The hRad51 and RecA proteins show significant differences in cooperative binding to single-stranded DNA*. J Mol Biol, 1999. **293**(4): p. 769-780.
10. Dunn, K., S. Chrysogelos, and J. Griffith, *Electron microscopic visualization of recA-DNA filaments: evidence for a cyclic extension of duplex DNA*. Cell, 1982. **28**(4): p. 757-765.
11. Flory, J. and C.M. Radding, *Visualization of recA protein and its association with DNA: a priming effect of single-strand-binding protein*. Cell, 1982. **28**(4): p. 747-756.
12. Hegner, M., S.B. Smith, and C. Bustamante, *Polymerization and mechanical properties of single RecA-DNA filaments*. Proc Natl Acad Sci U S A, 1999. **96**(18): p. 10109-10114.
13. Jain, S.K., M.M. Cox, and R.B. Inman, *On the role of ATP hydrolysis in RecA protein-mediated DNA strand exchange. III. Unidirectional branch migration and extensive hybrid DNA formation*. J Biol Chem, 1994. **269**(32): p. 20653-20661.
14. Kim, H.K., et al., *ADP stabilizes the human Rad51-single stranded DNA complex and promotes its DNA annealing activity*. Genes Cells, 2002. **7**(11): p. 1125-1134.
15. Kim, J.I., M.M. Cox, and R.B. Inman, *On the role of ATP hydrolysis in RecA protein-mediated DNA strand exchange. I. Bypassing a short heterologous insert in one DNA substrate*. J Biol Chem, 1992. **267**(23): p. 16438-16443.
16. Kim, J.I., M.M. Cox, and R.B. Inman, *On the role of ATP hydrolysis in RecA protein-mediated DNA strand exchange. II. Four-strand exchanges*. J Biol Chem, 1992. **267**(23): p. 16444-16449.
17. Konola, J.T., K.M. Logan, and K.L. Knight, *Functional characterization of residues in the P-loop motif of the RecA protein ATP binding site*. J Mol Biol, 1994. **237**(1): p. 20-34.
18. Kowalczykowski, S.C., *Biochemistry of genetic recombination: energetics and mechanism of DNA strand exchange*. Annu Rev Biophys Biophys Chem, 1991. **20**: p. 539-575.
19. Kowalczykowski, S.C. and R.A. Krupp, *DNA-strand exchange promoted by RecA protein in the absence of ATP: implications for the mechanism of energy transduction in protein-promoted nucleic acid transactions*. Proc Natl Acad Sci U S A, 1995. **92**(8): p. 3478-3482.
20. Liu, Y., et al., *Conformational changes modulate the activity of human RAD51 protein*. J Mol Biol, 2004. **337**(4): p. 817-827.
21. Menetski, J.P., D.G. Bear, and S.C. Kowalczykowski, *Stable DNA heteroduplex formation catalyzed by the Escherichia coli RecA protein in the absence of ATP hydrolysis*. Proc Natl Acad Sci U S A, 1990. **87**(1): p. 21-25.
22. Namsaraev, E.A. and P. Berg, *Binding of Rad51p to DNA. Interaction of Rad51p with single- and double-stranded DNA*. J Biol Chem, 1998. **273**(11): p. 6177-6182.
23. Rehrauer, W.M. and S.C. Kowalczykowski, *Alteration of the nucleoside triphosphate (NTP) catalytic domain within Escherichia coli recA protein attenuates NTP hydrolysis but not joint molecule formation*. J Biol Chem, 1993. **268**(2): p. 1292-1297.
24. Ristic, D., et al., *Rad52 and Ku bind to different DNA structures produced early in double-strand break repair*. Nucleic Acids Res, 2003. **31**(18): p. 5229-5237.
25. Ristic, D., et al., *The architecture of the human Rad54-DNA complex provides evidence for protein translocation along DNA*. Proc Natl Acad Sci U S A, 2001. **98**(15): p. 8454-8460.
26. Seitz, E.M., et al., *RadA protein is an archaeal RecA protein homolog that catalyzes DNA strand exchange*. Genes Dev, 1998. **12**(9): p. 1248-1253.
27. Shan, Q. and M.M. Cox, *RecA filament dynamics during DNA strand exchange reactions*. J Biol Chem, 1997. **272**(17): p. 11063-11073.
28. Shim, K.S., et al., *hXRCC2 enhances ADP/ATP processing and strand exchange by hRAD51*. J Biol Chem, 2004. **279**(29): p. 30385-30394.
29. Shin, D.S., et al., *Full-length archaeal Rad51 structure and mutants: mechanisms for RAD51 assembly and control by BRCA2*. Embo J, 2003. **22**(17): p. 4566-4576.

30. Sigurdsson, S., et al., *Basis for avid homologous DNA strand exchange by human Rad51 and RPA*. J Biol Chem, 2001. **276**(12): p. 8798-8806.
31. Stark, J.M., et al., *ATP hydrolysis by mammalian RAD51 has a key role during homology-directed DNA repair*. J Biol Chem, 2002. **277**(23): p. 20185-20194.
32. Stasiak, A. and E. Di Capua, *The helicity of DNA in complexes with recA protein*. Nature, 1982. **299**(5879): p. 185-186.
33. Sung, P., et al., *Rad51 recombinase and recombination mediators*. J Biol Chem, 2003. **278**(44): p. 42729-42732.
34. Sung, P. and S.A. Stratton, *Yeast Rad51 recombinase mediates polar DNA strand exchange in the absence of ATP hydrolysis*. J Biol Chem, 1996. **271**(45): p. 27983-27986.
35. Tomblin, G. and R. Fishel, *Biochemical characterization of the human RAD51 protein. I. ATP hydrolysis*. J Biol Chem, 2002. **277**(17): p. 14417-14425.
36. Tomblin, G., et al., *Biochemical characterization of the human RAD51 protein. III. Modulation of DNA binding by adenosine nucleotides*. J Biol Chem, 2002. **277**(17): p. 14434-14442.
37. van Noort, J., et al., *Dual architectural roles of HU: formation of flexible hinges and rigid filaments*. Proc Natl Acad Sci U S A, 2004. **101**(18): p. 6969-6974.
38. VanLoock, M.S., et al., *ATP-mediated conformational changes in the RecA filament*. Structure (Camb), 2003. **11**(2): p. 187-196.
39. Wu, Y., et al., *Crystal structure of archaeal recombinase RADA: a snapshot of its extended conformation*. Mol Cell, 2004. **15**(3): p. 423-435.
40. Wyman, C., D. Ristic, and R. Kanaar, *Homologous recombination-mediated double-strand break repair*. DNA Repair (Amst), 2004. **3**(8-9): p. 827-833.
41. Xu, L. and K.J. Mariani, *A dynamic RecA filament permits DNA polymerase-catalyzed extension of the invading strand in recombination intermediates*. J Biol Chem, 2002. **277**(16): p. 14321-14328.
42. Yu, X. and E.H. Egelman, *Structural data suggest that the active and inactive forms of the RecA filament are not simply interconvertible*. J Mol Biol, 1992. **227**(1): p. 334-346.
43. Yu, X., et al., *Domain structure and dynamics in the helical filaments formed by RecA and Rad51 on DNA*. Proc Natl Acad Sci U S A, 2001. **98**(15): p. 8419-8424.
44. Yu, X., et al., *What is the structure of the RecA-DNA filament?* Curr Protein Pept Sci, 2004. **5**(2): p. 73-79.
45. Zaitseva, E.M., E.N. Zaitsev, and S.C. Kowalczykowski, *The DNA binding properties of Saccharomyces cerevisiae Rad51 protein*. J Biol Chem, 1999. **274**(5): p. 2907-2915.

Summary



Summary

DNA, the genetic material in the living cell, is continuously challenged by various endogenous and exogenous agents. DNA lesions, if not repaired properly, can lead to chromosomal aberrations, cell death or carcinogenesis. In order to maintain genome stability, the cell has specialized DNA repair mechanisms. Single molecule analysis of protein complexes involved in DNA repair by direct observation with scanning force microscopy is presented in chapter 2. The unique features of scanning force microscopy are explored in this chapter to describe multiple structural aspects of DNA repair protein complexes and to correlate these aspects with their DNA repair functions.

DNA double-strand breaks, one of the most toxic DNA lesions, can be repaired in an error-free manner by homologous recombination. Chapter 3 describes the role and basic steps of homologous recombination as well as the proteins involved in this process in *E. coli* and eucaryotes. Furthermore, the latest *in vivo* experiments, addressing the behavior of homologous recombination proteins in the context of the living cell, are presented.

DNA double-strand breaks are repaired by one of two main pathways, non-homologous end joining or homologous recombination. A competition between Ku70/80 and Rad52 for DNA end binding has been suggested to determine the choice of repair pathway. In order to test this idea, direct comparison of the binding of the Ku70/80 and Rad52 to different DNA substrates has been performed and reported in chapter 4. Scanning force microscopy analysis showed no evidence of competition of these two proteins for the same DNA substrates. Ku70/80 bound preferentially to DNA with free ends. Rad52 bound preferentially to single-stranded DNA and not DNA ends. Based on these DNA binding characteristics it is unlikely that competition between Rad52 and Ku70/80 can direct DNA double-strand break repair to either non-homologous end joining or homologous recombination.

The Rad51 protein mediates pairing between homologous DNA molecules. The Rad54 protein assists this reaction. To understand how Rad54 functions, interactions of the human Rad54 protein with double-stranded DNA are reported in chapter 5. Scanning force microscopy analysis of the structure of Rad54-DNA complexes provides evidence for protein translocation along DNA. We propose a model to explain how this activity of Rad54 may facilitate homologous recombination.

All the identified recombinases form helical filament on DNA, which is the catalytic core of homologous recombination. Chapter 6 reports analysis of nucleoprotein filaments formed by the human recombinase Rad51 in a variety of conditions by scanning force microscopy imaging. Stable and regular filaments with extended double-stranded DNA were observed under conditions that stimulated homologous recombination *in vitro*. Irregular filaments were produced under conditions that allowed formation of an ADP bound conformation Rad51. The assembly and disassembly of Rad51 filaments were, unlike RecA, not cooperative process but occurred from multiple places along the filament.

Samenvatting

DNA, het genetisch materiaal van de cel, wordt voortdurend bedreigd door verschillende endogene en exogene agentia. Wanneer DNA beschadigingen niet correct worden gerepareerd, kunnen zij leiden tot chromosomale instabiliteit, celdood of carcinogenese. De cel beschikt over diverse DNA herstelmechanismen die de integriteit van het genoom moeten bewaken.

Hoofdstuk 2 beschrijft studies aan individuele moleculen van eiwitcomplexen die betrokken zijn bij DNA herstel. Hierbij werd gebruik gemaakt van 'scanning force' microscopie. Dit type microscopie is bij uitstek geschikt om de structuur van DNA herstel enzymen te bestuderen en te correleren aan hun functie.

Dubbelstrengs-DNA breuken, behorende tot de meest toxische DNA schades, kunnen foutloos worden hersteld door het proces van homologe recombinatie. Hoofdstuk 3 beschrijft het moleculaire mechanisme van dit proces zoals het plaatsvindt in *E. coli* en eukaryote cellen. Daarnaast worden de meest recente inzichten behandeld die zijn verkregen uit onderzoek van recombinatie-eiwitten in de levende cel.

Er zijn twee herstelmechanismen voor dubbelstrengs-DNA breuken: niet-homologe end-joining en homologe recombinatie. Het is mogelijk dat de keuze tussen die twee mechanismen beslist wordt door de uitkomst van een competitie tussen Ku70/80 en Rad52 voor DNA-uiteinden. Om deze hypothese te testen, werd de binding van Ku70/80 en Rad52 aan verschillende DNA substraten bestudeerd met behulp van 'scanning force' microscopie. De resultaten van deze studie, beschreven in hoofdstuk 4, laten zien dat er geen directe competitie is tussen Ku70/80 en Rad52 voor hetzelfde DNA substraat. Ku70/80 bond bij voorkeur aan DNA met vrije uiteinden, terwijl Rad52 zich associeerde met enkelstrengs-DNA in plaats van DNA-uiteinden. Uit deze gegevens blijkt dat het niet waarschijnlijk is dat competitie tussen Ku70/80 en Rad52 het proces van dubbelstrengs breuk herstel in de richting van niet-homologe end-joining of homologe recombinatie stuurt.

De eiwitten Rad52 en Rad 54 zijn betrokken bij het samenhechten van homologe DNA moleculen. In hoofdstuk 5 zijn studies beschreven die betrekking hebben op de interactie van het menselijk Rad54 eiwit met dubbelstrengs-DNA. 'Scanning force' microscopische analyse toonde aan dat Rad54 zich kan verplaatsen langs het DNA-molecuul. Wij introduceren een model dat verklaart hoe deze activiteit van Rad54 het proces van homologe recombinatie kan faciliteren.

Alle geïdentificeerde recombinasen vormen helix-vormige nucleoproteïne filamenten die interageren met DNA. Het complex van dergelijke filamenten en het DNA-molecuul is de katalytische kern van het homologe recombinatie proces. Hoofdstuk 6 doet verslag van 'scanning force' microscopische analyse van nucleoproteïne filamenten die – onder verschillende condities – werden gevormd door het menselijk recombinase Rad51. Onder condities die homologe recombinatie *in vitro* stimuleren, werden stabiele en regelmatige filamenten met dubbelstrengs DNA waargenomen. Onregelmatige filamenten werden gevonden onder condities waar Rad51 een ADP-gebonden conformatie aanneemt. De formatie en deformatie van Rad51 filamenten vond plaats op meerdere plaatsen binnen een dergelijk filament en is dus geen coöperatief proces zoals de vorming van bacteriële RecA filamenten.

List of publications

Ristic D., Todorovic V., Kojic S. and Stefanovic D. (1997). Characterization of a helicase, DHEL III, from *Drosophila melanogaster* embryonic nuclei. *Biochem. Mol. Biol. Int.* 43, 723-731.

Kojic S., Todorovic V., Ristic D., Savic A. and Stefanovic D. (1998). Den1, den2 and den3, ATP-inhibited deoxyribonucleases from *Drosophila* embryonic nuclei. *Mol. Cell. Biochem.* 189, 207-212.

Ristic D., Wyman C., Paulusma C. and Kanaar R. (2001). The architecture of the human Rad54-DNA complex provides evidence for protein translocation along DNA. *Proc. Natl. Acad. Sci. U S A.* 98, 8454-8460.

Janicijevic A., Ristic D. and Wyman C. (2003). The molecular machines of DNA repair: scanning force microscopy analysis of their architecture. *J. Microsc.* 212, 264-272.

Ristic D., Modesti M., Kanaar R. and Wyman C. (2003). Rad52 and Ku bind to different DNA structures produced early in double-strand break repair. *Nucleic Acids Res.* 31, 5229-5237.

Wyman C., Ristic D. and Kanaar R. (2004). Homologous recombination-mediated double-strand break repair. *DNA Repair (Amst).* 3, 827-833.

Ristić D., Modesti M., van der Heijden T., Dekker C., Kanaar R. and Wyman C. (2004). ATP hydrolysis affects stability of hRad51 nucleoprotein filaments. Manuscript in preparation.

Curriculum vitae

Dejan Ristić, born 25.01.1970. in Sremska Mitrovica, Yugoslavia

- | | |
|-----------|---|
| 1984-1988 | High School "Stevan Petrovic Brile", Sremska Mitrovica, Yugoslavia
Secondary School Degree |
| 1989-1995 | Faculty of Biology, University of Belgrade, Yugoslavia
Bachelor of Science in Molecular Biology and Physiology |
| 1996-1998 | MSc in Molecular Genetics and Genetic Engineering at Faculty of
Biology, University of Belgrade, Yugoslavia |
| 1999-2004 | PhD student at the Department of Cell Biology an Genetics, Erasmus
MC, Rotterdam, the Netherlands |
| 2004- | Postdoctoral fellow at the Department of Cell Biology an Genetics,
Erasmus MC, Rotterdam, the Netherlands |

Acknowledgments

First, I would like to thank Jan Hoeijmakers for the warm welcome he extended to me. Jan, your enthusiasm, constant interest in other people's work and problems and the ability to always squeeze someone in your overbooked agenda make you a person someone can always rely on.

Roland, thank you for giving me the opportunity to participate in the study of homologous recombination and for everything you taught me. Your superb science overview, clear ideas and directions, patience and faith in me have helped me enormously right from the start till the very end of my PhD thesis.

Claire, thank you for introducing me to the world of SFM, the huge effort you invested in helping me to write this thesis and for your endless patience. Your rational approach to problems, optimism and humour has made my PhD days not only a learning experience but also a pleasant experience.

Niels, thank you for reading my manuscript so thoroughly and for all your comments and remarks.

Martijn, my paranimf, was the first person I always asked for opinions and help concerning experiments, countless Dutch bureaucracy documents, tax return forms.... Martijn, thank you for all your help and for those pleasant lab and out-of-the-lab moments.

Mauro, thank you for helping me with my experiments as well as for your infectious enthusiasm and humour.

Coen, thank you for helping me to find my way during my first days in the department. Your music input in our working environment was unforgettable.

Speaking of music...Cecile, thank you for your help with protein purification and for your effective singing attempts.

I would also like to thank all the present and past lab members (...Jeroen, Lieneke, Mies, Asia, Katsuhiro, Gusia, Raul, Masha, Sheba, Kris, Celine, Ana, Jacqueline, Maurice...) for creating an enjoyable lab environment.

Eric and Koos, thank you for translating the Summary for me, especially on such short notice.

Thijn, John, Fernando and Cees, our Delft connection, thank you for bringing the world of physics closer to us biologists.

Jan Jos (or Jos Jos as my little son calls you), our cyber Johnny, thank you for sharing with us the hidden beauty of the Netherlands and making us foreigners feel at home.

Laura, your laugh, colors, music, dance... have been enriching my life since we become friends. I am happy that we can share these exiting final moments of our PhD days.

Logistic team: Sjoeph, Ton, Pim, Leo, Jasperina, Marike and Rita, thank you for everything you have done for me.

At the end I would like to thank my family and friends for their constant interest in my work and especially for their involvement in all-important moments of my life. Mum, Dad and my sister Sanja, thank you for your support and your faith in me. Vesna and Miloš, the source of my strength and inspiration, thank you for your love and acceptance of all my mood swings (especially around deadlines).

Dejan